

**DECIPHERING SPERMIDINE MEDIATED
STRESS RESPONSE IN *Escherichia coli***



**THESIS
SUBMITTED FOR THE DEGREE OF
DOCTOR OF PHILOSOPHY
JAWAHARLAL NEHRU UNIVERSITY, NEW DELHI**

SEPTEMBER, 2022



**RAJESH KUMAR MISHRA
CSIR-INSTITUTE OF MICROBIAL TECHNOLOGY
CHANDIGARH, INDIA**



इमटेक
IMTECH

सूक्ष्मजीव प्रौद्योगिकी संस्थान
सेक्टर 39-ए, चण्डीगढ़ - 160 036 (भारत)
INSTITUTE OF MICROBIAL TECHNOLOGY
(A CONSTITUENT ESTABLISHMENT OF CSIR)
Sector 39-A, Chandigarh-160 036 (INDIA)

Chandigarh,

15/09/2022

Certificate

This is to certify that the research work embodied in this thesis entitled **“Deciphering spermidine-mediated stress response in *Escherichia coli*”**, has been carried out by Mr. Rajesh Kumar Mishra under the guidance of Dr. Dipak Dutta, Principal Scientist, at the CSIR-Institute of Microbial Technology, Chandigarh, India. This research work is original and has not been submitted, in part or as a whole, for a degree or diploma at this or any other institute or university.

Supervised by:

Dr. Dipak Dutta

Signature

डॉ. दीपक दत्ता/Dr. Dipak Dutta
प्रधान वैज्ञानिक/Principal Scientist
सीएसआईआर-सूक्ष्मजीव प्रौद्योगिकी संस्थान
CSIR-Institute of Microbial Technology
सेक्टर/Sector 39-A, चण्डीगढ़/Chandigarh-160036

Submitted by:

Mr. Rajesh Kumar Mishra

Signature

दूरभाष 0172-6665201 } Reception
0172-6665202 }
0172-6665..... (Direct)

फैक्स : { 0091-172-2690632 (COA)
0091-172-2690585 (Director)
0091-172-2690056 (Purchase)
एस. टी. डी. कोड : STD CODE : 172

तार : Gram : IMTECH
E.mail : system@imtech.res.in
Web : http://imtech.res.in

TABLE OF CONTENT

	Page No.
Abbreviations	
Abstract	
Acknowledgment	
Chapter 1: Introduction and literature review	1-30
1.1. Overview of polyamines	1
1.2. Biosynthesis and metabolism of polyamines	4
1.3. Polyamine homeostasis	5
1.4. Reactive oxygen species and oxidative stress	8
1.4.1. Intracellular ROS production	9
1.4.2. Damage due to O ₂ ⁻	11
1.4.2.1. Damage to Fe-S cluster	11
1.4.3. Damage due to H ₂ O ₂	12
1.4.3.1. Damage to Fe-S cluster	13
1.4.3.2. Damage to DNA	13
1.4.4. Regulatory response to oxidative stress	14
1.4.4.1. The SoxRS system	15
1.4.4.2. OxyR system	16
1.4.4.3. PerR system	18
1.4.5. Scavenger enzymes against ROS	19
1.4.5.1. SOD for degradation of O ₂ ⁻	19
1.4.5.2. Catalase and peroxidase for degradation of H ₂ O ₂	19
1.5. Importance of Fe in Bacteria	21
1.5.1 Fe homeostasis in bacteria	23
1.6. Mn homeostasis in bacteria	25
1.7. Polyamines and metal ions	27
1.8. Polyamines and oxidative stress	27
1.9. Polyamines and pathogenicity	29
1.10. Objective of present work	30

Chapter 2: Effect of over-accumulated spermidine on redox state of <i>E.coli</i>	31-48
2.1. Introduction	31
2.2. Materials and Methods	32
2.2.1. Bacterial strains, Plasmids, proteins and chemicals	32
2.2.2. Growth, viability, spermidine sensitivity and complementation assays	32
2.2.3. Estimating cellular spermidine levels	33
2.2.4. Relative ROS estimation	34
2.2.5. EPR spectroscopy	34
2.2.6. Estimation of intracellular NADP and NADPH	34
2.2.7. Intracellular glutathione measurement	35
2.2.8. Estimation of intracellular NAD and NADH	35
2.2.9. Determination of intracellular ATP level	36
2.3. Results	36
2.3.1. Overaccumulation of spermidine causes growth retardation in <i>E. coli</i>	36
2.3.2. Increased cellular spermidine inhibits overall oxidative stress while evoking less harmful O ₂ ⁻ production	38
2.3.3. Spermidine stress evokes O ₂ ⁻ production in $\Delta speG$ strain	43
2.3.4. O ₂ ⁻ production under spermidine stress affects cellular redox state	44
2.4. Discussion	47
Chapter 3: Effect of spermidine toxicity on gene expression profile	49-61
3.1. Introduction	49
3.2. Materials and Methods	51
3.2.1. Bacterial strains and broth	51
3.2.2. P1 phage preparation and transduction	51
3.2.3. Plasmid and bacterial constructs	52
3.2.4. Antibody production	53
3.2.5. Determining relative ROS levels in the cells	53

3.2.6. Quantitative real-time PCR (RT-qPCR)	53
3.2.7. β -galactosidase and GFP reporter assays	54
3.2.8. Western blotting experiments	54
3.3. Results	55
3.3.1. Spermidine blocks the induction of SoxR regulon	55
3.4. Discussion	61
Chapter 4: Biochemical impact of spermidine toxicity on Fe homeostasis	62-76
4.1. Introduction	62
4.2. Material and Methods	63
4.2.1. Bacterial strains and chemicals	63
4.2.2. Aconitase activity	63
4.2.3. ICP-MS analysis to estimate cellular Fe and Mn content	63
4.2.4. Spot assay	63
4.2.4. RNA isolation	64
4.2.5. Isothermal titration calorimetry	64
4.2.6. 2,2'-Bipyridyl and NBT assays	65
4.3. Results	65
4.3.1. Spermidine affects ISC biogenesis	65
4.3.2. Free spermidine directly interacts with Fe	68
4.3.3. Free spermidine interacts and oxidizes Fe ²⁺ ion to generate O ₂ ⁻ radicals <i>in-vitro</i>	68
4.3.3. Free spermidine interacts and oxidizes Fe ²⁺ ion to generate O ₂ ⁻ radicals <i>in-vitro</i>	70
4.4 Discussion	74
References	77-96
Appendix	97-111

PUBLICATIONS

1. **Cobalt and Nickel impair DNA metabolism by the oxidative stress independent pathway.** Vineet Kumar, **Rajesh Kumar Mishra**, Gurusharan Kaur and Dipak Dutta. **Metallomics**, 2017, 9, 1596 DOI: 10.1039/C7MT00231A.
2. **Free spermidine evokes superoxide radicals that manifest toxicity.** Vineet Kumar, **Rajesh Kumar Mishra**, Debarghya Ghose, Arunima Kalita, Anand Prakash, Gopa Mitra, Amit Arora and Dipak Dutta. **eLife**, 2022, DOI: 10.7554/eLife.77704.
3. **An intrinsic alkalization circuit turns on *mntP*-riboswitch under manganese stress in *Escherichia coli*.** Arunima Kalita, Rajesh Mishra, Vineet Kumar, Amit Arora, and Dipak Dutta. (Under review in Microbiology spectrum).
4. **A novel Rho terminator in Mn^{2+} responsive 5'-UTR riboswitch element of manganese importer *mntP* gene functions to mitigate oxidative stress by regulating intracellular Mn levels in *E. coli*.** Anand Prakash, Arunima Kalita, Kanika Kuthial, Rajesh Kumar Mishra and Dipak Dutta. (Manuscript under preparation).
5. **Contribution of root associated zinc solubilizing *Pseudomonas aeruginosa* on plant Growth and translocation of zinc in Basmati rice variety.** Shohini Chakraborty; Biraj Sarkar; Rajesh Kumar Mishra; Dipak Dutta; Sukanta Majumdar (Under Communication).

ACKNOWLEDGEMENT

I want to dedicate my thesis to my parents and my family for having faith in me. I begin my thanks to almighty God giving strength and patience to complete the journey.

Firstly, I would like to express my sincere thanks to my mentor **Dr. Dipak Dutta** for his guidance and support. The unique part of him is he always has given me full freedom and space to work in lab because of that I could learnt a lot. He is an excellent mentor who know how to bring out best in a student and help them succeed. I am heartily thankful to him for tolerating me those years of Ph.D. I am indebted to him for his scientific inventiveness, analytical power, and trouble-shooting abilities, which always helped me during my entire Ph.D. tenure. I'd like to express my gratitude to him for believing in me and teaching me to have faith in myself. **Thank you, Sir**, for giving me the opportunity to join your research team and creating an invaluable space for me to do this research. Your words of confidence and encouragement were immensely important, especially during the seemingly tough moments. I am grateful for the freedom you have given me to forge my own path, as well as the guidance and support you have provided when needed. I admire everything you've done for me.

Beside my guide, I extend my thanks to **Dr, Sanjeev Khosla**, Director IMTECH, Former Director **Dr. Anil Koul** for providing such a nice facility to persue science. I am also thankful to **Dr. S. Karthikeyan, Dr. Charu Sharma, Dr. Balwinder singh** for coordinating IMTECH JNU Ph.D program. I extend my thank to Student's affair department for making process smooth. I am also thankful to my RAC members **Dr. Pradip Sen, Dr. Mani Shankar Bhattacharya**, and **Dr. Hemraj Nandanwar** for their valuable inputs in my study. I am thankful to CSIR-IMTECH facilities especially FACS and ITC. I am thankful to Deepak Bhat for taking care of sequencing facilities and appreciate his efforts during confocal training.

I extend my special thanks to my former lab senior **Dr. Vineet Kumar, Dr. Amit Bhardwaj** and **Dr. Gurusharan Kaur**. I have learnt so mant things from them to understand the physiology in *E. coli*. I especially thanks to Dr. Vineet for his patience and

having believe in me during our paper work. I always remember our scientific discussions which always gives me confident to learn new things and grasp it quickly.

I would like to thank hostel warden, **Dr. Dipak Sharma**, for creating an excellent atmosphere and facility in hostel. I am also thankful to hostel staff **Mrs. Mamta** and **Mr. Ganesh** for caretaking each and every facility related to hostel. I extend my thanks to mess workers for providing delicious food. I would like to appreciate HR Committee and MMC for their good works.

I am also thankful to technical staffs for their sincere work, especially **Mr. Ashok Rana** for taking care of instruments, **library staffs, BIC department, Canteen staffs, ESD, store and Purchase dept., Gardeners and Security guards** for being well organized and dedication for their works.

I always feels proud to be the part of DD lab. I am thankful for my lab members **Debarghya sir, Arunima, Kanika, Anand sir** for making lab environment healthy. I am thankful to **Debarghya sir** and **Arunima** for helping me during my experiments and data analysis. I especially thanks **Debarghya sir** for the trouble shooting and discussions. I am also thankful to my former lab juniors **Ankita** and **Sourav**. I wish them best of luck in future.

I especially thanks **Dr. Nirja** for always motivating and having faith in me during my tough times. I have learnt a lot from her and she has taught me how to be happy in bad situations. I am thankful to her for all the scientific inputs during HPLC experiments, We have so much scientific discusions during our paper work.

I literally don't have words to thank S.N.G.R.H. group. Sometimes your friends become your family and I am lucky to have them. **Dr. Harsh** (party singer and wicket keeper Batsman, Mahi mar rha hai), **Dr Gaurav** (a next level thinker, you can'tpredict him, some day you will find him on mars or moon), **Dr. Sumit** (Dukh harta, simple and clean hearted, Guitarist), **Hilal Bhai** (nice human being and a great philosopher, cold drink mat piya karo....), **Dr. Naushad**, (a well scripted person, rotlu but a true achiever).

I am really lucky to be the part of SB16 especially our cricket team. I especially thanks my batchmate **Manish, Happy, Rahul, Chubey, Sanpreet, Khadim, Manish** (All-rounder and dream11 game changer), **Nishant, Khadim, Sapna, Lucky, Puja, Megha, saloni, Jagrity, Raghavendra, Shukla**. We shared a lots of memory together. I especially thanks to **Gunjan, Sumeeta**, and **Gaurav** for being with me during my worst phase of my life. I am really sorry if I forgot any name. I am also thankful to my juniors especially **Radhe, Parth, Pravin, Shivani, Shweta, Sharmila Abhinit, Nisha, Nandita Ambar Bhawar, Ashish, Chankit, Mahesh, Braj, Sachin, Rinku, Kshitij, Shobit, Manna, Rajan, Pranaya** for helping me during experiments and other activities.

My sincere thanks to my Seniors, **Dr. Ajit, Dr. Prabhat, Dr. Kanti, Dr. Jeetu** with whom, I did plenty of parties and having lots of memories during SSBMT Tournament. I sincerely thanks **Praveen sir, Pandeyji, Mehta sir, Deepak Sir** for their love and support,

I would like to acknowledge my Harmonica Group BHOR. I am really happy to be part of it. I would like to thank **Robin Tah, Abhishekh da, Captain, Samiranda, Sanu, Matrika Uncle** and **Binayda** for their love and supports during these years. I love to acknowledge my friend **Raja, Sunny, Pradip, Arunda, Heera, Monojit, Chhotu** for their support and love.

I am very grateful to almighty god for blessing me with my family. My papa, who worked really hard to avail us all the needfuls throughout the life, My mother who always taught me how to go ahead in life. I am really lucky to have my elder brother **Mr. Prasenjit Kumar Mishra**, who had sacrificed a lot just to see me smiling. I love my Didi, jiju and Aadarsh for their love and support.

ABBREVIATION

%	Percent
°C	Degree Celsius
A ₄₅₀	Absorbance at 450nm
<i>B. subtilis</i>	<i>Bacillus subtilis</i>
Bp	Base pair
CaCl ₂	Calcium Chloride
Cam	Chloramphenicol
CMH	1-Hydroxy-3-methoxycarbonyl-2,2,5,5-tetramethylpyrrolidine
Da	Dalton
DETC	Diethyldithiocarbamate
DHE	Dihydroethidium
DMTU	Dimethyl thiourea
DNA	Deoxyribonucleic acids
DTNB	5,5'-dithio-bis-(2-nitrobenzoic acid)
<i>E. coli</i>	<i>Escherichia coli</i>
EDTA	Ethylenediamine-tetra-acetate
EPR	Electron paramagnetic resonance
Fe ²⁺	Ferrous
Fe ³⁺	Ferric
G	Gram

g/l	gram per litre
gDNA	Genomic/Chromosomal DNA
GSH	Reduced glutathione
GSSG	Oxidised glutathione
H2DCFDA	2',7' dichlorodihydrofluorescein diacetate
Hr	Hours
IPTG	Isopropyl β -D-1-thiogalactopyranoside
ISC	Iron sulfur cluster
K ₂ HPO ₄	Dipotassium hydrogen phosphate
Kan	Kanamycin
Kbp	Kilobase pairs
KCl	Potassium Chloride
kDa	Kilodalton
KH ₂ PO ₄	Potassium dihydrogen phosphate
L	Litre
M	Molar
mCi	Millicurie
MFI	Mean fluorescence intensity
Mg	Milligram
mg/ml	Milligram per millilitre
MgCl ₂	Magnesium Chloride

MgSO ₄	Magnesium Sulphate
Min/mins	Minutes
ml	Millilitre
mM	Millimolar
N	Normal
Na ₂ HPO ₄	Disodium hydrogen phosphate
NaCl	Sodium Chloride
NAD	Nicotinamide adenine di-nucleotide
NADP	Nicotinamide adenine di-nucleotide phosphate
NaH ₂ PO ₄	Sodium dihydrogen phosphate
NaOH	Sodium hydroxide
NBT	Nitro blue tetrazolium
NEB	New England Biolab Inc.
Ng	Nanogram
Ni-NTA	Nickel- Nitrilotriacetic acid
nM	Nanomolar
Nm	Nanometer
Nt	Nucleotides
OM	Outer membrane
ONPG	Ortho-nitrophenyl- β-galactoside
PAGE	Polyacrylamide gel electrophoresis

PAGE	Polyacrylamide Gel Electrophoresis
PAO	Polyamine oxidase
PBS	Phosphate buffer saline
PCR	Polymerase chain reaction
PCR	Polymerase Chain Reaction
PMSF	Phenylmethanesulphonyl fluoride
PPP	Pentose phosphate pathway
RNA	Ribonucleic acids
Rpm	Revolutions per minute
RT	Room temperature
<i>S. aureus</i>	<i>Staphylococcus aureus</i>
s/sec	Seconds
SDS	Sodium dodecyl sulfate
SDS	Sodium Dodecyl sulphate
SP	Sodium pyruvate
SSAT	Spermine/spermidine N1 acetyl transferase
TE	Tris-EDTA
Tris	Tris(hydroxymethyl)amino methane
TU	Thiourea
UA	Uric acid
V	Volt

W	Watt
Xg	times gravity
Mg	Microgram
$\mu\text{g/ml}$	Microgram per millilitre
MI	Microlitre

ABSTRACT

Spermidine is polycationic polyamine present in all life forms. Spermidine has shown to have a diverse array of functions in biological systems. They are essential for the growth and vitality of an organism. Plenty of studies have shown the positive aspect of spermidine function. But the study on toxicity caused by overaccumulation of spermidine still needs to be focused on. To address spermidine toxicity, we studied the effect of accumulated spermidine on the physiology of *E. coli*.

Chapter I is a review of literature where I tried to emphasize all the relevant literature regarding polyamine homeostasis and its functioning in both prokaryotes and eukaryotes. Since the previous study has emphasized the role of spermidine as an anti-ROS agent so I also have studied the relationship between spermidine and reactive oxygen species.

The Chapter II, we focused on spermidine toxicity and its impact on the redox state. For this study, we used a spermidine-sensitive *E. coli* strain. We have validated the previous studies that showed spermidine as an anti-ROS agent. However, our study showed, that instead of working as an anti-ROS agent, spermidine overaccumulation causes superoxide production that causes an imbalance of redox potential and also affects energy metabolism.

In Chapter III, we explored our microarray data to observe the impact of spermidine on transcriptional profile. To support and validate the microarray data we performed RT-qPCR. We further used different reporter constructs to justify microarray. Among the highly upregulated genes, we have chosen iron-sulfur cluster biogenesis to further study the effect of spermidine. We suspect spermidine which causes superoxide production, can dissolve Fe from the core of iron-sulfur cluster protein hence causing its inactivation.

In Chapter IV, our study focused on the impact of spermidine on metal homeostasis. We have shown that spermidine stress affected Fe homeostasis. We found that spermidine can directly interact with Fe. Interaction of 13 molecules of Fe^{2+} to 10 molecules of spermidine causes oxidation of the former and produces 13 molecules of O_2^- a molecule in aerobic conditions.

CHAPTER-I

INTRODUCTION AND LITERATURE REVIEW

1.1. Overview of polyamines

Polyamines are polycationic compounds present in eukaryotes, bacteria, and archaea. They are required for cell growth and proliferation. At physiological pH, nearly all polyamines found in nature are linear and flexible aliphatic chains with two or more positively charged amine groups. Cadaverine, putrescine, and spermidine are the major polyamines found in almost all life forms. Additionally, higher Eukaryotes synthesize spermine as well. Gram-negative bacteria are known to synthesize the majority of polyamines whereas Gram-positive bacteria had substantially lower polyamine concentrations and in fact, are deprived of detectable polyamines. Additionally, numerous yeasts are also known to have spermidine and spermine in trace amounts (Tabor and Tabor, 1984a). Cadaverine, putrescine, and spermidine are three major polyamines in *E. coli*. Putrescine and spermidine had intracellular concentrations of 10-30mM and 1-3 mM, respectively, in *E. coli* (Shah and Swiatlo, 2008). Cadaverine is least prevalent of all naturally occurring bacterial polyamines and is normally absent in *E. coli*. In contrast, cadaverine can be synthesised by *E. coli* during anaerobic growth when the organism is exposed to low pH or when putrescine biosynthesis is inhibited (Shah and Swiatlo, 2008).

Polyamines affect a wide variety of biological processes (Figure 1.2), including nucleic acid and protein metabolism, ion channel function, cell growth, and differentiation, mitochondrial activity, autophagy, aging, antioxidant defense, and actin polymerization (Casero et al., 2018; Gawlitta et al., 1981; Madeo et al., 2018; Miller-Fleming et al., 2015; Oriol and Audit, 1978). Cationic amine groups exhibit a strong affinity for negatively charged molecules such as RNA, DNA, and phospholipids (Igarashi and Kashiwagi, 2000; Miyamoto et al., 1993; Schuber, 1989; Tabor and Tabor, 1984a). Polyamine, especially spermidine has been shown to play a vital role in the “Central dogma of Life” and is also known to stimulate DNA replication and replication fork movement (Geiger and Morris, 1980). Furthermore, polyamines are known to prevent open circle plasmid DNA formation and thereby suggesting their role in protecting DNA from damage. Polyamines have been reported to protect DNA against reactive oxygen species (ROS) such as singlet oxygen, hydroxyl radicals ($\bullet\text{OH}$), and hydrogen peroxide (H_2O_2) (Balasundaram et al., 1993; Casero et

al., 2018; Ha et al., 1998a, 1998b; Jung and Kim, 2003; Khan et al., 1992a, 1992b; Pegg, 2018). Indeed, knocking out polyamine biosynthesis enzymes from *E. coli* and yeast confers toxicity to oxygen, superoxide anion radical (O_2^-), and H_2O_2 (Balasundaram et al., 1993; Chattopadhyay et al., 2003a, 2006a; Eisenberg et al., 2009). Polyamines induce the synthesis of several different proteins necessary for cell growth and viability by altering the structure of certain messenger RNAs. eIF5A is the only protein known to contain a spermidine derivative, i.e. hypusine, operates at the translational level as well (Igarashi and Kashiwagi, 2019). Spermidine along with Mg^{2+} has a great role in assembling different subunits of ribosomal complexes, which otherwise can dissociate. (Igarashi and Kashiwagi, 2000). Additionally, polyamines enhance ribosomal fidelity during polypeptide synthesis (Igarashi and Kashiwagi, 2019; Jelenc and Kurland, 1979). Polyamines also help in the assembly of 30S ribosomal subunits (Igarashi et al., 1981). Polyamines promote the synthesis of OppA, an oligopeptide uptake system and periplasmic substrate-binding protein. Additionally, polyamines indirectly enhances the mRNA synthesis of at least 58 genes by translational activation of CyaA (adenylate cyclase), RpoS, FecI, and Fis. There is a positive link between the build-up of polyamines and polyphosphates (Motomura and Tomota, 2006; Oves-Costales et al., 2007) where polyphosphates provide energy and function as a buffer against alkaline conditions (Pick et al., 1990). Since polyamines are so basic, they can be critical for bacterial survival in the acidic environment of the gastrointestinal tract. (Chattopadhyay and Tabor, 2013; Chattopadhyay et al., 2015).

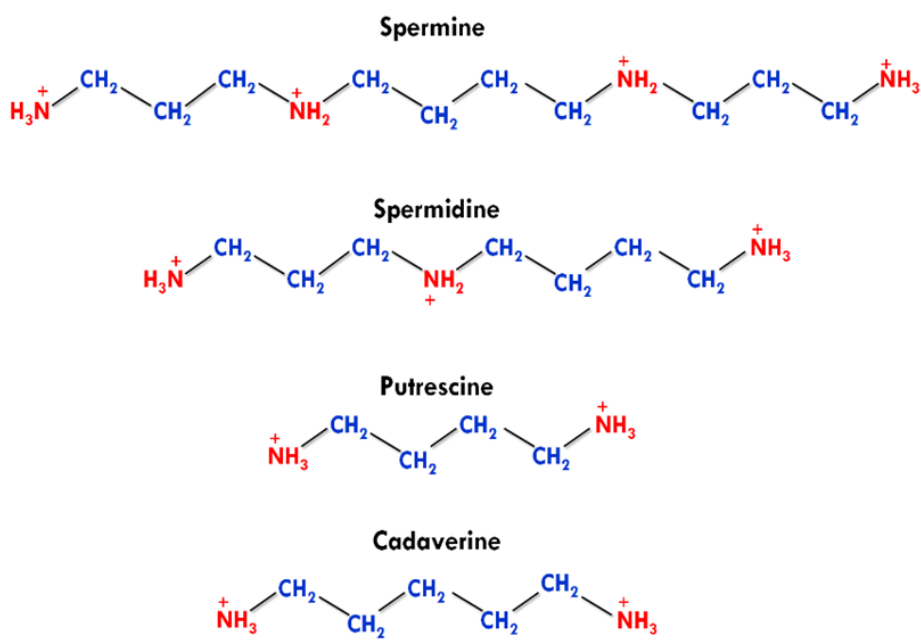


Figure 1.1. Structures of different natural polyamines. (Adopted from Sagar et al., 2021).

Internal Polyamine level in humans may be accomplished in three ways: through intestinal bacteria, endogenous production, and dietary supply (exogenous). These systems control intracellular PA levels by regulating synthesis, catabolism, and transport concomitantly. However, the exogenous diet provides the maximum quantity of PAs than the process of endogenous biosynthesis. Dietary polyamines play a crucial role in maintaining the PAs inside the body because malfunctioning the PA biosynthesis can lower its level inside the cell which may lead to several health disorders (Buyukuslu, 2015). Various food items contain the required amounts of polyamines i.e., plant-derived foods have mostly Putrescene and Spermidine, and meat products mainly contain Spermine, while dairy products are rich in spermidine and putrescene (Buyukuslu, 2015). Several studies have estimated the mean intake value of Polyamines and the suggested daily dietary intake of it is varied from 250 to 700 μmol (Buyukuslu, 2015; Buyukuslu et al., 2014; Nishibori et al., 2007). A controlled diet, solely or with clinical applications, can be used as an effective treatment against various cancer, cardiovascular diseases, Huntington's disease, Alzheimer's disease, and Parkinson's disease (Sagar et al., 2021). Spermidine supplementation has proved to be beneficial in cardiovascular diseases by promoting autophagy. Polyamines (spermine and spermidine) promote the proliferation and maturation of the gastrointestinal tract and are involved in the differentiation and development of the immune system (Atiya Ali et al., 2014; Buts et al., 1995; Gómez-Gallego et al., 2017; Löser, 2000; Pérez-Cano et al., 2010; Plaza-Zamora et al., 2005; Romain et al., 1992; Sabater-Molina et al., 2009). In addition, due to their antioxidant properties, polyamines can participate in the regulation of the inflammatory response (Kalač, 2014; Soda, 2010).

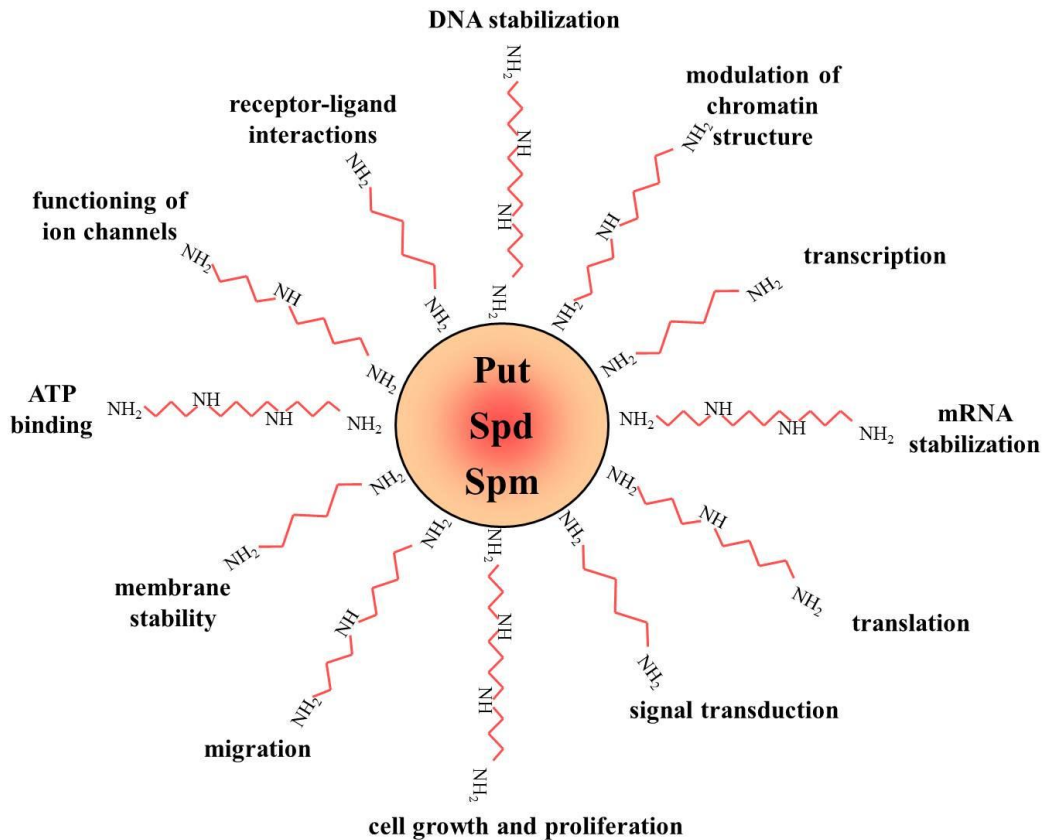


Figure 1.2. Physiological and molecular Function of polyamine in *E. coli*. (Adopted from Kahana’s lab page, Weizmann Institute of Science)

1.2. Biosynthesis and Metabolism of polyamine

Polyamine biosynthesis in *E. coli* involves a cascade of events involving a variety of gene products (Figure 1.3). Putrescine is synthesized through two distinct decarboxylation mechanisms. Arginine decarboxylase (encoded by the *speA* gene) decarboxylates arginine to agmatine in one mechanism. The agmatine ureohydrolase enzyme then converts it to putrescine and urea (encoded by *speB* gene). The second decarboxylation pathway is mediated by ornithine decarboxylase (encoded by the *speC* gene), which catalyzes the conversion of ornithine to putrescine directly (Keseler et al., 2013a; Tabor and Tabor, 1985). In *E. coli*, spermidine biosynthesis is carried out by spermidine synthase (encoded by the *speE* gene), which uses putrescine as a substrate and decarboxylated S-adenosyl methionine as a cofactor (Figure 1.3). SAM-decarboxylase synthesizes decarboxylated S-adenosyl methionine (SAM) from S-adenosyl-methionine (encoded by *speD* gene) (Keseler et al., 2013b).

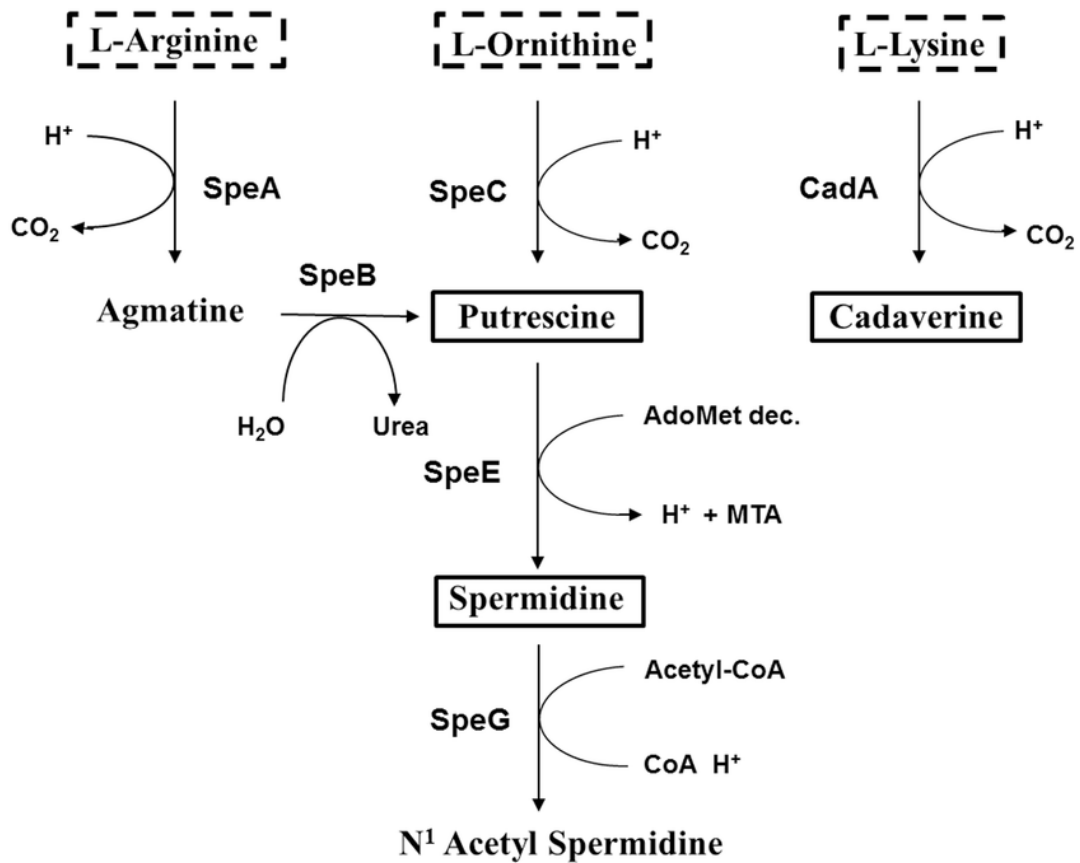


Figure 1.3. Biosynthetic pathways for polyamines in *E. coli*. Cadaverine synthesis occurs predominantly when lysine is abundant in the growth medium or putrescine synthesis is blocked. SpeA – arginine decarboxylase, SpeB – agmatine ureohydrolase, SpeC – ornithine decarboxylase, SpeD – SAM decarboxylase, SpeE – spermidine synthase, MetK – methionine adenosyltransferase, CadA – lysine decarboxylase. (Adopted from Campilongo et al., 2014).

1.3. Polyamine homeostasis

Despite their importance as cellular entities, excess polyamines have a detrimental influence on a variety of cellular activities. Spermidine at higher concentrations causes growth retardation in *E. coli* and impairs the function of the cytoplasmic membrane (Bachrach and Cohen, 1961). As a result, *E. coli* maintains polyamine levels in three distinct ways: through polyamine synthesis, transport, and polyamine modification for destruction or inactivation. To maintain optimal polyamine production, *E. coli* modifies the amounts of ornithine decarboxylase, arginine decarboxylase, and SAM decarboxylase (Kashiwagi and Igarashi, 1988; Morris and Fillingame, 1974; Shah and Swiatlo, 2008; Wright et al., 1986). Polyamine transport is facilitated by the *E. coli* pot operon PotABCD which forms a spermidine-specific transport mechanism that imports spermidine at the expense of ATP

hydrolysis (Fukuchi et al., 1995; Igarashi and Kashiwagi, 1999; Miyamoto et al., 1993). The putrescine-specific transport system is comprised of PotFGHI, which is responsible for bringing putrescine into the cell via ATP hydrolysis (Pistocchi et al., 1993). For a long time, the outflow of polyamines was unknown but later on

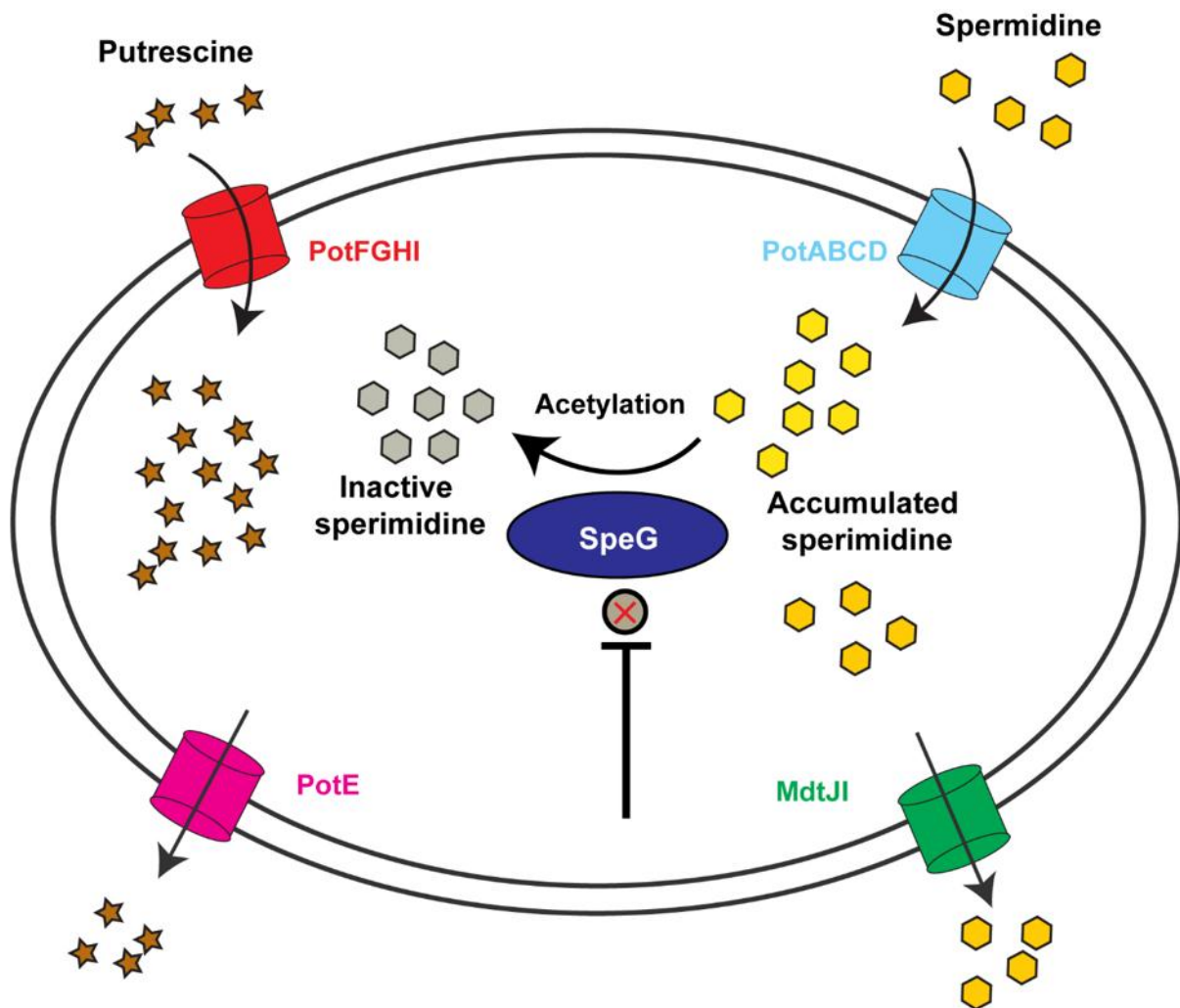


Figure 1.4. Regulation of Polyamines in *E. coli*. PotFGHI and Pot ABCD imports putrescine and spermidine, respectively. Accumulated putrescine either exports via potE exporter or gets converted to spermidine. There are two fates of accumulated spermidine in this regulation i.e., either it gets exported via MdtJI exporter or gets deactivated by N- acetyl transferase, an enzyme encoded by *speG*. Blocking of SpeG causes accumulation of active spermidine inside the cell.

MdtJI and PotE were identified as the exporters of spermidine and putrescine, respectively (Higashi et al., 2008; Miyamoto et al., 1993; Schiller et al., 2000). If the level of polyamine in the cell increases, the cell recovers the functioning level of polyamine through

chemical inactivation or destruction. Acetylation is required for the chemical inactivation of spermidine and putrescine, while oxidation is used to break down putrescine and spermine (Igarashi and Kashiwagi, 1999; Rabellotti et al., 1998). Spermidine N (1)-acetyltransferase from *E. coli* acetylates spermidine at the N1 and N8 sites (Fukuchi et al., 1994). As a result, deletion of the spermidine N-acetyltransferase gene (*speG*) in *E. coli* results in spermidine hypersensitivity. Acetylation of spermidine is critical for the cell's polyamine turnover. However, the effect of acetylation on polyamine turnover is not well understood.

While the majority of prokaryotes, including *E. coli*, produce cadaverine, putrescine, and spermidine, higher eukaryotes also synthesize spermine. Additionally, *E. coli* acquires spermidine and putrescine from its environment (Igarashi and Kashiwagi, 2000; Miller-Fleming et al., 2015). Higher polyamines, spermidine, and spermine, are converted back to putrescine in the Eukaryotic system, however, this is not the case in *E. coli* (Figure 1.4.). The cytosolic spermidine/spermine N1-acetyltransferase (SSAT) is the rate-limiting enzyme in polyamine catabolism. SSAT acetylates spermine and spermidine, and the acetylated spermine and spermidine subsequently enter the peroxisome, where they are oxidised by polyamine oxidase (PAO) and produce acetaminopropanal as byproducts of this oxidation (Figure 1.5). To produce putrescine from spermidine, SSAT must be present. In the cytoplasm, an enzyme called spermine oxidase (SMO) can turn spermine back into spermidine. SMO prefers spermine to its acetylated counterpart, acetyl-spermine, whereas PAO favors acetyl-spermine. (Madeo et al., 2018).

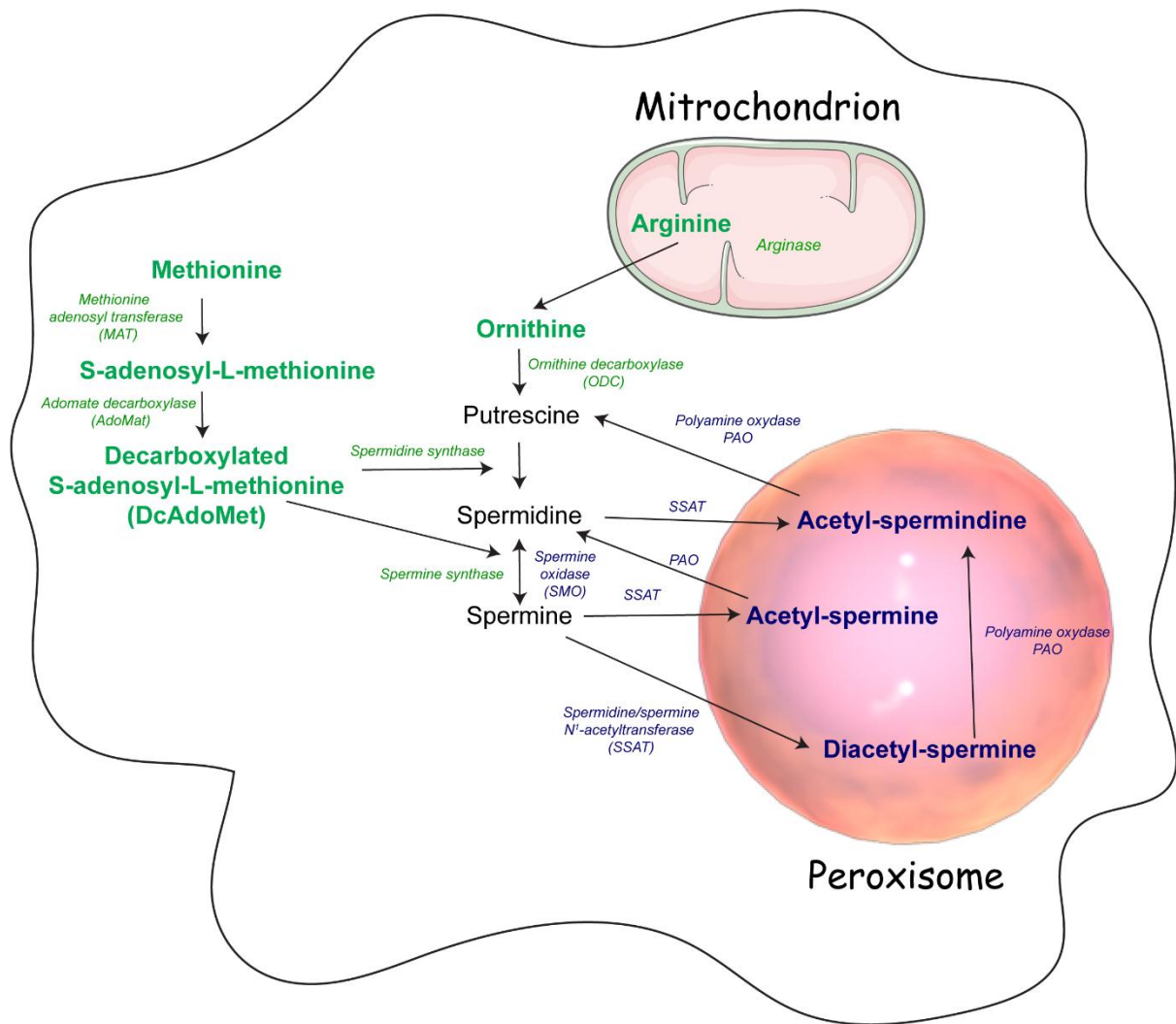


Figure 1.5. Polyamine metabolism in Eukaryotes. Green shows biosynthesis; blue is showing catabolism; black: Synthesis of polyamine (Adapted from Minois et al., 2011).

1.4. Reactive oxygen species and oxidative stress

ROS are required in small amounts for cellular growth and signaling. An imbalance between ROS formation and its neutralization can lead to oxidative stress. ROS are normally generated as by-products of oxygen metabolism, but environmental stress factors (i.e., UV, ionizing radiations, pollutants, and heavy metals) and xenobiotics (i.e., anticlastic drugs) greatly increases ROS production that leads to cell and tissue damage. O₂ diffuses across biological membranes as readily as water does because it is hydrophobic. Hence it is very difficult for the cells to respire rapidly enough to drop the internal oxygen concentration as that of the external environment. In anaerobic microhabitats, certain bacteria can avoid

oxidative stress, while others must deal with intracellular molecular oxygen. For example, obligate anaerobes are unable to tolerate even minute quantities of oxygen as compared to aerobes that survive well in oxygen-rich environments where as, microaerophiles thrive on a very small amount (few micromolar) of oxygen. The oxygen concentrations above their natural environments have a negative impact on the development, mutagenesis, and even mortality of most of these microorganisms. *E. coli*, a facultative anaerobe, fits this description as well. O₂ is a reactive chemical that oxidizes other molecules. According to Molecular-orbital rules, molecular oxygen accepts electrons singly, not in pairs. This restriction prevents oxygen from oxidizing organic biomolecules but allows it to oxidize transition metals, which are good univalent electron donors.

1.4.1. Intracellular ROS production

Molecular oxygen (O₂) has an even number of electrons; the two outermost orbital electrons are arranged in discrete orbitals as unpaired and spin-aligned electrons. This arrangement allows them to accept one electron at a time. Due to its slightly negative (-0.16) univalent reduction potential, O₂ has a low affinity for the first electron and can only accept electrons from good univalent electron donors, such as metal centres, flavins, and respiration quinones. The flavins of dehydrogenases were shown to be the principal sources of O₂ and H₂O₂ (Kusssmaul and Hirst, 2006; Messner and Imlay, 1999). H₂O₂ is produced at a high rate even in mutants lacking respiratory enzymes, effectuating researchers to conclude that O₂ and H₂O₂ are mostly formed by the accidental autoxidation of non-respiratory flavoproteins (Korshunov and Imlay, 2010; Seaver and Imlay, 2004). Flavoproteins such as glutathione reductase, lipoamide dehydrogenase, and glutamate synthetase have been shown to generate ROS in vitro, and they are ubiquitous throughout metabolism (Massey et al., 1969). Oxidation of flavoprotein in dihydroflavin results in flavosemiquinone and O₂⁻ via electron transport chain (Figure 1.6B). Most of the time, a second electron transfer happens before O₂⁻ can leave the active site and enter the bulk solution, resulting in H₂O₂ production. As a result, these enzymes are likely responsible for the generation of both O₂⁻ and H₂O₂. Autoxidation of flavin enzymes depends on molecular oxygen exposure, midpoint potential, and electron residence time (Messner and Imlay, 1999). Consequently, ROS stress is likely related to the concentrations of the cell's most autoxidizable enzymes. Facultative and obligate anaerobic bacteria enter aerobic environments with high levels of O₂⁻ produced by fumarate reductase, an abundant anaerobic respiratory enzyme that interacts extremely

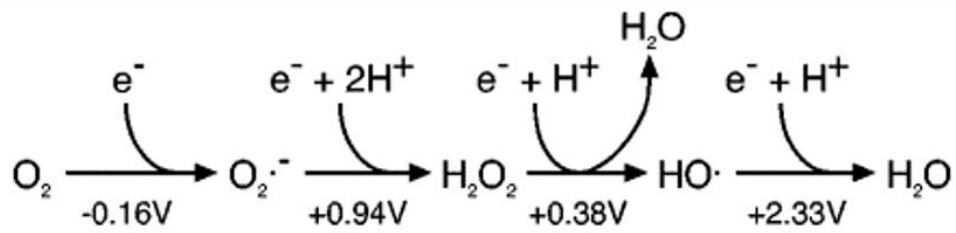
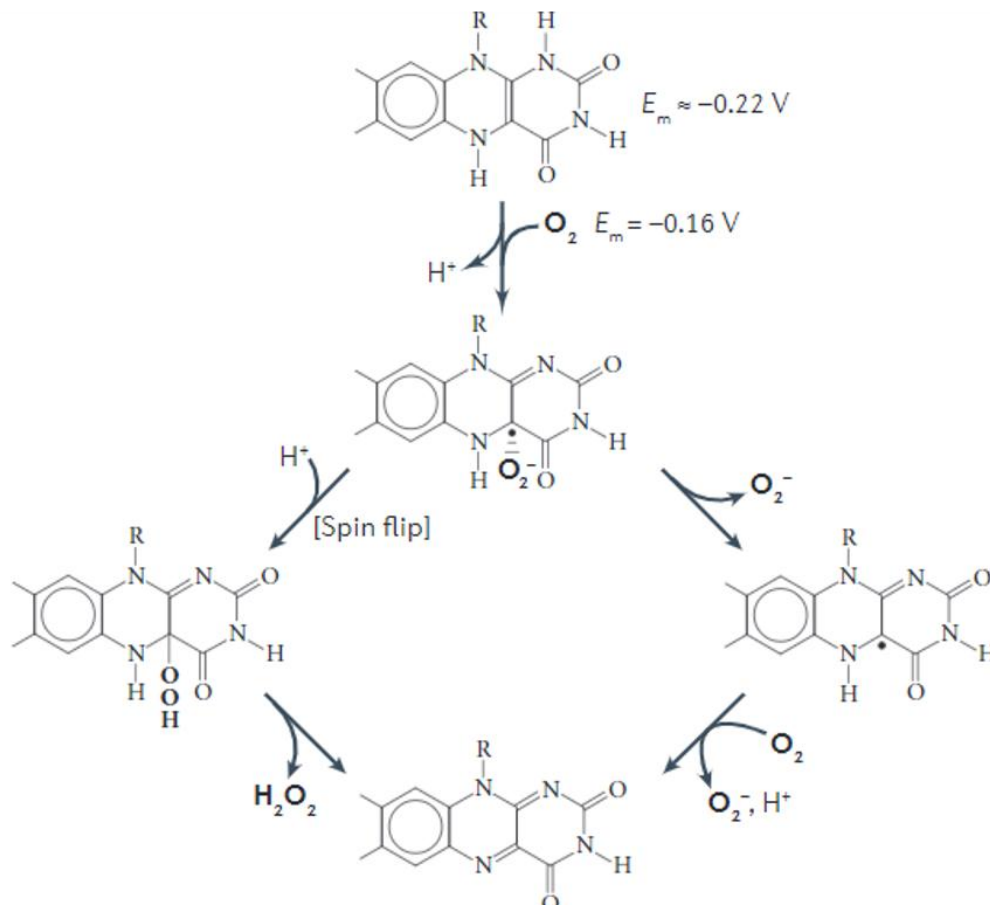
A.**B.**

Figure 1. 6. Common ROS production in *E. coli*. **A.** Reduction potential of Oxygen molecule; $\text{O}_2^{\cdot-}$, H_2O_2 , and $\text{HO}\cdot$ all have standard reduction potentials except for O_2 , these chemicals are potentially powerful univalent oxidants. **B.** Two pathways of flavoprotein produce $\text{O}_2^{\cdot-}$, and H_2O_2 Enzymatic flavins have univalent reduction potentials as low as O_2 , allowing autoxidation. Flavosemiquinone or $\text{O}_2^{\cdot-}$ must flip an electron spin to facilitate H_2O_2 release (left route). The right route yields two $\text{O}_2^{\cdot-}$ molecules. Most enzymes investigated to use the left route. (Adopted from Imlay, 2013).

quickly with oxygen (Imlay, 1995). For hyperoxia to be hazardous, there must be an increase in ROS production since the rate of enzyme autoxidation is likewise dependent on collision frequency (Seaver and Imlay, 2004). Menaquinone (the low-potential electron carrier in *E.*

coli respiratory chain) autoxidation contributes to a small fraction of ROS formation (Korshunov and Imlay, 2006). It autoxidizes in proportion to the oxygen content just as redox enzymes.

Apart from cytoplasmic O_2^- , *E. coli* also can synthesize a periplasmic copper-zinc superoxide dismutase (SOD) that is encoded by *sodC* (Benov and Fridovich, 1999). *sodC* mutant in *E. coli* shows a significant phenotypic defect which indicates that superoxide in the periplasm is harmful (Gordon, 2008). The release of O_2^- in periplasmic space depends upon the oxidation of menaquinone (Kóňa and Brinck, 2006). The rate of periplasmic superoxide formation (3 $\mu\text{M/s}$) is almost equal to cytoplasmic O_2^- formation (5 $\mu\text{M/s}$). When pathogenic bacteria are subjected to O_2 fluxes from the phagocytic NADPH oxidase, periplasmic O_2^- stress may be even larger. This is the reason why *Salmonella* species produce more SodC isozymes to maintain their full virulence.

1.4.2. Damage due to O_2^-

O_2^- works either as a weak univalent reductant or a stronger univalent oxidant. There hasn't been a single report that claims any damage to the biomolecules by O_2^- so far (Beyer and Fridovich, 1987; Farr et al., 1986; Figueroa-Bossi and Bossi, 1999; Sakai et al., 2006). O_2^- doesn't react with nucleic acids and *in vitro*. Recent studies reveal that they may oxidize short-chain sugars (Nnyepi et al., 2007). These observations raised questions concerning the biological importance of O_2^- and the role of SOD. Carlos and Touati created *E. coli* mutants without manganese (Mn) and iron (Fe) cofactor MnSOD and FeSOD (Canvin et al., 1996). These mutants grow well in oxygen-free medium but poorly in oxygen. They were complemented by the mammalian copper-zinc SOD (Napolitano et al., 2000), which confirmed that the abnormalities were caused by a deficiency in O_2^- dismutation.

1.4.2.1. Damage to Fe-S clusters

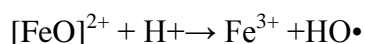
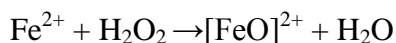
SOD mutants cannot synthesize branched-chain amino acids such as leucine, isoleucine, and valine as O_2^- inactivates dihydroxy acid dehydratase, an enzyme required in branched-chain synthesis (Figueroa-Bossi and Bossi, 1999; Krishnakumar et al., 2004). Catabolic metabolization in the citric acid cycle is defected due to the damage of Aconitase and Fumerase enzyme, which belongs to the family of dehydratase having (4Fe-4S) cluster (Liochev and Fridovich, 1992; Wilmes-Riesenberg et al., 1996). Apart from these enzymes, other metabolic enzymes of the same family such as serine dehydratase, threonine deaminase, isopropyl malate isomerase, and 6-phosphogluconate dehydratase are also getting affected by

O_2^- . Each enzyme's exposed Fe atom acts as a Lewis acid, binding to the substrate and removing the hydroxide anion from it during the reaction (Kusssmaul and Hirst, 2006). O_2^- may bind to Fe and form complexes with it. When the cluster is protonated, H_2O_2 and an oxidised $[4Fe-4S]^{3+}$ cluster can be generated. Fe^{2+} is liberated from the cluster during hydrolysis, and this results in an inactive $[3Fe-4S]^+$ cluster (Figure 1.6). It has been calculated that the O_2^- concentration in aerobic *E. coli* is 10^{-10} M, implying that the half-life of a dehydratase would be 30 minutes or less (González-Flecha and Demple, 1999). Furthermore, cells constantly reactivate damaged clusters, ensuring an active enzyme pool in aerobic wild-type cells. The enzymes that include Fe-S buried in polypeptides such as respiratory dehydrogenase and other electron transport enzymes are not harmed by O_2^- . Destruction of dehydratase clusters indirectly contributes to the high mutation rate in SOD mutant cells. The "free" (unincorporated) Fe in cells is large in SOD mutants due to the constant release of Fe from their clusters. Nucleic acids may attach to some of the lost Fe by accident and further interacts with H_2O_2 which causes damage to the nucleic acid.

Mutants with reduced levels of SOD are unable to utilize sulfate as their primary supply of sulfur. This phenotype's remains a mystery. In SOD mutants, the Transketolase enzyme which is responsible for the biosynthesis of the aromatic compound is also getting inactivated.

1.4.3. Damage caused by H_2O_2

H_2O_2 is not a radical species, and in principle, it can operate either as a univalent or divalent oxidant. In both circumstances, however, the dioxygen pair must be cleaved and despite the overall thermodynamic driving force, this bond-breaking step imposes high energy of activation that makes H_2O_2 inert towards most biomolecules. In the cellular environment, H_2O_2 can be univalent and reduces Fe^{2+} ions to generate a harmful $\bullet OH$ and Fe^{3+} ion via the Fenton reaction.



After releasing from the complex, the $\bullet OH$, becomes a potent oxidant ($E_o' = +2.3$ V; Fig. 1.7) that reacts at diffusion-limited speeds (10^8 to 10^{10} $M^{-1} s^{-1}$) with most organic molecules (D'Orazio et al., 2008). Unlike O_2^- and H_2O_2 that oxidize the catalytic Fe atom of dehydratase clusters, causing Fe^{3+} loss and enzyme deactivation, $\bullet OH$ could degrade active-site residues of these enzymes. Fe can be used to restore enzyme activity after H_2O_2

inactivates them in vitro. As a result, before the ferryl radical ($[\text{FeO}]^{2+}$) can decompose into the harmless hydroxide anion (OH^-), it removes another electron from the cluster (Figure 1.6), thus making the radical harmless (Jang and Imlay, 2007a).

1.4.3.1. Damage to Fe-S cluster

An oxidation of the [4Fe-4S] clusters of dehydratase enzymes involved in cellular metabolic pathways such as the TCA cycle, pentose phosphate pathway, and other branched biosynthesis causes their inactivation (Imlay, 2013). Solvent-exposed Fe atoms in these clusters bind substrate directly, deprotonating it and then abstracting a hydroxide anion. H_2O_2 can oxidize the exposed Fe atom to an unstable $[\text{4Fe-4S}]^{3+}$ state (Figure 1.7). This valence is unstable, and the cluster soon disintegrates into a $[\text{3Fe-4S}]^+$ form that lacks the catalytic, solvent-exposed Fe atom. In this action, the $\bullet\text{OH}$ pulls a second electron from the Fe-S cluster, releasing a hydroxide anion, (rather than a $\bullet\text{OH}$) into the active site, and hence polypeptide oxidation is avoided. The steady-state activity of these enzymes reflects the balance between oxidation and repair rates (Jang and Imlay, 2007). Dissociation of metal from the active site causes loss of activity of these enzymes. A little amount i.e., $0.5 \mu\text{M}$ H_2O_2 is enough to harm cells, hence the concentration of scavenging enzymes is calibrated to keep H_2O_2 below this threshold level. Unlike O_2^- , H_2O_2 are nonpolar and uncharged molecule which can easily get diffuse the membrane, hence it is getting more difficult for bacteria to survive in an H_2O_2 -rich environment. Most bacteria maintain inducible defensive regulons regulated by OxyR or PerR transcription factors.

1.4.3.2. Damage to DNA

E. coli cells develop into long filaments after exposure to H_2O_2 , showing DNA damage that limits replication. The hypothesis is that certain free Fe atoms bond to nucleic acids and create $\bullet\text{OH}$ on the DNA surface when exposed to H_2O_2 (Poole, 2005). An electron can be removed from the ribose moiety by a $\bullet\text{OH}$, which results in the formation of a ribosyl radical and the addition of molecular oxygen leads to strand breakage

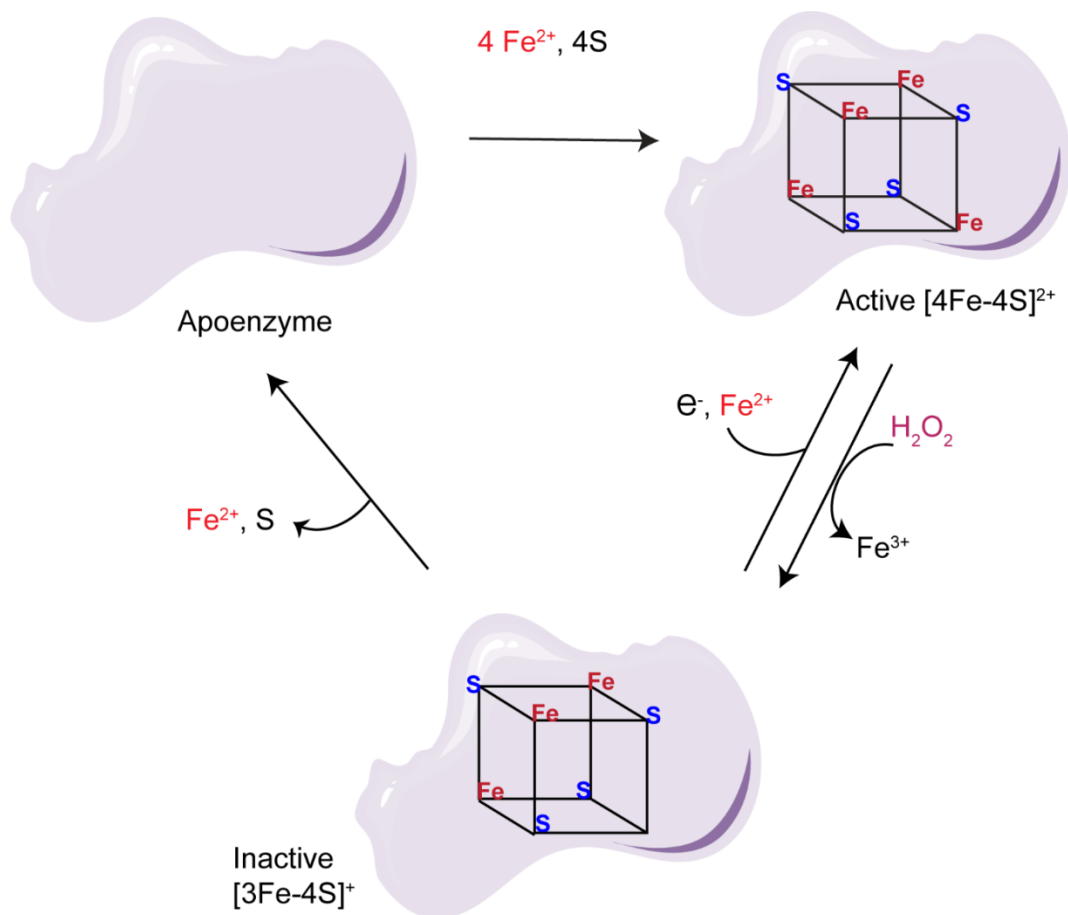


Figure 1. 7. The damage that H_2O_2 does to $[\text{4Fe-4S}]^{2+}$ cluster enzymes. The dehydratase enzyme's catalytic Fe atom reacts with H_2O_2 and breaks apart, leaving behind an inactive $[\text{3Fe-4S}]^+$ cluster. By reducing and metalizing that cluster, it can be made to work again. In some dehydratases, the cluster breaks apart completely to make an apoenzyme. OxyR induces the Suf system to restore the holoenzyme.

(Ding and Demple, 1997; Horsburgh et al., 2002). Many different adducts can be produced when $\bullet\text{OH}$ remove electrons from DNA bases. DNA oxidation produces an unusual amount of 8-hydroxyguanine, which is formed when an electron tunnels from the low-potential guanine to a neighbouring base radical and converts the original radical to a normal base.

1.4.4. Regulatory response to oxidative stress

Bacteria are unable to regulate their surroundings, thus they have developed robust transcriptional responses to protect themselves from external threats. Enteric bacteria rapidly make transition from anaerobic to fully aerobic environments, necessitate inducible antioxidant systems that may be activated and deactivated according to the environmental

condition. The SoxRS and OxyR systems, found in *E. coli* and *Salmonella*, provide two archetypal examples of oxidative stress responses.

1.4.4.1. The SoxRS system

Bacteria contain transcriptional regulators that can detect ROS redox signals and control antioxidant systems (Lushchak and Storey, 2021). SoxRS regulates O_2^- and redox-cycling molecules (Figure 1.8B, but not H_2O_2 (Gu and Imlay, 2011a)). SoxR is a homodimer whose activity relies on its oxidation state (Hidalgo et al., 1997). After sensing O_2^- , SoxR induces the transcription of *soxS* gene. SoxS, in turn, promotes more than 100 genes involved in antioxidant defense, damage repair, and cell metabolism (Nunoshiba et al., 1992; Wu and Weiss, 1992). SoxS regulates *sodA*, *nfo*, *zwf*, *fumC*, *acnA*, *fur*, and *ntrA* (González-Flecha and Demple, 2000; Pomposiello et al., 2003; Touati, 2000). During oxidative stress, *rseC* and *rsxABCDGE* inactivates SoxR and decreases its concentration inside the cell by inhibiting SoxRS activation (Koo et al., 2003). As the oxidative stress diminishes, SoxS gets degraded by proteolysis. Apart from *E. coli*, Actinobacteria and Proteobacteria also have SoxR. In non-enteric bacteria such as *Pseudomonas aeruginosa* or *Streptomyces coelicolor*, SoxS is absent. SoxR directly activates in response to redox-cycling agents (Chiang and Schellhorn, 2012; Fujikawa et al., 2017; Mettert and Kiley, 2015).

Table 1.1 Genes controlled by SoxRS system

Gene (s)	Product
<i>Soda</i>	Mn-dependent O_2^- dismutase
<i>Nfo</i>	Endonuclease IV
<i>Fur</i>	Fe regulatory protein
<i>Zwf</i>	Glucose-6- phosphate dehydrogenase
<i>Fpr</i>	NADPH:flavodoxin oxidoreductase
<i>fldA</i>	Flavodoxin A
<i>fldB</i>	Flavodoxin B
<i>acrAB</i>	Drug efflux pump
<i>tolC</i>	Outer membrane component of efflux pump
<i>micF</i>	Antisense RNA to OmpF porin
<i>nfsA</i>	NADPH nitroreductase
<i>nfnB</i>	Dihydropteridine reductase
<i>rimK</i>	Modification of ribosomal protein S6
<i>ribA</i>	cGMP hydrolase
<i>mdaB</i>	NADPH quinone reductase

1.4.4.2. OxyR system

The OxyR system is critical in the detection and maintenance of the organism's cellular H₂O₂ levels. OxyR is a transcriptional regulator of the LysR family, present in most Gram-negative bacteria, but it has also been detected in Gram-positive bacteria such as *S. aureus* and *S. coelicolor* (Morikawa et al., 2006). After sensing H₂O₂, OxyR gets oxidised and becomes active. OxyR is a tetramer that binds to target genes' 5' promoter regions (Figure 1.8) via a conserved sequence pattern (González-Flecha & Demple, 1999). In *E. coli*, the OxyR regulates more than 20 different gene. H₂O₂ involved in several molecular mechanisms of adaptive response to redox stress, such as detoxification by activating *katE* and *ahpCF*, it also activates heme biosynthesis genes (*hemH*), redox state maintaining genes such as *grxA*, *gorA*, and *trxC*. OxyR also stimulates the production of OxyS, a short regulatory RNA that induces in response to peroxide stress (González-Flecha & Demple, 1999). This sRNA appears to play a role in the protection against H₂O₂-induced mutagenesis (Altuvia et al., 1997). Furthermore, OxyS depletion has been shown to result in much higher levels of H₂O₂ in *E. coli* (González-Flecha & Demple, 1999). OxyR detects H₂O₂ levels via specific cysteine residue (C199). The peroxide molecule interacts with the thiol group on C199, establishing an intramolecular disulfide bond and causing conformational changes that modify OxyR's DNA binding properties, allowing efficient interaction with RNA polymerase. Under normal conditions, OxyR exists in its reduced form whereas an increased H₂O₂ level causes OxyR to oxidize quickly: This chemical process is then reversed through feedback regulation, as oxidized OxyR increases the expression of the *grxA* and *gor* genes, which encode glutaredoxin 1 and glutathione reductase, respectively, both of which function to reduce OxyR. OxyR system has been studied primarily in *E. coli*, later it has been seen in other bacteria that have evolved to adapt their specific OxyR regulon to better suit their environmental niches: they may differ in the molecular mechanism of H₂O₂ regulation and the number of OxyR homologs, or the type of genes present in their regulon.

Table 1.2 Genes controlled by OxyR system

Gene (s)	Product
<i>katG</i>	Catalase (HPI)
<i>ahpCF</i>	NADH peroxidase (alkylhydroperoxide reductase)
<i>dps</i>	Fe-storage protein
<i>Fur</i>	Fe regulatory protein
<i>sufABCDSE</i>	Fe-S cluster assembly system
<i>mntH</i>	ISC importer
<i>hemH</i>	Ferrochetalase
<i>trxC</i>	Thioredoxin C
<i>grxA</i>	Glutaredoxin
<i>gor</i>	Glutathione reductase
<i>dsbG</i>	Periplasmic disulfide isomerase
<i>oxyS</i>	Small regulatory RNA

A.

B.

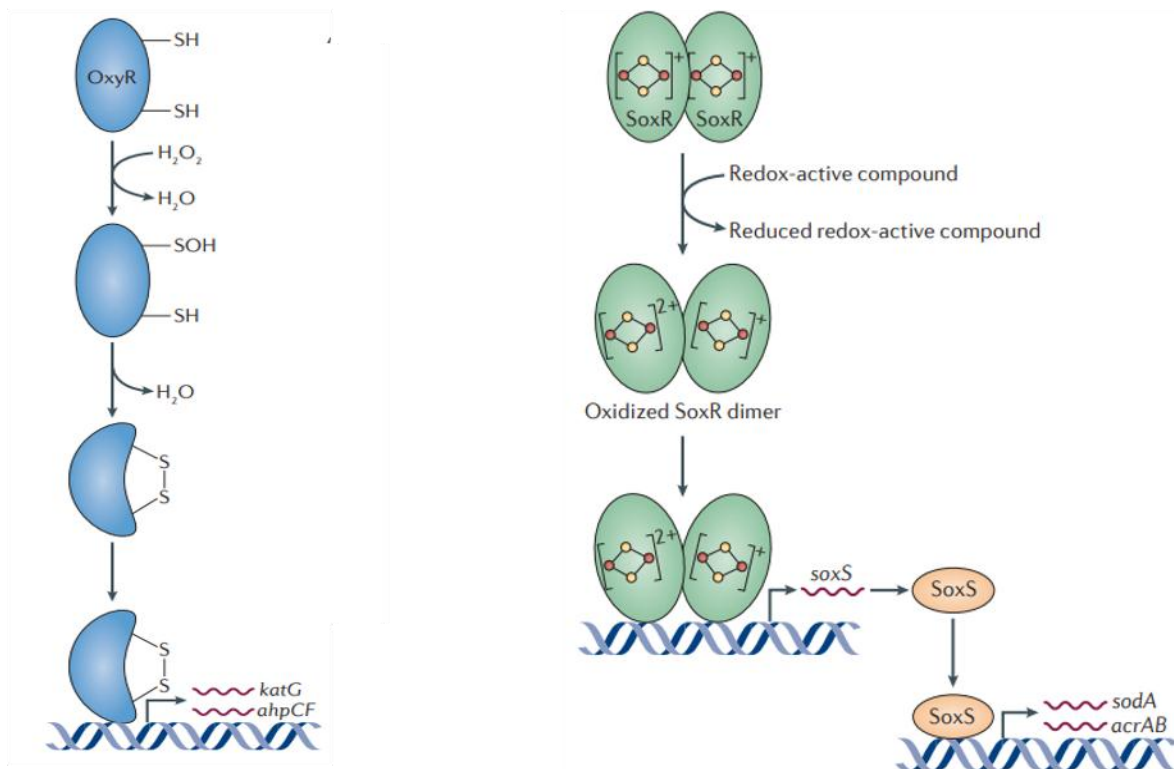


Figure 1. 8. *Escherichia coli* transcriptional regulator activation. The OxyR system responds to H_2O_2 , whereas the SoxRS system responds to redox-active substances. **A.** OxyR is activated when a Cys residue interacts with H_2O_2 to produce sulphenic acid, which condenses with Cys40 residue. The resulting disulfide bond locks OxyR into a conformation that allows it to operate as a positive

transcription factor for OxyR regulon members such as *katG* and *ahpCF*. **B.** Each SoxR monomer comprises a [2Fe–2S] cluster. The dimer is activated by redox-active compounds, often phenazines or quinones generated by plants and microorganisms. Oxidized SoxR increases transcription of *soxS*, and the SoxS protein works as a secondary transcription factor to activate SoxRS regulon members, including *sodA* (encoding Mn-cofactor O₂⁻ dismutase) and *acrAB* (encoding a multidrug efflux pump).

1.4.4.3. PerR system

The PerR system is the most common mechanism in Gram-positive bacteria for avoiding peroxide oxidative stress. PerR is a metalloregulatory transcription factor that belongs to the ferric uptake regulator (Fur) superfamily. It was discovered in *Bacillus subtilis* as the primary regulator of the H₂O₂ response (Bsat et al., 1998). PerR has also been detected in Gram-negative bacteria (Li et al., 2004; Van Vliet et al., 1999), mostly in conjunction with OxyR (Wu et al., 2006). PerR is a transcriptional factor that functions as a dimer in response to metal ions within the cell via metal-catalyzed oxidation (Mongkolsuk and Helmann, 2002). Each subunit has a structural site that binds to zinc (Zn²⁺) irreversibly and a regulatory metal binding site (Jacquamet et al., 2009). PerR binds to manganese Mn²⁺ or Fe²⁺ ions in *B. subtilis*, depending on ion availabilities (Sen and Imlay, 2021). The metal-bound conformation of PerR binds to DNA at a particular Per box either in the promoter region or downstream of it (Fuangthong and Helmann, 2003), serving as a repressor (Dubbs and Mongkolsuk, 2012). The oxidation of Fe²⁺ into Fe³⁺ at the regulatory site provides the basis for PerR regulation. The binding of the regulatory metal under non-stress conditions stabilizes the conformation of the PerR dimer to better interact with DNA, resulting in suppression of the PerR regulon (Jacquamet et al., 2009). Excess peroxide promotes the oxidation of Fe in the regulatory sites of PerR through the Fenton reaction when intracellular H₂O₂ levels rise (Lee and Helmann, 2006). PerR then suffers conformational changes that prevent it from interacting with DNA (Imlay, 2015), resulting in the deactivation of PerR-regulated genes. The majority of these genes are engaged in oxidative stress metabolism and protection (*kat*, *ahpCF* operon, *mrgA*), while some are involved in metal homeostasis (*hemAXCDBL* operon) and surfactant synthesis (*srfA*) (Hayashi et al., 2005). Various bacteria, may have evolved to use PerR in different ways to better adapt their environmental niche.

1.4.5. Scavenger enzymes against ROS

Bacteria and other species can only tolerate a certain quantity of non-harmful ROS. Bacteria have evolved several methods to combat oxidative stress and prevent the imbalance of ROS levels that leads to cell damage. O_2^- and H_2O_2 react so quickly with vulnerable targets (Nucleic acid, protein, and membrane lipids), and therefore to mitigate this effect, sufficient scavenger enzymes must be synthesized. The existence of scavenging enzymes that consume ROS (SODs, catalases, and peroxidases) is crucial in bacteria's self-defense mechanisms against oxidative stress.

1.4.5.1. SOD efficiently dismutates O_2^- .

Bacteria and other species can only tolerate a limited quantity of non-harmful ROS. Bacteria have developed many methods to combat oxidative stress and prevent the imbalance of ROS levels that leads to cell damage. SODs are activated by RNA polymerase sigma factor RpoS (also known as σ_{38} , Sigma S, or KatF) that senses O_2 , and are highly upregulated when aerobic cells enter the stationary phase (Imlay, 2009). The existence of scavenging enzymes that consume ROS (SODs, catalases, and peroxidases) is crucial in self-defense mechanisms against oxidative stress in bacteria. SOD is a metalloenzyme that neutralises O_2^- to H_2O_2 and molecular oxygen. *E. coli* possesses two cytoplasmic enzymes (Fe-SOD and Mn-SOD) and one periplasmic enzyme (Cu-Zn-SOD) (Imlay, 2013). To avoid O_2^- toxicity, high cytoplasmic SOD titres maintain steady-state O_2^- levels at a sub-nanomolar concentration (Imlay and Fridovich, 1991). Because Mn-SOD and Fe-SOD are structurally and kinetically similar, SOD activity is present throughout a wide range of metal bioavailability. When Fe levels are high, Fur (Ferric uptake regulator) inhibits Mn-SOD transcription while Fe-SOD is synthesized and activated at lower Fe concentration hence Fur is deactivated and transcription of both Mn-SOD and the siRNA RyhB, which represses Fe-SOD mRNA, occurs (Massé and Gottesman; Tardat and Touati, 1991). Due to the biological availability of Fe, the Fe-SOD enzyme has been favored by evolution in anaerobic conditions. Periplasmic SOD protects bacteria against O_2^- those escapes from respiratory chain components to the cytoplasmic membrane.

1.4.5.2. Catalase and peroxidase degrade H_2O_2

Catalases are found in almost all bacteria, except for Gram-positive bacteria such as *streptococci*, *enterococci*, and *leuconostocs* (Mishra and Imlay, 2012). The enzymes that can degrade H_2O_2 in *E. coli* are alkyl hydroperoxide reductase (Ahp), catalase G (KatG), and

catalase E (KatE) (Seaver and Imlay, 2004). Ahp is a thiol-based peroxidase with two components (AhpC-AhpF) that transfers electrons from NADH to H_2O_2 , reducing it to water. KatG is a catalase-peroxidase that is weakly expressed in exponential cells. When cells are stressed by exogenous H_2O_2 , the transcriptional regulator OxyR strongly induces both ahpCF and katG. KatE is only found in stationary phase cells because it is induced by the RpoS system (Schellhorn and Hassan, 1988). Peroxidases are the primary scavengers at low H_2O_2 concentrations, whereas catalases are used at higher H_2O_2 concentrations or when cells are starved (Imlay, 2013). Furthermore, in the periplasm of *E. coli*, cytochrome c peroxidase (Ccp) receives electrons from the respiratory chain and directly transfers them to H_2O_2 . Instead of removing H_2O_2 , Ccp enables the cell to use it as a terminal oxidant to support respiration (Khademian and Imlay, 2017). This function is only useful when molecular oxygen is unavailable.

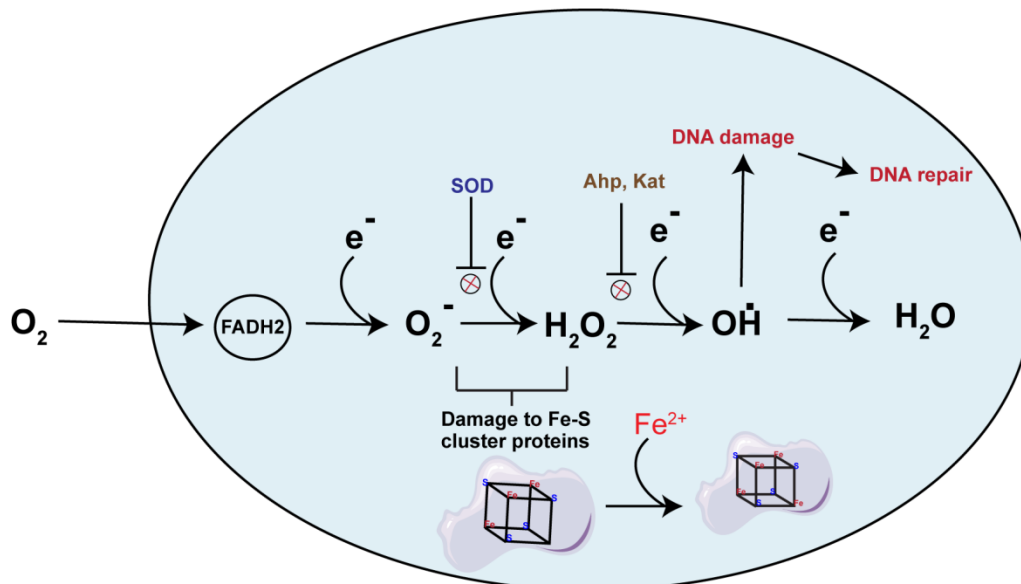


Figure 1.9. An overview of the damage induced by reactive oxygen species in *E. coli*. Redox enzymes, such as FADH2, oxidise flavoproteins by a process called autoxidation, which produces reactive oxygen species (ROS) such as H_2O_2 and O_2^- . These oxidants can be controlled by enzymes like catalases (Kats) and peroxidases (such alkyl hydroperoxide reductase (Ahp)), as well as superoxide dismutases (SODs). However, both species can harm mononuclear Fe enzymes and [4Fe-4S] dehydratases. Damaged enzymes are continually being repaired; therefore, their steady-state activity reflects the equilibrium between the damaging and healing processes. The pool of unincorporated Fe^{2+} , which has a loose association with macromolecules like DNA, also reacts directly with H_2O_2 . This process

results in DNA damage from $\bullet\text{OH}$ that must be repaired by repair enzymes. The cell's intrinsic defense mechanisms ensure that these types of damage occur at such a low frequency that they have no discernible impact on the cell's capacity to divide and survive. Intracellular oxidant levels rise when oxygen-generating redox chemicals and/or H_2O_2 enter the cell, largely impairing the most susceptible enzymes and leading to the breakdown of metabolic processes. Under these circumstances, cell recovery depends on the induction of defense regulons directed by OxyR and SoxRS.

1.5. Importance of Fe in Bacteria

Fe is an important metal and is the most abundant trace metal found in the cellular system. It constitutes Fe-S cluster (ISC) proteins. Most of the cellular Fe can be found in the form of ISCs ([2Fe-2S], [4Fe-4S], [3Fe-4S],) or heme (Figure 1.10). ISCs and heme are essential components of the protein complexes that comprise the electron transport chain (ETC) and the tricarboxylic acid cycle (TCA) (Keseler et al., 2013a). ETC and TCA cycles are the sources of ATP production inside the cell, Hence Fe scarcity might affect ATP production. *E. coli* cells maintain about 1mM Fe in the cytoplasm for survival (Chattopadhyay et al., 2006b; Finney and O'halloran, 2002). For instance, the complex of NADH dehydrogenase I (NDH-1) has nine ISC centers for electron transport. Similarly, succinate dehydrogenase (SDH or SdhABCD), terminal oxidases, aconitases (AcnA and B), and fumarase (FumABC) enzymes utilize these cofactors extensively during the ETC and TCA cycles, respectively (Keseler et al., 2013a). Heme is also a critical component of hemoglobin in higher eukaryotes, which transport oxygen to the tissues. Additionally, Fe in its ionic form works as a cofactor for mononuclear Fe enzymes (Anjem and Imlay, 2012). The well-characterized *isc* gene network in *E. coli* is responsible for the synthesis of ISC-containing proteins (Roche et al., 2013). The *isc* operon is composed of clusters of genes *iscRSUA-hscBA-iscX-fdx*. IscU and IscA act as scaffolds for the assembly of ISCs, whereas IscS aids in sulfur mobilization. HscA and HscB form a chaperone/cochaperone system similar to the DnaKJ chaperone/cochaperone system involved in ISC assembly (Giel et al., 2006). ISC regulator (IscR) is a transcription factor (Giel et al., 2006) When the cellular Fe level is elevated, the IscR complexes with [2Fe-2S], repressing transcription of the *isc* operon, including *iscR*. Thus, IscR is negatively regulated (Figure 1.11). However, when Fe is depleted, the apo-IscR form is unable to bind to the operator site of the *isc* promoter, hence

suppressing all *isc* operon genes. The apo-IscR form, on the other hand, acts as an activator for the *sufABCDSE* operon genes, which comprise an alternate ISC biogenesis system (Py and Barras, 2010). Thus, IscR coordinately regulates the expression of the *iscRSUA-hscBA-iscX-fdx* and *sufABCDSE* operons via suppression by [2Fe-2S]-IscR and activation by apo-IscR. Additionally, the *suf* system is activated and inhibited by OxyR and Fur regulators. Thus, loss of the *suf* system has a detrimental effect on *E. coli* when it is exposed to oxidative stress. Thus, the observations indicate that the Suf system is capable of functioning under both oxidative stress and Fe deficiency situations.

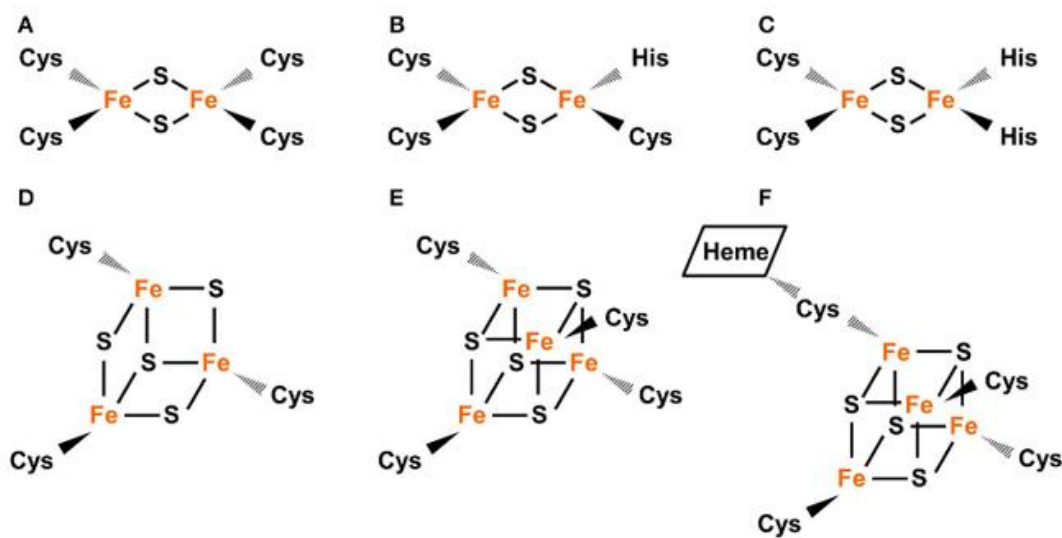


Figure 1.10. Common types of Fe-S clusters. **A.** The plant-type Fd is a classic 2Fe-2S molecule, with four Cys residues serving as coordination sites (ferredoxin). **B.** Coordination of 2Fe-2S by three Cys and one His residues. **C.** Coordination of the Fe-2S by two Cys and two His residues, as seen in PetC (photosynthetic electron transfer), is an example of a Rieske type 2 coordination scheme. **D.** Similar to that of Fd-GOGATs (ferredoxin-dependent Gln oxoglutarate aminotransferases), 3Fe-4S is coordinated by three Cys residues. **E.** Similar to PsaA, PsaB (Photosystem I protein-C), and PsaC, 4Fe-4S is coordinated by four Cys residues. **F.** Like NiR (nitrite reductase) and SiR (siroheme reductase), 4Fe-4S is coordinated by four Cys residues with a thiolate ligand that serves as both heme and heme sulphide (sulfite reductase) (Adopted from Lu, 2018).

Bacteria stores an ample amount of Fe inside the cell. Many bacteria, for instance, create siderophores to bind and import Fe²⁺. They do this by storing surplus Fe in ferritins during times of plenty, and then, when supplies are low, triggering a Fe-sparing response

controlled by the short RNA (sRNA) RyhB, which prevents the production of enzymes that require Fe but aren't strictly necessary.

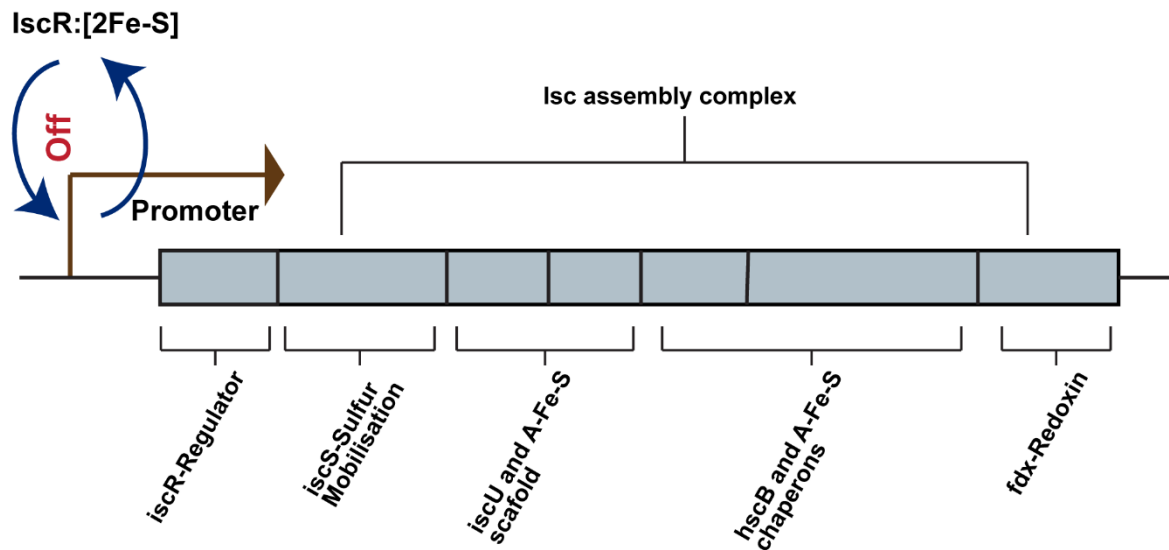


Figure 1.11. A diagrammatic representation to show the ISC biogenesis system. IscR, when paired with Fe, forms the *isc* operon repressor holo-*IscR*.

Heme production in *E. coli* begins with L-glutamate and progresses via 5-amino-levulinate to uroporphyrinogen III. Following that, uroporphyrinogen III is converted to protoheme IX, which is then turned into the various heme classes required for cytochromes (Keseler et al., 2013a). There is currently no information on the transcriptional control of heme biosynthesis genes in *E. coli* (Keseler et al., 2013a).

1.5.1. Fe homeostasis in bacteria

The cytoplasm of *E. coli* maintains roughly 1mM Fe to sustain life (Finney and O'halloran, 2002). For this reason, Fe -starved bacteria have to devise ways of coping with their ancestors' metabolic apparatus. During the availability of excess Fe, many bacteria synthesize siderophores to solubilize and import Fe²⁺; when the Fe is scarce, they initiate an Fe-sparing response, regulated by the small RNA (sRNA) RyhB, to prioritize Fe use by shutting down the synthesis of Fe -requiring enzymes that are abundant but not essential.(Boukhalfa and Crumbliss, 2002). There are around 500 distinct types of siderophores known till date (Boukhalfa and Crumbliss, 2002). Once extracellular siderophores have captured Fe³⁺ in gram-negative bacteria, they attach to the particular outer membrane ferri-siderophore receptors consisting of FepA, FecA, and FhuA proteins (Figure 1.12) in the membrane (McHugh et al., 2003). The movement of the ferri-siderophore over

the outer membrane is an energy-dependent process. This energy is provided by cytosolic membrane potential (electrochemical gradient) and the TonB-ExbB-ExbD system (Andrews et al., 2003). It is proposed that the membrane electrochemical potential is utilized by ExbB and ExbD proteins to activate TonB. A conformational shift in the outer membrane receptors for ferri-siderophore is induced by the energized TonB, which then transports ferri-siderophore to the periplasm (Bradbeer et al., 1976). OM receptors and TonB systems are not required in Gram-positive bacteria since they lack an OM. ABC transporters and periplasmic binding proteins carry ligand-bound siderophores from the periplasm to the cytoplasm (Andrews et al., 2003). For example, FhuD and FecB are the periplasmic binding proteins, while FecCDE and FepCDEG are ABC transporters in *E. coli* (Keseler et al., 2013b). Ferri-siderophore complexes are dissociated inside cells to release the complexed Fe for utilization in cellular metabolism. The Fe^{3+} ion of the ferri-siderophore complex is thought to be reduced in this process, causing Fe^{2+} to dissociate. The esterase protein, which is encoded by the *fes* gene, is required for the usage of ferri-enterobactin also in the enterobactin synthesizing, exporting, and uptake gene cluster (*ent-fec*) (Andrews et al., 2003). In addition to ferric ion transport, bacteria use a siderophore-independent method to transport Fe^{2+} ions. Fe^{2+} ion transporter is encoded by the *feoAB* genes in *E. coli*, which are active in anaerobic conditions. Fe^{2+} transport via FeoB is dependent on ATP or GTP for energy (Kammler et al., 1993; McHugh et al., 2003). A relationship exists between Fe^{2+} ion transport and extracellular ferric reductase activity in *E. coli* and *Helicobacter pylori* (Worst et al., 1998). There is a decreased affinity for Fe^{2+} ion importation by membrane-bound MntH, a transporter that also brings Mn into the cell (Makui et al., 2000). Many bacteria store internal reserves of Fe in storage proteins because the availability of soluble Fe in the environment is limited and the acquisition of Fe is a costly process. When external Fe sources are limited, the stored Fe can be utilized to boost growth and metabolism. Prokaryote's primary Fe storage proteins include classic ferritins, heme-containing bacterioferritins, and smaller Dps proteins (Bsat et al., 1998). Dps, FtnA, Bfr, and Bfd are the most important *E. coli* Fe storage proteins (Andrews et al., 2003). A total of roughly 100 genes, including the Fe homeostasis genes previously described, are controlled by Fur, the global Fe-dependent transcription regulator found in *E. coli* and most other bacteria. The genes involved in acquiring or synthesizing siderophores and Fe storage are silenced when the cytoplasmic concentration of Fe^{2+} is high (Keseler et al., 2013). The Fe metabolism is similarly regulated by *ryhB*, according to Massé and Gottesman, 2002. RyhB is suppressed by *fur* and this affects the downstream targets. Fe storage proteins are controlled by *ryhB* in a Fur-dependent way. This explains why Fe

homeostasis has a two-tiered regulatory system. A Fe exporter FieF has also been discovered in *E. coli* (Keseler et al., 2013b).

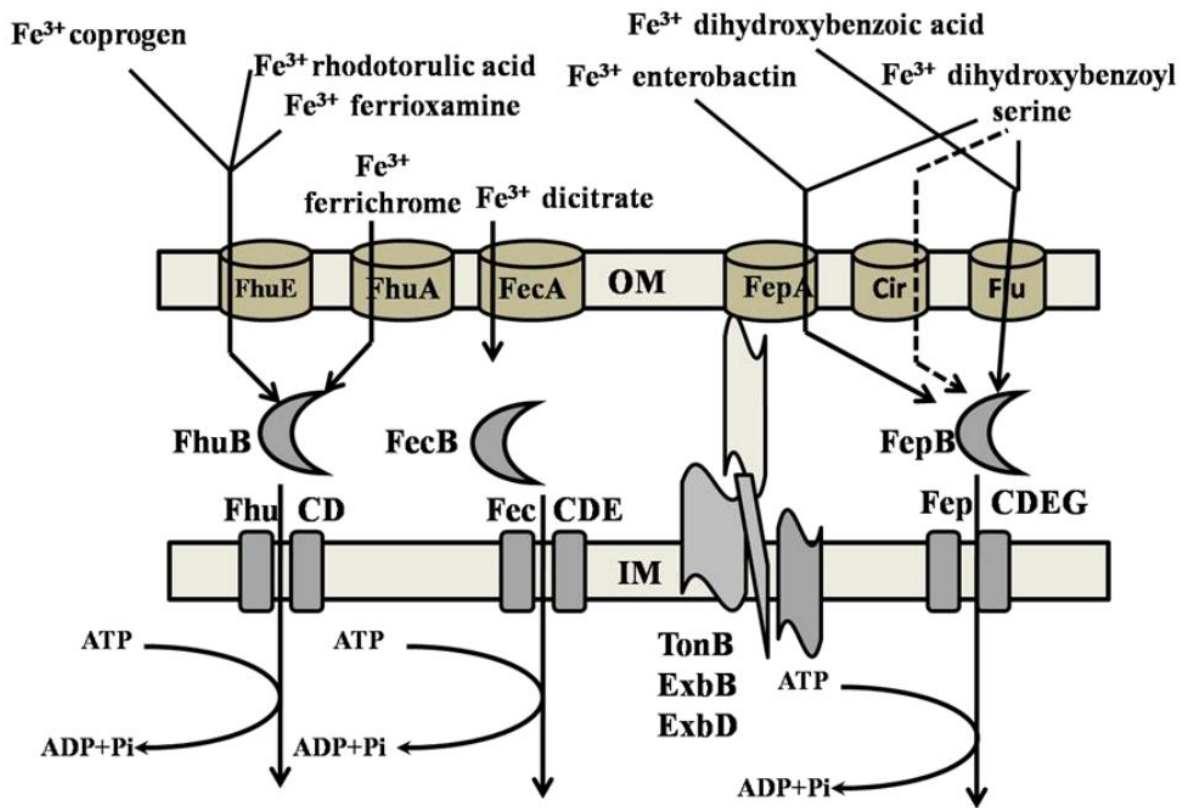


Figure 1.12. Siderophore-dependent Fe transport mechanisms in *E. coli*. The diagram depicts the uptake of Ferric ions in siderophore complexes and the release of functional Fe by proteins such as FhuB, FecB, and FepB. The ferri-siderophore receptors are FepA, FecA, and FhuA, while the ABC transporters are FhuCD, FecCDE, and FepCDEG (Adopted from Andrews et al., 2003).

1.6. Mn homeostasis in Bacteria

Mn is an essential trace element that participates in a wide range of cellular molecular processes. Several enzymes require Mn as a cofactor because it may fill in for the absence of other ions, such as Fe and Mg. In addition to detoxifying reactive oxygen species (ROS), Mn-using enzymes are involved in a variety of metabolic processes, including protein glycosylation, polyamine production, DNA synthesis, nucleic acid degradation, phospholipid biosynthesis and processing, polysaccharide biosynthesis and protein catabolism. Most of the time, Mn serves as either a reduction/oxidation centre to aid the process (e.g., the role of SOD in the detoxification of O₂⁻ radicals) or a Lewis acid in acid-base reactions. Oxidative stress

causes an increase in Mn transport in cells. The cell's cytoplasmic O_2^- radicals are quenched by Mn-SOD, which is activated when Mn levels are increased. As a result, Mn is predominantly an antioxidant metal that aids in the detoxification of ROS. A vast range of bacteria and the mitochondria of higher organisms have MnSOD, which is interesting because they are found everywhere. As an added benefit, Mn complexed with phosphate and/or oxalates can aid to reduce ROS levels in the system (Anjem and Imlay, 2012)(Anjem et al., 2009). To put it another way, Mn serves as a universal antioxidant metal throughout the body's system. Transcriptional control of MnSOD in *E. coli* and *B. subtilis* is provided by SoxRS and PerR, respectively (Anjem et al., 2009). Mn-SOD levels in bacteria are likewise regulated by Fur, the ferric uptake regulator. SOD enzymes, like FeSOD and CuSOD, also exist in organisms (such as *E. coli*) to deal with O_2^- radicals that are produced under normal circumstances (Fee, 1991). Even while Mn concentrations in *E. coli* and the majority of other organisms are kept to a few micromolar levels, certain lactic acid bacteria can reach millimolar levels of Mn within the cell. Their capacity to withstand higher levels of oxidative stress or even the lack of SOD is connected with this enhanced level of Mn (Archibald and Fridovich, 1981). Lactic acid bacteria, unlike *E. coli* and other bacteria, require a much less quantity of Fe (Jakubovics and Jenkinson, 2001). O_2^- may be eliminated from the organism by polyphosphorus or pyrophosphorus complexed with Mn, whereas Mn-bicarbonate may be able to neutralize H_2O_2 (Stadtman et al., 1990). Mn may have a non-enzymatic oxidative stress protection system that is yet to be discovered (Archibald and Fridovich, 1981). Similarly, the radio-resistant *Deinococcus radiodurans* bacterium accumulates a high concentration of Mn compared to a low concentration of the metal Fe (Slade and Radman, 2011). Because *D. radioduran* radiation-damaged proteins undergo some oxidation processes, a radio-resistant mechanism involving the Mn-complex has been postulated (Daly et al., 2004)(Daly et al., 2004). Several enzymes, including DNA and RNA polymerases, can use Mn as a replacement for Mg ions in the active center (Bock et al., 1999; Sissi and Palumbo, 2009; Song and Hunt, 1988; Vashishtha et al., 2016). An additional finding depicts that under oxidative stress conditions, Mn may take the place of Fe in four mononuclear Fe enzymes, namely ribulose 5 phosphate 3-epimerase, peptide deformylase, threonine dehydrogenase, and cytosine deaminase (Anjem and Imlay, 2012). In the presence of oxidative stress, several enzymes benefit from this swap. NrdAB and NrdEF are two distinct ribonucleotide reductases in *E. coli*. Under conditions of Fe deprivation and oxidative stress, the Mn-dependent ribonucleotide reductase (NrdEF) is activated and ensures dNTP synthesis for chromosomal replication in *E. coli* (Martin and Imlay, 2011).

1.7. Polyamine and metal ions

Polyamine mimics cations such as Zn^{2+} , Ca^{2+} , and Mg^{2+} by competing for their binding sites on membrane receptors, enzymes, and other biological activities due to its cationic nature. For instance, polyamine frequently replaces Mg^{2+} ions in ribosomes, which are essential for translation. Moreover, polyamines not only reduce the requirement for Mg^{2+} but also elevate protein synthesis above the maximum level obtained by high Mg^{2+} alone (Ogasawara et al., 1989). Similarly, Ca^{2+} is substituted for the anionic position on the phospholipid membrane by polyamine, which affects receptor-mediated signal transmission (Koenig et al., 1987). Polyamine acts as a strong chelator and forms complexes with other cationic ions such as Ni^{2+} , Co^{2+} , Cu^{2+} , and Zn^{2+} (Bertsch et al., 1958; Hares et al., 1956). Additionally, halogen and pseudo-halogen complexes of Cd^{2+} and Hg^{2+} have been reported to have 1,3-diamino propane, putrescine, and cadaverine. Diamines act as a bridge or chelating ligands in these compounds (Jastrzab et al., 2017). A study of Cu^{2+} complexes with linear triamines revealed that the most stable complexes have a five or six-ring structure (Antonelli et al., 1984; Jastrzab et al., 2017; Weatherburn et al., 2002).

Fe co-transport in enterocytes was mediated by an interaction between Fe and polyamines followed by the uptake of the polyamine-Fe complexes by the enterocytes' polyamine transport mechanism. Additionally, polyamines have an effect on Fe homeostasis in CHO cells (Gaboriau et al., 2004). Similarly, polyamines in *E. coli* upregulate FecI at the translational level (Yoshida et al., 2004). FecI is a sigma factor (σ^{18}) that regulates the transcription of Fe uptake operon (fecABCDE). Therefore, increased transcription of fecABCDE mRNAs suggests that polyamines control Fe uptake in *E. coli* via FecI activation (Yoshida et al., 2004). Therefore, it appears that polyamines have a major role in metal ion homeostasis and their function. Polyamines in bacteria can scavenge Fe and free radicals, leading to acid resistance, promote biofilm formation, regulate the expression of virulence factors, and mediate immune evasion during the establishment of bacterial infection (Rai et al., 2016) (Rai et al., 2016).

1.8. Polyamine and oxidative stress

Natural PAs are capable of functioning as a free radical scavenger and protects DNA and Phospholipids from oxidative damage. Polyamine also scavenges HO^{\cdot} and $O_2^{\cdot-}$ in comparison to other highly effective antioxidants such as Vitamins C and E (Bors et al.,

1989; Khan et al., 1992c, 1992b). Spermidine and other polyamines can protect DNA from strand breakage by scavenging reactive oxygen species (Chattopadhyay et al., 2003a; Jung and Kim, 2003; Khan et al., 1992c; Rider et al., 2007). Polyamines significantly reduce the percentage of the open circular form of plasmid DNA at the concentration of 10mM (Khan *et al.*,1992). In the absence of spermidine, *E. coli* cells were shown to be extremely susceptible to paraquat in an oxygen-rich environment, suggesting that spermidine may have a protective effect against O₂⁻ induced cell death (Minton et al., 1990). In an alternative study, it was further investigated that when *E. coli* mutants missing polyamine were cultivated in 95% oxygen or exposed to H₂O₂, they were very vulnerable to ROS toxicity (Chattopadhyay et al., 2006b).

Recently, a module was enlarged to include polyamine-inducible genes involved in the production of SODs, glutathione (GSH), and catalases (Jung and Kim, 2003; Sakamoto et al., 2015). Thus, polyamines have been demonstrated to stimulate the expression of proteins essential for an effective antioxidant response in addition to their direct action on ROS in *E. coli*. Exogenous polyamines are required for ROS protection in *Saccharomyces cerevisiae* mutants lacking in spermidine and spermine, even when SOD is overexpressed (Balasundaram et al., 1993; Chattopadhyay et al., 2003b). Microarray investigation of spermidine-treated spermine-deficient yeast mutants revealed that spermidine boosted the expression of at least 500 genes by more than twofold, including several oxidative stress response genes (Chattopadhyay et al., 2009). Tpo1, a polyamine exporter from *S. cerevisiae*, was recently discovered to participate in the oxidative stress response by modulating intracellular spermidine and spermine levels in response to H₂O₂, thereby invoking the production of proteins required for oxidant tolerance, such as SODs and heat shock proteins, governing the duration of cell cycle arrest, and allowing adaptation to elevated H₂O₂ levels (Krüger et al., 2013). Spermine and spermidine also protect mammalian cells from ROS-mediated damage, and their loss is known to halt cellular proliferation. Due to a mutation in the spermine synthase gene, the Gy11 embryonic fibroblast cell line lacks spermine (Rider et al., 2007). This cell are more sensitive to the cytotoxic effects of H₂O₂ than normal cells, and lowering their polyamine levels, causes DNA damage and apoptosis even in the absence of H₂O₂. Furthermore, reducing cellular GSH increased the sensitivity of polyamine-depleted cells to H₂O₂, showing that polyamines are involved in a protective mechanism against ROS that is independent of GSH (Rider et al., 2007).

Maintaining an optimum level of polyamines, which is tightly regulated at the transport, synthesis, and degradation levels are crucial. Several oxidases in catabolic processes produce reactive aldehydes such as acrolein and H₂O₂. These metabolites, especially those derived from spermine, can be extremely hazardous, causing damage to proteins, DNA, and other biological components. Infection or cell damage can increase their production by releasing free polyamines and activating the oxidative catabolic pathways. Because polyamines play an important physiological role in defending against oxidative damage, a decrease in polyamine content may enhance these compounds' harmful potential. Polyamine catabolism increases have been linked to the development of ailments such as stroke, different neurological diseases, renal failure, liver disease, and cancer. These discoveries open up new avenues for illness detection, prevention, and therapy (Hoet and Nemery, 2000; Pegg, 2013). At lower temperatures, spermidine replaces ribosomal confined Mg²⁺, causing ribosome deactivation, which further affects protein synthesis (Limsuwun and Jones, 2000).

1.9. Polyamine and pathogenicity

Polyamines can influence the virulence mechanisms of pathogens. Polyamines are also important in biofilm development and antimicrobial resistance (Gilbertsen and Williams, 2014). Polyamines can modify the virulence mechanism of a range of illnesses. Although the *cadA* gene is present in the majority of *E. coli* strains, *Shigella* does not have it. *CadA* expression in *Shigella* reduces enterotoxin activity. Cadaverine pre-treatment of eukaryotic cells makes them less susceptible to *Shigella* enterotoxins. (Maurelli et al., 1998; Shah and Swiatlo, 2008). Notably, spermine/spermidine N-acetyl transferase (SSAT or SpeG), which degrades spermidine and spermine, is the cell's most effective polyamine homeostasis component (Miller-Fleming et al., 2015). Surprisingly, *S. aureus* neither synthesizes nor encodes polyamine or the SpeG enzyme. As a result, *S. aureus* strains are predisposed to hypersensitivity to spermidine (Joshi, 2012). However, the *S. aureus* USA-300 lineage is especially pathogenic due to the acquisition of the *speG* gene nested in the Arginine Catabolic Mobile Element (ACME) (Joshi, 2012). Spermidine homeostasis regulated by SpeG is critical for bacterial pathogenesis. The absence of *speG* prevents the *Salmonella enterica* pathogen from replicating in host cells (Putignani et al., 2017). *Staphylococcus aureus* lacks both de novo polyamine production pathways and a polyamine inactivation mechanism controlled by SpeG. As a result, *S. aureus* strains are predisposed to hypersensitivity to spermidine. However, *S. aureus* USA-300 strains emerged by the

acquisition of the *speG* gene nested within the Arginine Catabolic Mobile Element (ACME), which confers severe pathogenicity (Joshi, 2012). Nonetheless, the presence of SpeG does not automatically favor pathogenesis, as evolutionary silencing of the *speG* gene in *Shigella* species might facilitate harmful lifestyles as well (Barbagallo et al., 2011). *Bacillus anthracis* utilizes spermidine in the manufacture of the siderophore petrobactin. Petrobactin is required for Fe uptake and pathogenicity but does not interact with siderocalin, a host protein that interacts with bacterial siderophores (Oves-Costales et al., 2007). Polyamine has a huge role in Biofilm production that enhances the virulent properties of pathogenic cholera agent *Vibrio cholerae* (Karatan et al., 2005), the plague bacterium *Yersinia pestis* (Patel et al., 2006), the model Gram-positive species *Bacillus subtilis* (Burrell et al., 2010), *E. coli* (Sakamoto et al., 2015) and *Neisseria gonorrhoeae* (Goytia et al.).

1.10. Objectives of the present work

To understand the mechanism of spermidine toxicity and its role in metal homeostasis, we adapted several approaches *viz.* genetics, microarray, proteomics, and biochemical. To validate our experiments, we have chosen *E. coli* as our model organism. The effects of spermidine on Fe homeostasis, envelope biogenesis, redox balance maintenance, etc. were addressed by using a spermidine-sensitive strain $\Delta speG$ of *E. coli*. The objectives of the study are divided broadly as below:

1. Effect of over-accumulated spermidine on redox state of *E. coli*
2. Effect of spermidine toxicity on gene expression profile
3. Biochemical impact of spermidine toxicity on Fe homeostasis

CHAPTER II

EFFECT OF OVER ACCUMULATED SPERMIDINE ON REDOX STATE OF *E. COLI*

2.1. Introduction

Polyamines are ubiquitously present in all life forms. They tweak a diverse array of biological processes, e.g., nucleic acid and protein metabolism, ion channel functions, cell growth and differentiation, mitochondrial function, autophagy and aging, protection from oxidative damage, actin polymerization, and perhaps many more (Casero et al., 2018; Gawlitta et al., 1981; Madeo et al., 2018; Michael, 2018; Miller-Fleming et al., 2015; Oriol and Audit, 1978; Pegg, 2016, 2018; Pohjanpelto et al., 1981; Tabor and Tabor, 1984a; Wallace et al., 2003). The cationic amine groups of polyamines can avidly bind to negatively charged molecules, such as RNA, DNA, phospholipids, etc. (Igarashi et al., 2000; Miyamoto et al., 1993; Schuber, 1989; Tabor and Tabor, 1984). Polyamines have been demonstrated to protect DNA from reactive oxygen species (ROS) such as singlet oxygen, $\bullet\text{OH}$, or H_2O_2 (Balasundaram et al., 1993; Ha et al., 1998a, 1998b; Jung and Kim, 2003; Khan et al., 1992c, 1992b; LØVaas, 1996; Pegg, 2018; Stewart et al., 2018). Indeed, knocking out polyamine biosynthesis enzymes from *E. coli* and yeast confers toxicity to oxygen, O_2^- , and H_2O_2 (Balasundaram et al., 1993; Chattopadhyay et al., 2003a, 2006b; Eisenberg et al., 2009).

Most prokaryotes, including *E. coli*, synthesize cadaverine, putrescine, and spermidine, while higher eukaryotes additionally synthesize spermine. *E. coli* also acquires spermidine and putrescine from the surrounding medium (Igarashi and Kashiwagi, 2000; Miller-Fleming et al., 2015). However, polyamine in excess is toxic to the organisms unless polyamine homeostasis in the cell is operated at the levels of export, synthesis, inactivation, and degradation (Miller-Fleming et al., 2015). Notably, spermine/spermidine N-acetyl transferase (SSAT or SpeG), which inactivates spermidine and spermine, constitutes the most potent polyamine homeostasis component of the cells (Miller-Fleming et al., 2015). Interestingly, *Staphylococcus aureus* neither synthesizes polyamine nor encodes for the SpeG enzyme. Thus, *S. aureus* strains are inherently hypersensitive to spermidine (Joshi, 2012). However, *S. aureus* USA-300 lineage, which evolved through acquiring *speG* gene nested in the Arginine Catabolic Mobile Element (ACME), is exceptionally pathogenic (Joshi, 2012). The mechanism behind such a phenomenon is entirely unknown.

Besides, a specific mechanism of SpeG function conferring pathogenic fitness to *S. aureus* USA300 strain is unknown. Here, we provide evidence that although spermidine mitigates oxidative stress by lowering $\bullet\text{OH}$ and H_2O_2 levels, excess of it simultaneously triggers the production of O_2^- radicals, thereby causing toxicity in the *E. coli* ΔspeG strain as well as naturally *SpeG*-deficient *S. aureus* RN4220 strain. However, wild-type *E. coli* and *S. aureus* USA300 with a horizontally-acquired *speG* gene tolerate applied exogenous spermidine stress. Furthermore, we demonstrate that while RNA-bound spermidine inhibits Fe oxidation, free spermidine interacts and oxidizes the Fe to evoke O_2^- radicals.

Despite a tremendous volume of work unravelling the biological importance of spermidine and its homeostasis mechanisms, the molecular details of its toxicity are not understood. In this study, we decipher the molecular mechanism of spermidine toxicity in bacteria.

2.2. Material and Methods

2.2.1. Bacterial strains, plasmids, proteins, and chemicals

Bacterial strains and plasmids used in this study are listed in Appendix Table 1. BW25113 strain of *E. coli* was used as WT in this study. *S. aureus* RN4220 strain is a gift from Ravi PN Mishra lab, CSIR IMTECH, India. *S. aureus* USA300 strain was purchased from ATCC (ATCC BAA-1717). Oligonucleotides were purchased from IDT. Bacterial broths and agar media were purchased from BD Difco. The knockout strains of *E. coli* were procured from the KEIO library (Baba et al., 2006), verified by PCR, and freshly transduced into the WT background by P1 phage. The double and triple knockout mutants were generated following the standard procedure described by Datsenko and Wanner (Datsenko and Wanner, 2000). *E. coli* strain JRG3533 was a generous gift from Dr. Rachna Chaba, IISER Mohali, India. RKM1 strain was constructed by P1 transduction of *sodA-lacZ:Cm^R* genotype of JRG3533 to BW25113 ΔsoxS strain.

speG gene was PCR amplified by DG12-DG13 primer pairs (Appendix Table 2), respectively. *sodA* and *speG* were additionally subcloned in pBAD/Myc-His A vector to get *sodA* and *speG* multicopy expressions for complementation assays.

2.2.2. Growth, viability, spermidine sensitivity, and complementation assays

The growth curves described in the results were generated using an automated BioscreenC growth analyzer (Oy growth curves Ab Ltd.). To do this, overnight cultures of

bacterial strains were diluted in a new LB medium and cultivated in the presence and absence of spermidine concentrations ranging from 3.2 mM to 6.4 mM. Wherever indicated, 10 mM of each ROS quencher (thiourea, Tiron, sodium pyruvate, ascorbate, and NAC) was utilized. Serially diluted *E. coli* strains were spread over the LB-Agar surface supplemented with 6.4 mM spermidine for viability experiments. The number of colonies formed was used to measure viability under spermidine stress. Zones of inhibition (ZOI) were assessed in aerobic and anaerobic settings following overnight growth of the bacteria in the presence of 6.4 mM spermidine in wells on agar plates. The anaerobic state was established using AnaeroGas Pack 3.5L pouches in an anaerobic petri dish jar. To conduct complementation tests, the pBAD-*zwf* and pBAD-*sodA* plasmids were transformed into $\Delta speG\Delta zwf$, and $\Delta speG\Delta sodA$, respectively, and growth assays in the presence of spermidine were performed. Because leaky expressions of *zwf* and *sodA* were sufficient to repair growth abnormalities, arabinose induction was omitted.

2.2.3. Estimating cellular spermidine levels

Cells were grown in presence or absence of spermidine for 4 hr. The cells were washed with 1 M NaCl at 37°C for 10 min; 500 nmol of hexane-diamine (internal standard) was added and the pellets were resuspended in 750 μ l of 10% perchloric acid. The cells were lysed by freeze-thawing using liquid nitrogen, and 800 μ l of saturated sodium carbonate and 800 μ l of 10 mg/ml of dansyl chloride were added to the supernatants. The dansylation was carried out at 60°C for 3 hr in dark. The reaction was stopped using 400 μ l of 100 mg/ml proline and kept at 60°C for 30 min; 400 μ l toluene was added to each sample and mixed thoroughly. The organic layer was collected and dried using a speed vac; 2 ml 80% acetonitrile was added and sonicated to dissolve the dry samples. The samples were then passed through 0.22 μ m filter and injected to HPLC system (Agilent 1260 Infinity II) attached with a reversed-phase C-18 column (Agilent ZORBAX Eclipse Plus C18 of dimension 4.6 \times 100 mm, 3.5 μ m). Acetonitrile gradient (0–100%) with 0.8 ml/min flow rate was used for all samples. A PDA detector was used to monitor the elution peaks. The corresponding mass of individual peaks was detected using either a single quadrupole Agilent MSD using the ESI source or a separate Agilent LC-MS/MS equipment. Pure spermidine and hexane-diamine were also dansylated and determined their 100% tri- or di-dansylation. The dansylated spermidine was also used to generate a standard curve. The peak areas of spermidine (mAu*s) were normalized with the average peak area of internal standards. The absolute amounts of spermidine were calculated from the standard curve.

2.2.4. Relative ROS estimation

The cellular overall ROS and O_2^- anion concentrations were determined using H2DCFDA (10 μ M) and DHE (2.5 μ M), respectively. A 16-hour-grown overnight culture was diluted at a 1:100 ratio. The cells were then cultivated with or without 3.2 mM spermidine for 4 hours until they reached the mid-log phase followed by cell pelleting and washing twice with 1XPBS buffer. An equal number of pelleted cells were treated with DHE or H2DCFDA probes for one hour. The results for 0.05 million cells were obtained using the BD accuri F13 laser (for DHE) and the F11 laser (for H2DCFDA). The mean fluorescence intensity (MFI) of triplicate tests was determined.

The growth conditions for detecting H_2O_2 were similar to those described above. Cells were harvested and washed with 1X M9 minimal medium. An equal number of cells (2.5 mg each) were suspended in 6 ml of M9 minimal medium and incubated at 37°C at 200 rpm for varying intervals to allow H_2O_2 to be liberated. At different time points, cells were pelleted and the supernatant was used to quantify H_2O_2 release using a fluorometric H_2O_2 assay kit MAK165 (Sigma).

2.2.5. EPR spectroscopy

The protocol was adopted from Thomas et al., 2015, with slight modifications. The *AspeG* strain harboring pDAK1 empty vector or pSodA was grown in the presence or absence of 3.2 mM spermidine for 2 hr and then 0.001% arabinose was added and further grown for 2 more hours; 100 mg cell pellets were quickly resuspended in 700 μ l of KDD buffer, pH 7.4 (99 mM NaCl, 4.69 mM KCl, 2.5 mM CaCl₂, 1.2 mM MgSO₄, 25 mM NaHCO₃, 1.03 mM KH₂PO₄, 5.6 mM D-glucose, 20 mM HEPES, 5 μ M DETC, and 25 μ M deferoxamine); 100 μ l cell suspensions were preincubated with or without 20 mM DMTU and 200 μ M UA for 5 min; and 500 μ M of CMH spin probe (Enzo Life Sciences) were added and incubated for 30 min at 37°C. EPR spectra were acquired using a Bruker EMX MicroX EPR spectrometer with the following settings: center field, 3438 G, sweep width, 500 G; microwave frequency, 9.45 GHz; microwave power, 8.04 mW; modulation frequency 100 kHz; modulation amplitude, 5.64 G; conversion time, 40 ms; time constant, 40.96 ms; receiver gain, 1120; data points 1024; number of X-Scans, 5.

2.2.6. Estimation of intracellular NADP and NADPH

Relative NADP/NADPH levels were measured using NADP/NADPH assay Kit (Sigma MAK038) with slight modifications. *E. coli* cells were grown in the presence or

absence of 3.2mM Spermidine until the culture enters into log phase. The cell pellets were collected and washed twice with 1X cold PBS. NADPH/NADP extraction was done with 400 μ L of extraction buffer. Cell lysis was done by continuous freeze thaw cycles in liquid nitrogen followed by subsequent sonication (Instrument name). The cell debris was separated by centrifugation for 5 minutes at 4°C at 15000 rpm. The supernatants were collected and passed through a 10 kDa spin column (Millipore). 10 μ l of 0.1 N NaOH (for NADPH) and 10 μ l of 0.1 N HCl (for NADP) was added drop-wise to 50 microliter sample each for the measurement of NADP and NADPH respectively. Samples were incubated at 60°C in a water bath for 50 min and were immediately transferred to the ice for 5 min. The sample was then centrifuged at 13000 rpm for 2 min and 50 μ l of each sample was used in reaction mixture. Briefly, the reaction mixture (200 μ l) was composed of 50 μ l supernatant, 198 μ l NADP buffer and 2 μ l enzyme and After 10 min, developer (10 μ l) was added and kept at RT for 5 min. Absorbance was measured at 450nm.

2.2.7. Intracellular Glutathione measurement

Total glutathione (GSt), as well as its oxidized (GSSH) and reduced forms (GSH), were measured using a kit (Sigma CS0260) with minor modifications (Rahman et al., 2007). Overnight cell cultures were diluted 100 times and were allowed to grow for four hours in the presence and absence of spermidine. Cells were pelleted at 5000 rpm for 5 minutes at room temperature and the bacterial pellets were washed twice with 1X ice cold PBS. Bacterial pellets containing 20 mg of cell mass were dissolved in autoclaved Milli-Q water and heated at 95°C. The supernatant was collected after centrifuging the solutions at 13000 rpm. A reaction mixture containing 700 μ l KPE buffer along with 100 μ l of the sample was incubated for 30 sec after adding 60 μ l of DTNB (0.6mM) and 0.3U. At the end of reaction, 60 μ l of NADPH (0.2mM) was added for conversion of GSSG to GSH and absorbance was measured at 450 nm. The cell extracts were treated with 2-vinyl pyridine (10mM) for 1 hour before adding NADPH, DTNB, and GR, which covalently reacts with GSH, to compute the oxidized form of glutathione (GSSG). Triethanolamine is used to neutralize the excess 2-vinyl pyridine

2.2.8. Estimation of intracellular NAD and NADH

Relative NAD/NADH levels were determined using NAD/NADH assay Kit (Sigma MAK038) with slight modifications. Concisely, overnight grown cultures were diluted and cultivated in the presence or absence of 3.2mM Spermidine for 4 hours. The cell pellets were

collected and washed with 1X cold PBS. NADH/NAD extraction was done with 400 μ L of extraction buffer. Cell lysis was done by continuous freeze thaw cycles in liquid nitrogen followed by subsequent sonication. The cell debris was separated by centrifugation for 5 minutes at 4°C at 15000 rpm. The supernatants were collected and passed through a 10 kDa spin column (Millipore). Four freeze-thaw cycles on liquid nitrogen and subsequent short sonication were done to lyse the cells. The cell debris was removed by centrifugation for 5 minutes at 4°C at 15000 rpm. The supernatants were collected and passed through a 10 kDa spin column (Millipore). 10 μ l of 0.1 M HCl (for NADH) and 10 μ l of 0.1 M NaOH (for NAD⁺) were applied drop-wise to 50 microliter sample. Samples were incubated at 60°C in a water bath for 50 min and were immediately moved to the ice for 5 min. The sample was then centrifuged at 13000 rpm for 2 min and 50 μ l of each sample was used in reaction mixture. Briefly, the reaction mixture (200 μ l) was composed of 50 μ l supernatant, 198 μ l NAD buffer and 2 μ l enzyme and After 10 min, developer (10 μ l) was added and kept at RT for 5 min. Absorbance was measured at 450nm.

2.2.9. Determination of intracellular ATP level

Relative ATP estimation was done using ATP Bioluminescence Assay Kit CLS II (Roche). The overnight culture was diluted in the ratio of 1:100 and cultures were grown for 4 hours with and without spermidine treatment. The cells were then pelleted and washed with 1X chilled PBS. 5 mg of each cell pellet were then resuspended in ATP extraction buffer (100 mM Tris, pH 7.75 and 4mM EDTA, pH 8.0) and were incubated for 2 minutes at 100°C. The samples were centrifuged for 5 minutes at 1000g and the supernatant was transferred to fresh microfuge tubes. 50 μ l of sample and 50 μ l of luciferase reagent were added to the black 96 well microplates and luminescence was recorded using a luminometer. The relative light unit (RLU) values were recorded. Finally, relative ATP levels were normalized against per milligrams of proteins.

2.3. Results

2.3.1. Overaccumulation of spermidine causes growth retardation in *E. coli*

The addition of exogenous spermidine to the growing media was used to establish the working concentrations that adequately inhibited the development of *Δ speG*, but not the WT strain. Spermidine concentrations up to 6.4 mM slowed the proliferation of WT cells (Figure 2.1). On the contrary, the *Δ speG* strain showed dramatic growth retardation when spermidine

levels exceeded 3.2 mM. As a result, we settled on a spermidine concentration of 3.2 mM for the remainder of our research.

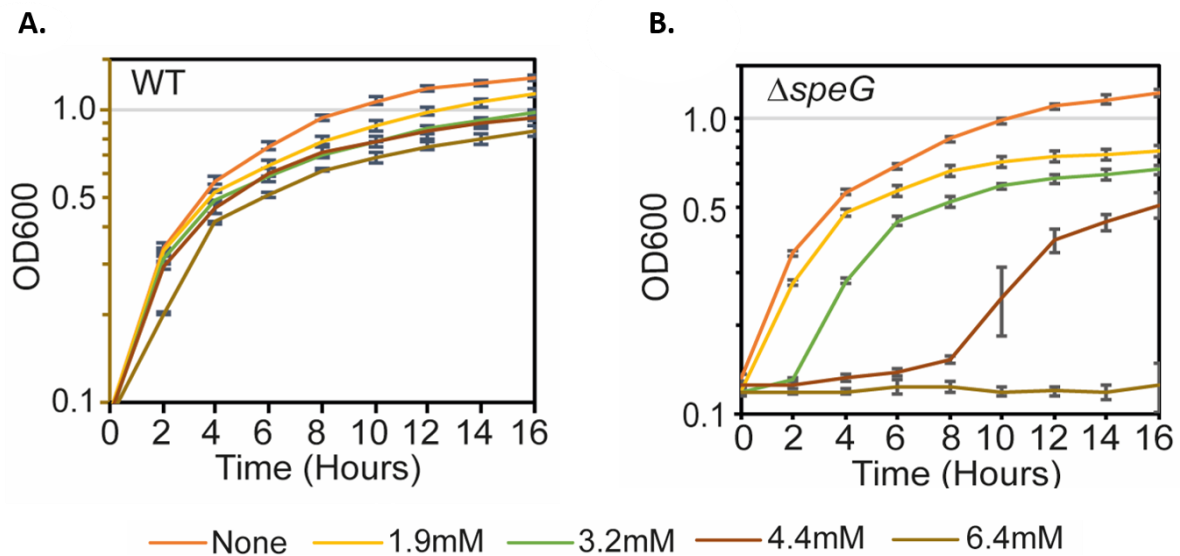


Figure 2.1. Growth difference between WT and $\Delta speG$ strain. $\Delta speG$ strain shows hypersensitivity in presence of spermidine. A. The spermidine concentration-dependent growth curve of wild-type (WT) cells in presence of various concentration of spermidine (1.9mM, 3.2mM, 4.4mM, and 6.4mM). Even at spermidine concentrations of 6.4 mM, WT displays a slight growth sickness. **B.** The spermidine concentration-dependent growth curve of $\Delta speG$ cells in presence of various concentration of spermidine (1.9mM, 3.2mM, 4.4mM, and 6.4mM). An extended lag phase has been seen in presence of 4.4mM spermidine and there was no growth at the concentration of 6.4mM.

HPLC analysis was carried out to determine the concentration of spermidine inside the cell. The $\Delta speG$ strain's intracellular spermidine levels increase when growing media was supplemented with 3.2 mM exogenous spermidine, while no such increase was observed in the WT cells (Figure 2.2). The SpeG function appears to have converted the extra spermidine to N1-, and N8-acetyl-spermidines, maintaining the quantity of spermidine in the WT cells (Miller-Fleming et al., 2015). Spermidine synthase-defective, $\Delta speE$ strain of *E. coli* also obtained a low quantity of spermidine from the LB media.

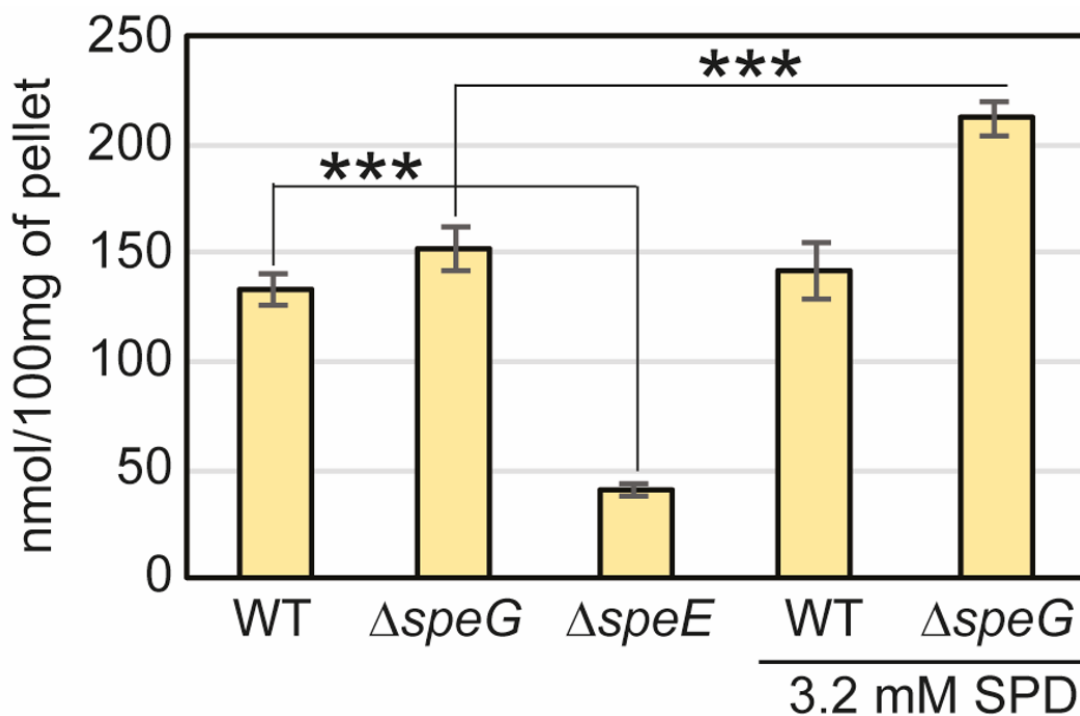


Figure 2.2. The bar diagram represents intracellular spermidine levels in different strains in the presence or absence of spermidine.

2.3.2. Increased cellular spermidine inhibits overall oxidative stress while evoking less harmful O_2^- production

The anti-ROS properties of polyamine spermidine are widely established (Balasundaram et al., 1993; Chattopadhyay et al., 2003; Chattopadhyay et al., 2006; Ha et al., 1998a; Ha, et al., 1998b; Khan et al., 1992a; Khan et al., 1992b; Pegg, 2018; Stewart et al., 2018). Polyamines have been implicated in preventing ROS generation in previous in vivo experiments that were done under polyamine deficient circumstances. Thus, assessing ROS levels both in spermidine-enriched and spermidine-deficient conditions were missing. To address this, we incubated *E. coli* strains with 2',7'-dichlorodihydrofluorescein diacetate (H2DCFDA), and dihydroethidium (DHE) probes, which generate fluorescent compounds reacting with one-electron-oxidizing species. While H2DCFDA is a generic ROS probe that nonspecifically reacts with many ROS species, the DHE is somewhat specific to the O_2^- anions in the system (Chen et al., 2013; Kalyanaraman et al., 2012). The relative mean fluorescence intensity (MFI) of H2DCFDA was increased about 1.5-fold in the spermidine synthase-defective ($\Delta speE$) strain, while no change was observed in the $\Delta speG$ strain (Figure 2.3A). However, spermidine treatment significantly decreased the H2DCFDA fluorescence in

WT, $\Delta speG$, and $\Delta speE$ strains (Figure 2.3A). Interestingly, despite no apparent increase in the spermidine level in WT cells under spermidine stress (Figure 2.2), a significant decrease in the H2DCFDA fluorescence was observed (Figure 2.3A). The acetylated products of spermidine might have some role in the decreased ROS levels causing decreased H2DCFDA fluorescence in spermidine-fed WT cells.

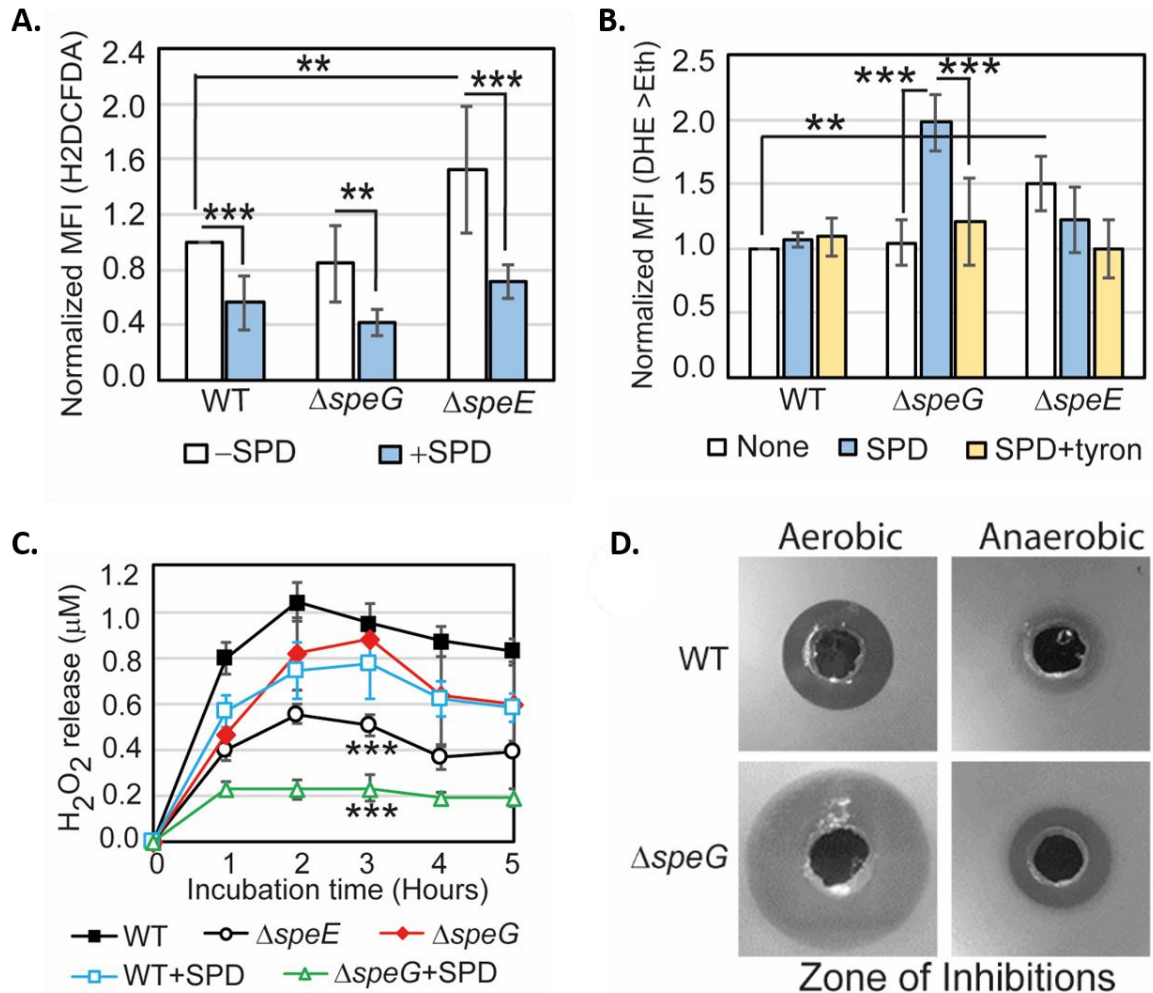


Figure 2.3. Spermidine stress and intracellular ROS in *E. coli*. **A.** The relative MFI values for the H2DCFDA, which is an indicator of $\bullet OH$ radical production, obtained by flow cytometry analyses are plotted. **B.** The relative MFI values of DHE probe, which is an indicator of O_2^- radical production, obtained by flow cytometry analyses are plotted. **C.** The absolute H₂O₂ production for a span of 5 hours from the different *E. coli* strains are shown. *** are P values generated compared with WT value. **D.** ZOI surrounding spermidine well on the agar plates were shown for the WT and $\Delta speG$ strains of *E. coli* under aerobic and anaerobic conditions.

Similarly, the relative MFI of DHE probe was increased significantly (1.5-fold) in $\Delta speE$ strain (Figure 2.3B). These findings are consistent with the observations that spermidine is an anti-ROS agent (Balasundaram et al., 1993; Chattopadhyay et al., 2003; Chattopadhyay et al., 2006; Ha et al., 1998a; Ha et al., 1998b; Khan, et al., 1992a; Khan et al., 1992b; Pegg, 2018; Stewart et al., 2018).

Surprisingly, the relative MFI of DHE probe was increased significantly (2-fold) in the spermidine-fed $\Delta speG$ as compared to WT strain of *E. coli* (Figure 2.3B). Tyron (Tr), an O_2^- quencher, decreased the MFI of DHE in the spermidine-fed $\Delta speG$ strain (Figure 2.3B). These observations indicate that although spermidine accumulation in the $\Delta speG$ strain reduces overall ROS levels and oxidative stress (Figure 2.3A), it may simultaneously evoke less harmful O_2^- production (Balasundaram et al., 1993; Chattopadhyay et al., 2003; Chattopadhyay et al., 2006; Ha et al., 1998a; Ha et al., 1998b; Khan et al., 1992a; Khan et al., 1992b; Pegg, 2018; Stewart et al., 2018). In another assay, we observed that the $\Delta speE$ and spermidine-fed $\Delta speG$ strains release substantially low levels of H_2O_2 compared to the untreated counterpart and WT cells (Figure 2.3C).

Next, we allowed WT and $\Delta speG$ strains to grow against the spermidine-diffusing wells on agar plates in aerobic and anaerobic conditions (Figure 2.3D). A far wider zone of inhibition (ZOI) for $\Delta speG$ strain was observed compared to WT under aerobic condition (Figure 2.3D), while a narrow ZOI was observed under anaerobic conditions for both strains (Figure 2.3D). This data further specifies that O_2^- production in aerobic condition could be reason for the observed spermidine toxicity.

Similar to the results for *E. coli* $\Delta speG$ strain, spermidine stress also decreases the levels of overall ROS, as indicated by the modest decrease (0.65-fold) in H2DCFDA fluorescence, in *S. aureus* RN4220 strain (Fig. 2.4C), suggesting that spermidine has a mild effect of minimizing the most hazardous $\bullet OH$ radical in RN4220 strain. On the other hand, no significant change in the H2DCFDA fluorescence was observed in *S. aureus* USA300 strain (Figure 2.4C). However, in contrast to *E. coli* $\Delta speG$ strain, the *S. aureus* RN4220 and USA300 strains exhibited low levels of H_2O_2 production. Further treatment with spermidine had no discernible effect on the H_2O_2 levels (Figure 2.4D).

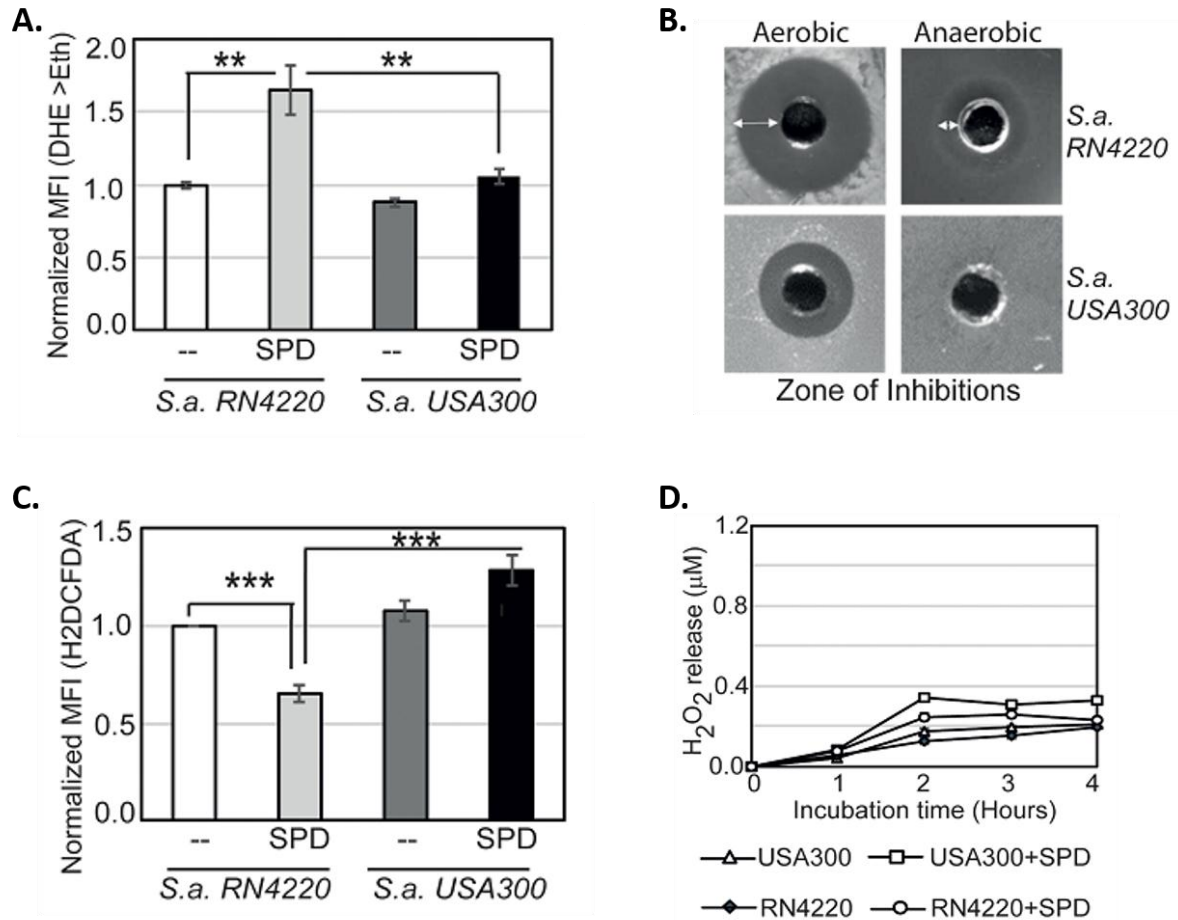


Figure 2.4. O₂⁻ and other ROS production in *S. aureus*. **A.** spermidine -treatment to the *speG*-negative *S. aureus* RN4220 strain enhances DHE fluorescence (1.5-fold). However, the *speG*-positive *S. aureus* USA 300 strain resists the effect of spermidine. These data suggest that spermidine -stimulated O₂⁻ radical production in *S. aureus* strains also depends on the absence of *speG* function. **B.** ZOI surrounding spermidine well on the agar plate was determined for the *S. aureus* (*S.a.*) RN4220 and USA300 strain under aerobic and anaerobic conditions. The observation suggests that spermidine is more toxic in aerobic conditions and in the absence of *speG* gene in RN4220 strain. **C.** spermidine treatment modestly decreased the H2DCFDA fluorescence (0.65-fold) in the *S. aureus* RN4220 strain. On the other hand, USA300 strain resists this effect of spermidine. **D.** H₂O₂ production from *S. aureus* strains in the presence or absence of spermidine for 5 hours was shown. The data indicate that a very low level of H₂O₂ was liberated from the *S. aureus* strains compared to the liberation from the *E. coli* strain (Fig. 2.3C). Besides, the absence and presence of *speG* function in RN4220 and USA300 strains, respectively, has no visible effects on the H₂O₂ liberation. Whenever mentioned, the *** denote P values <0.001 and <0.01, respectively; unpaired T-test.

If spermidine induces O_2^- production, SOD genes (e.g., *sodA* and *sodB*) would play vital roles. Therefore, the serial dilutions of WT, $\Delta speG$, $\Delta sodA$,

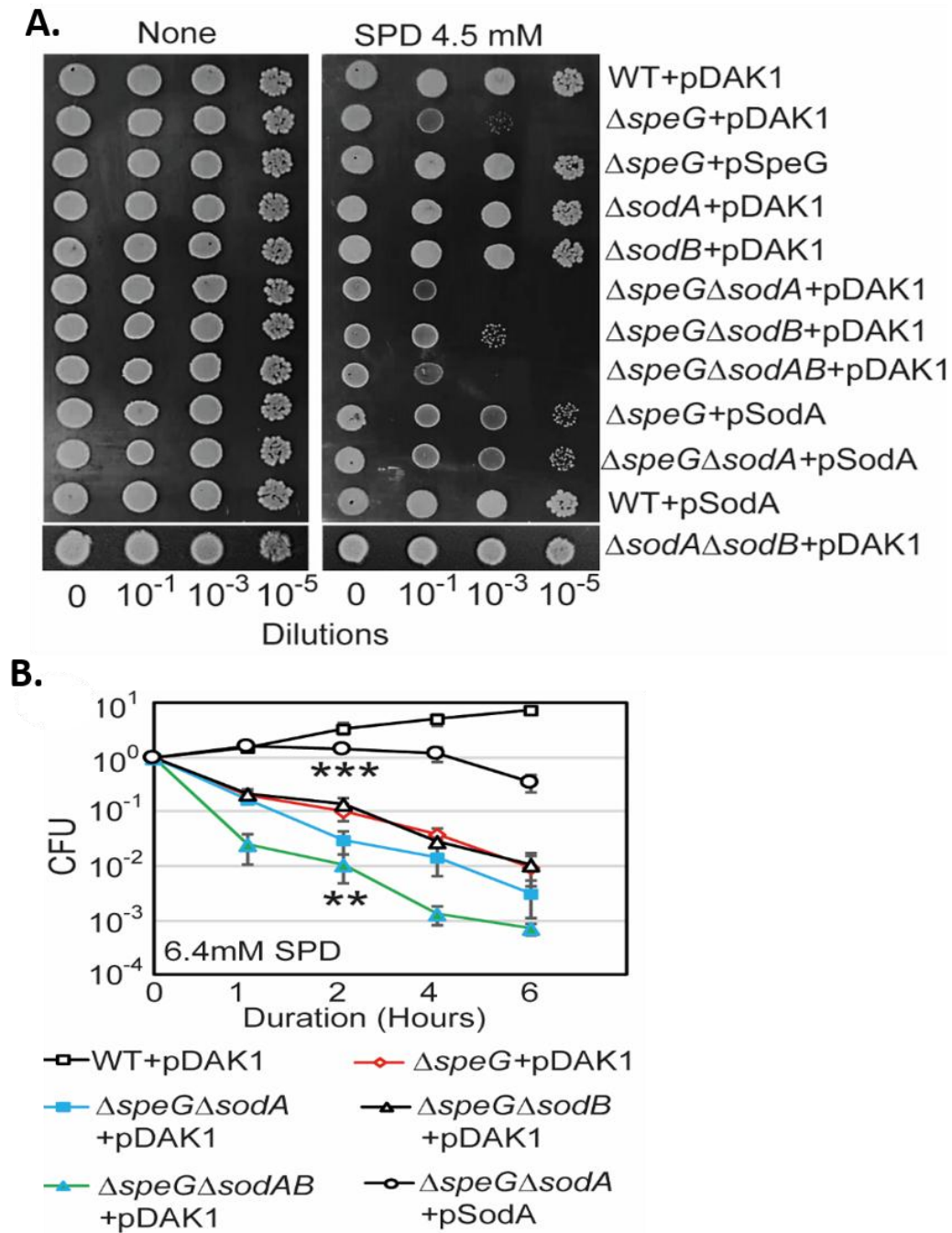


Figure 2.5. Spermidine stress and intracellular ROS in *E. coli*. **A.** Serially diluted *E. coli* cells were spotted on LB-agar plates to show their sensitivity to spermidine. **B.** Viability of different knockout strains was plotted from the CFU counts in different time intervals after treatment with a lethal dose of spermidine. ** and *** are P values generated compared with the values of $\Delta speG$ and $\Delta speG\Delta sodA$, respectively.

$\Delta sodB$, and corresponding double and triple mutants, viz. $\Delta speG\Delta sodA$, $\Delta speG\Delta sodB$, $\Delta sodA\Delta sodB$, and $\Delta speG\Delta sodA\Delta sodB$, were transformed with either empty vector, pDAK1, or pSodA vectors. The $\Delta speG\Delta sodA$ and $\Delta speG\Delta sodA\Delta sodB$ mutants containing empty vector exhibited higher growth defects than $\Delta speG$ strain on LB-agar plate supplemented with spermidine (Figure 2.5A).

However, the cell viability of the double mutants was similar to the $\Delta speG$ strain, while the triple mutant exhibited an accelerated loss of cell viability, in the presence of spermidine (Figure 2.5B). The multicopy induction of SodA from pSodA plasmid suppressed the growth defect in the $\Delta speG$ and $\Delta speG\Delta sodA$ strains (Figure 2.5B). The multicopy induction of SodA and pSodA plasmid also improved the viability of $\Delta speG\Delta sodA$ strain (Figure 2.5B). Unlike $\Delta speG$ strain, the single mutants displays growth and viability similar to the WT strain in the presence or absence of spermidine. This data suggests that the absence of SOD enzymes aggravates O_2^- toxicity in the spermidine-fed $\Delta speG$ strain.

2.3.3. Spermidine stress evokes O_2^- production in $\Delta speG$ strain

Although the above experiments apparently suggested the production of O_2^- anions under spermidine stress, they are not direct and confirmatory, as the ROS probes often react with multiple ROS species (Kalyanaraman et al., 2012). Spermidine transport is a proton motive force (PMF)-dependent process (Kashiwagi et al., 1986). Therefore, the observed narrower ZOI in the presence of spermidine under anaerobic conditions (Figure 2.3D) could also be due to the low PMF under anaerobic conditions. Thus, to determine the relative levels of intracellular O_2^- species, we performed EPR using a cell-permeable cyclic hydroxylamine spin-probe, 1-hydroxy-3-methoxycarbonyl-2,2,5,5-tetramethylpyrrolidine (CMH) (Dikalov et al., 2018). Compared to spin-trap agents, a lower level of CMH reacts at a much faster rate with O_2^- anion, producing highly stable and EPR-sensitive nitroxide radicals (Dikalov et al., 2018). However, peroxyxynitrite and $\bullet OH$ radicals can also oxidize CMH (Dikalov et al., 2018; Thomas et al., 2015).

In the first set of reactions, the unfed and spermidine-fed $\Delta speG$ cells carrying an empty vector were incubated with CMH. In the second set, portions of the unfed and spermidine-fed $\Delta speG$ cells carrying an empty vector were preincubated with dimethyl thiourea (DMTU) and uric acid (UA), the scavengers for the $\bullet OH$ and peroxyxynitrite ($ONOO^-$) radicals, respectively, before CMH addition. In the third set, the unfed and spermidine-fed $\Delta speG$ cells harboring pSodA plasmid were incubated with CMH. In the first set, a high level

of EPR signals were detected with more signals in the unfed sample than the spermidine-fed one (Figure 2.6B and 2.6C). This data indicates that the overall ROS production is higher in the absence of exogenous spermidine, which is consistent with the notion that spermidine is an anti-ROS agent (Balasundaram et al., 1993; Chattopadhyay et al., 2003, 2006; Ha et al., 1998; Ha et al., 1998b; Khan et al., 1992; Khan et al., 1992b; Pegg, 2018; Stewart et al., 2018). In contrast, the EPR signal was higher in the spermidine-fed cells than in unfed ones in the second set (Figure 2.6D and 2.6E), suggesting that the signals represent CMH oxidation by O_2^- anions. Finally, the decrease in EPR signals under the multicopy expression of SodA (Figure 2.6F and 2.6G) suggests that the signals in the second set were indeed generated from O_2^- -mediated oxidation of CMH.

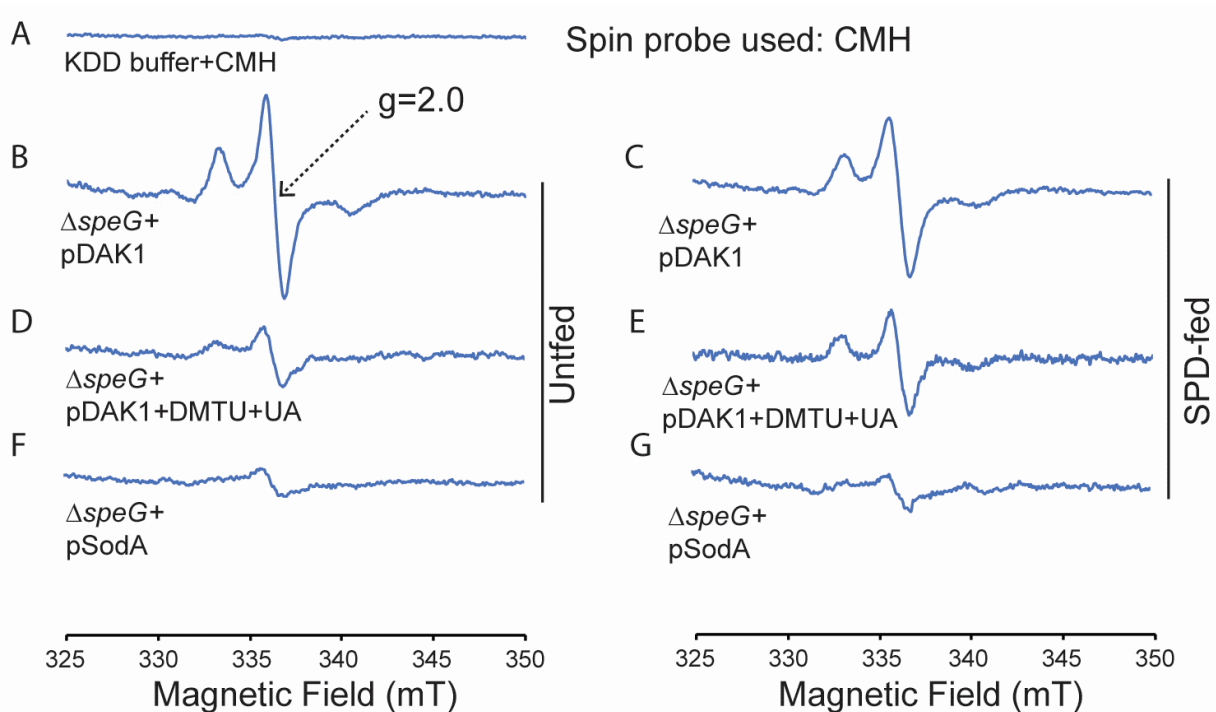


Figure 2.6. Spermidine stress and intracellular ROS in *E. coli*. **A.** CMH probe incubated with KDD buffer before EPR analysis. **B, C, D.** EPR spectra $\Delta speG$ strain with the plasmids pDAK1 (empty vector), or pSodA were grown without spermidine and performed EPR adding CMH probe. **E, F, G.** $\Delta speG$ strain with the plasmids pDAK1 (empty vector), or pSodA were grown with spermidine and performed EPR adding CMH spin probe.

2.3.4. O_2^- production under spermidine stress affects cellular redox state

Antioxidant chemicals, viz. Tyron (Tr), sodium pyruvate (SP), and thiourea (TU) scavenge O_2^- , H_2O_2 , and $\bullet OH$, respectively (Bleeke et al., 2004; Franco et al., 2007). Whereas, N-acetylcysteine (NAC) and ascorbate counterbalance oxidative stress by replenishing

glutathione levels and donating electrons to reducing partners (Nimse and Pal, 2015; Sun, 2010). We showed that Tr, NAC, and ascorbate, but not SP and TU, rescued the spermidine-mediated growth inhibition phenotype (Figure 2.7A). This observation further suggests that the O_2^- stress-derived redox imbalance could be the route of spermidine toxicity.

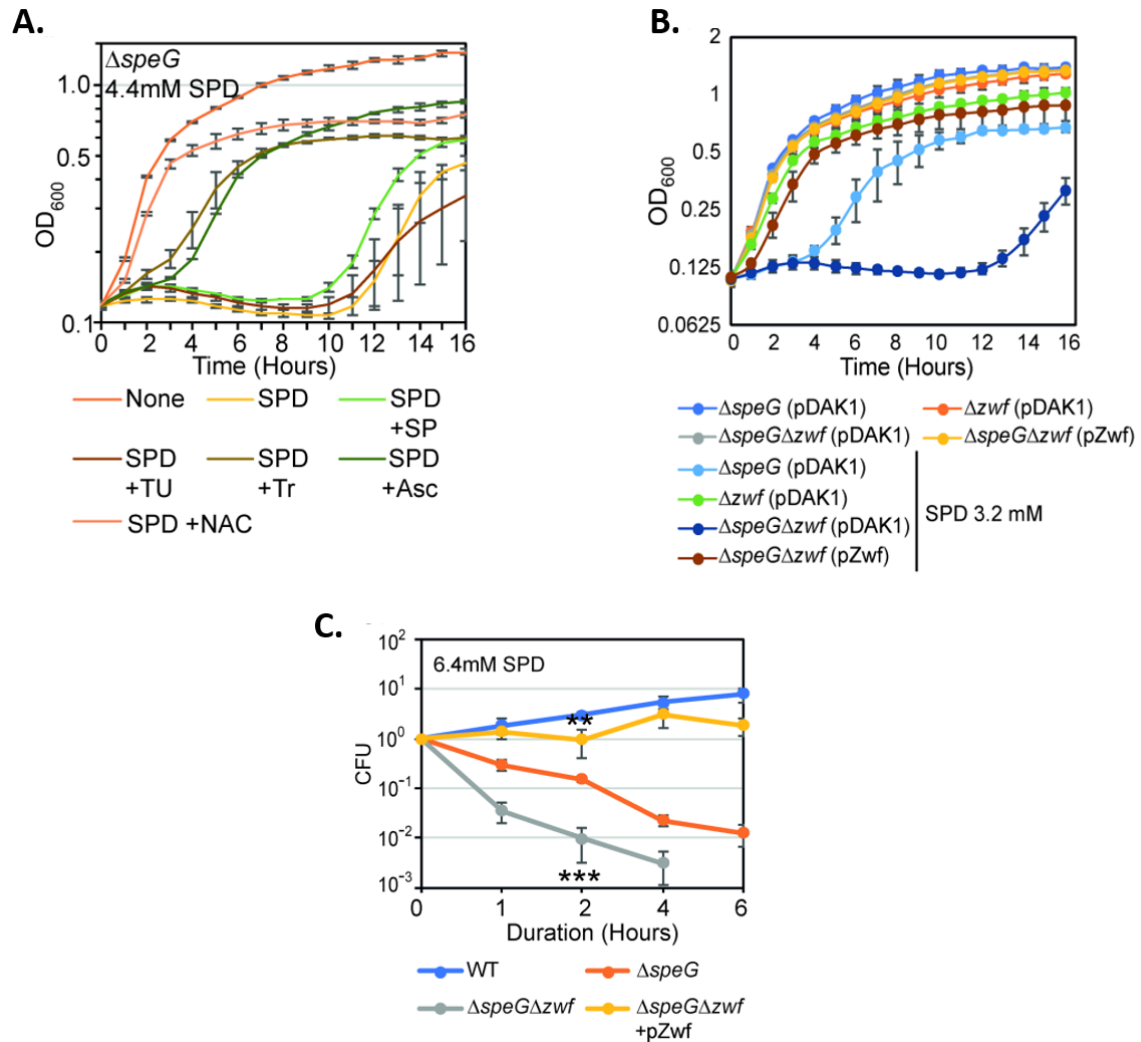


Figure 2.7. O_2^- production affects redox balance in the spermidine-fed $\Delta speG$ strain. A. Growth curves show that Tyron (Tr), Ascorbate (Asc) and N-acetyl cysteine (NAC) can overcome spermidine stress while sodium pyruvate (SP) and Thiourea (TU) fails to do so. **B.** Growth curves show that $\Delta speG\Delta zwf$ strain is hypersensitive to spermidine in comparison to $\Delta speG$ strain. Complementation of $\Delta speG\Delta zwf$ strain with pZwf plasmid overcomes this spermidine hypersensitivity. **C.** CFUs were obtained for different *E. coli* strains pre-treated with spermidine for desired time points and plotted to show the reduced viability of $\Delta speG\Delta zwf$ strain in comparison to the $\Delta speG$ strain.

The reduced nicotinamide adenine dinucleotide phosphate (NADPH) is a potent reducing agent. NADPH drives glutathione and thioredoxin cycles, thereby producing reduced forms of glutathione (GST), glutaredoxins, and thioredoxins to cope up with oxidative stress. A large fraction of NADPH in *E. coli* is provided by a Glucose-6-phosphate

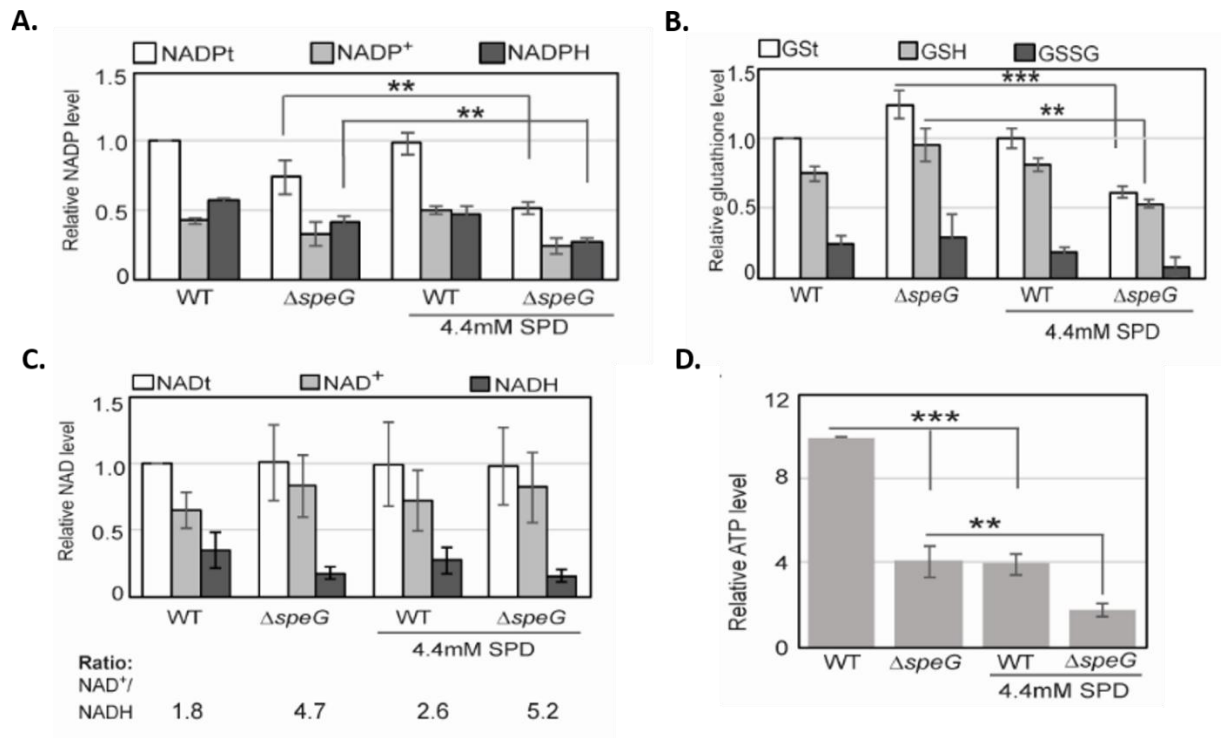


Figure 2.8. O₂⁻ production affects redox balance in the spermidine-fed $\Delta speG$ strain. A. Relative levels of NADPt and NADPH were significantly decreased in the $\Delta speG$ strain under spermidine stress. **B.** Relative levels of GST, GSH, and GSSG were significantly decreased in the spermidine -fed $\Delta speG$ strain. **C.** No significant change in the relative total NAD (NADt), NAD⁺, and NADH levels were recorded. However, NAD⁺ to NADH ratio was significantly increased in the $\Delta speG$ strain compared to WT cells. No further increase of the ratio was observed by adding spermidine in the growth medium of WT and $\Delta speG$ strain. **D.** The relative level of ATP declined in $\Delta speG$ strain and spermidine-fed WT cells in comparison to the unfed WT. spermidine supplementation decreased the ATP level further in the spermidine -fed $\Delta speG$ strain. Error bars in the panels are mean \pm SD from the three independent experiments. Whenever mentioned, the *** and ** denote P values.

1-dehydrogenase (Zwf) catalysed reaction (Olavarría et al., 2012). We observed that both the growth and viability of $\Delta speG\Delta zwf$ double mutant were significantly affected compared to the $\Delta speG$ strain under spermidine stress (Figure 2.7B and 2.7C).

Complementing $\Delta speG \Delta zwf$ with a plasmid, pBAD-*zwf*, rescues the growth defect and mortality under spermidine stress (Figure 2.7B and 2.7C). We compared the levels of the total NADP (NADP_t), total glutathione (GS_t), and their oxidized (NADP⁺ and GSSG) and reduced (NADPH and GSH) species in the WT and $\Delta speG$ strains grown in the absence and presence of spermidine. The relative levels of total and reduced species of NADP and GST were decreased significantly in the spermidine-fed $\Delta speG$ strain (Figure 2.8A and 2.8B). NAD serves as the precursor for NADP production. However, the levels of total (NAD_t), oxidized (NAD⁺), and reduced (NADH) did not alter significantly (Figure 2.8C). Nevertheless, the NAD⁺ to NADH ratio was significantly increased in the $\Delta speG$ strain compared to WT cells (Figure 2.8C). No significant increase in the ratios was observed by adding spermidine in the growth medium of WT and $\Delta speG$ strain (Figure 2.8C). In consistence with the increased ratio of NAD⁺ to NADH, the level of ATP was declined in $\Delta speG$ strain compared to the unfed WT (Figure 2.8D). ATP level was further decreased in the spermidine-fed $\Delta speG$ strain (Figure 2.8D).

2.4. Discussion

We found that the $\Delta speG$ strain of *E. coli* was sensitive to spermidine throughout the growth phase, implying that spermidine acetylation, detoxification, and homeostasis regulation are important for survival and propagation. Our findings explain why spermidine homeostasis is so finely controlled in bacteria. We investigated and validated the notion that spermidine is anti-oxidant (Figures 2.1A). Simultaneously, it presents compelling evidence that excess spermidine, which stays as a free species, induces the generation of hazardous quantities of O₂⁻ radicals in *E. coli* (Figures 2.1B). All the studies earlier were based on ROS dye, which was somehow apparent and nonspecific so, in our study, we use the Spin probe detection method to capture O₂⁻ (Figures 2.1B). Our research illustrates how the horizontal acquisition of the *speG* gene in *S. aureus* USA 300 strain could give the bacteria a harmful advantage. *S. aureus*, a Gram-positive commensal that lives on human skin, frequently causes serious disease when it gains access to deeper tissues. *S. aureus* does not produce spermidine. Furthermore, horizontal transfer of the $\Delta speG$ gene in *S. aureus* USA300 may give an advantage in inactivating host-originated spermidine/spermine, which requires further

investigation. The antioxidants NAC, Tr, and ascorbate restored the $\Delta speG$ strain's spermidine sensitivity.

Furthermore, we show that the presence of a G6PDH enzyme, which plays a function in NADPH in the PPP, is required for the growth of $\Delta speG$ strain. Estimation of NADPH, NADH, and Glutathione supports our argument that spermidine stress affects redox status which further decreases cellular ATP production (Figure 2.8).

CHAPTER III

EFFECT OF SPERMIDINE TOXICITY ON GENE EXPRESSION PROFILE

3.1. Introduction

Spermidine has globally affected cell growth and metabolism process. Polyamines mostly form complex with RNA, thereby affecting various translational steps and stimulating the synthesis of some proteins both *in vitro* and *in vivo* (Igarashi et al., 1974; Atkins et al., 1975; Morris and Igarashi, 1984; Watanabe et al., 1991; Algranati and Goldemberg, 1977; Miyamoto et al., 1993). Polyamines improves the fidelity of ribosomes in polypeptide synthesis by translation (Igarashi et al., 1979; Jelenc and Kurland, 1979). Polyamines also help in the assembly of 30S ribosomal subunits (Igarashi et al., 1981). Thus, polyamines induce the synthesis of OppA, a periplasmic substrate-binding protein of the oligopeptide uptake system (Igarashi et al., 1997). Furthermore, translational upregulation of CyaA (adenylate cyclase), RpoS, FecI, and Fis transcriptional regulators by polyamines indirectly enhances the mRNA production of at least 58 genes (Yoshida et al., 2004). The effects of polyamines on DNA architecture, transcription, phosphorylation of proteins, cell cycle progression, apoptosis, and ion channels are also reviewed (Igarashi and Kashiwagi, 2010). Spermidine has globally affected cell growth and metabolism process. Apart from this, it has a huge impact on the physiology of cells as observed in microarray analysis. The genes that were >2-fold downregulated are involved in flagellar biogenesis, acid resistance, hydrogenase function, nitrogen metabolism, electron transport, aromatic and basic amino acid metabolism, etc. (Figure 3.1). Interestingly, transcription of the genes encoding chaperones, heat shock, and other stress factors (*groL*, *groS*, *dnaK*, *hdeAB*, *ibpAB*, *uspAB*, etc.) was also downregulated under spermidine stress. On the other hand, among the highly upregulated category, the genes that encode for the ribosome, RNA polymerase, transcription factors, DNA polymerase, and enzymes for the fatty acid biosynthesis and ISC biogenesis were prominent.

These observations indicate that apart from inducing O_2^- production discussed in chapter 2, the excess spermidine could interfere with broad cellular processes, such as protein folding and proteostasis, DNA, RNA and lipid metabolisms, and ISC biogenesis. Many operons regulated by Fis and IHF were activated or repressed in presence of spermidine which indicates that spermidine could activate Fis and IHF regulon. It has been found that

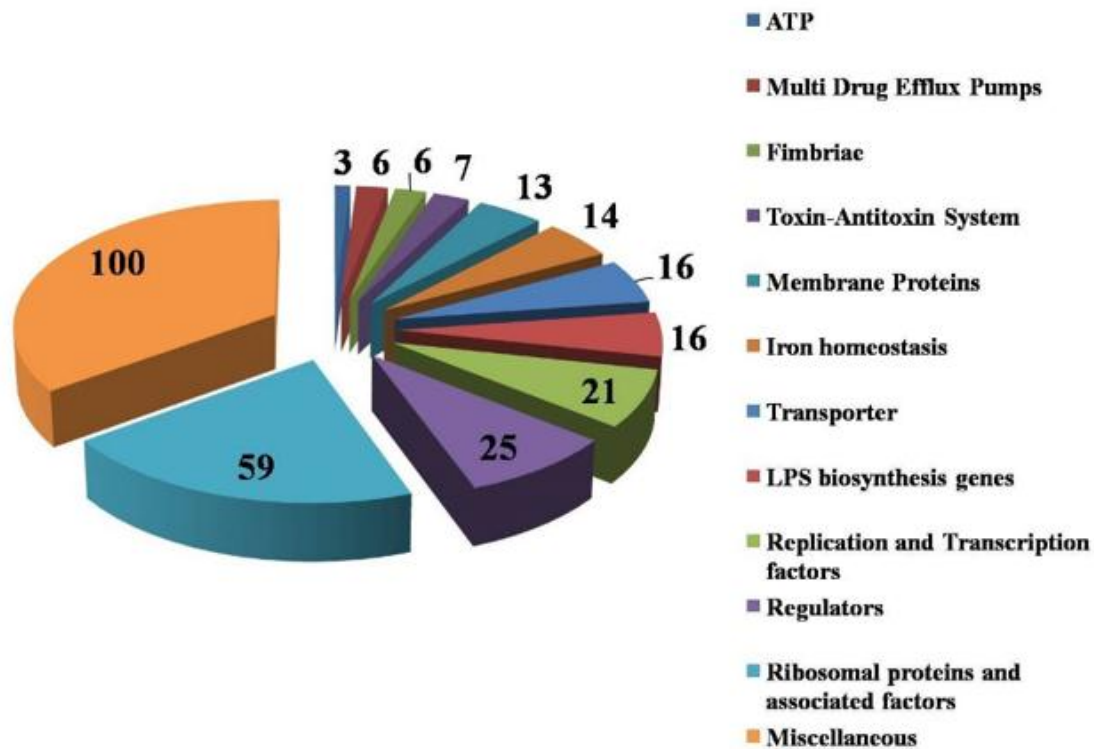


Figure 3.1. Pie chart representing the functional categories of upregulated genes under spermidine stress. (Done by Dr. Vineet kumar, former PhD student, Dr Dipak Dutta lab, CSIR-IMTECH)

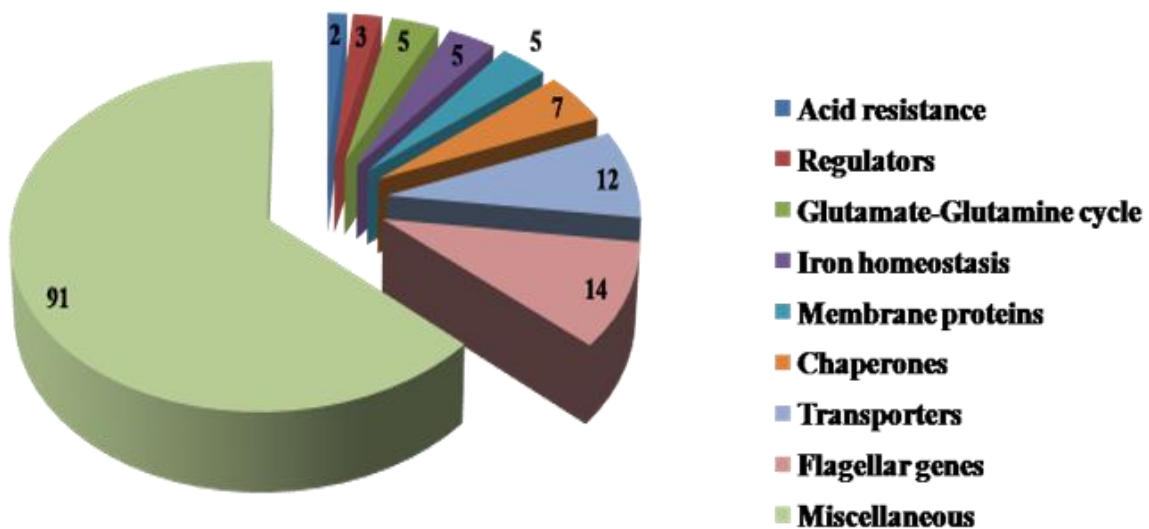


Figure 3.2 Pie chart representing the functional categories of downregulated genes under spermidine stress. (Done by Dr. Vineet kumar, former PhD student, Dr Dipak Dutta lab, CSIR-IMTECH)

polyamines affect the functioning of porins and hence decrease the permeability of the membrane (Iyer and Delcour, 1997; Dela Vega and Delcour, 1996).

A positive correlation between polyamine and polyphosphate accumulation (Motomura and Tomota, 2006). Polyphosphates, in turn, serve as an energy source and act as a buffer against alkaline conditions and metal accumulation (Pick et al., 1990). Since polyamines are highly basic, they can play a very important role in the survival of bacteria under the highly acidic pH of the stomach (Chattopadhyay and Tabor, 2013; Chattopadhyay et al., 2015).

3.2. Materials and Methods

3.2.1. Bacterial strains and broth

Bacterial strains and plasmids used in this study are listed in Appendix Table 1. BW25113 strain of *E. coli* was used as WT in this study. Oligonucleotides were purchased from IDT. Bacterial broths and agar media were purchased from BD Difco. The knockout strains of *E. coli* were procured from the KEIO library (Baba et al., 2006), verified by PCR, and freshly transduced into the WT background by P1 phage. The double and triple knockout mutants were generated following the standard procedure described by Datsenko and Wanner (Datsenko and Wanner, 2000). *E. coli* strain JRG3533 was a generous gift from Dr. Rachna Chaba, IISER Mohali, India. RKM1 strain was constructed by P1 transduction of *sodA-lacZ*:Cm^R genotype of JRG3533 to BW25113 Δ *soxS* strain.

3.2.2. P1 phage preparation and transduction

Overnight culture of donor strain with a suitable antibiotic was diluted 1:100 into 2 ml LB media with 5 mM CaCl₂. The cultures were incubated at 37°C for 30-45 minutes, or until they were slightly hazy. To this culture, 20 µl of P1 phage was added, and was allowed to grow for another 3-4 hours until it became clear. Now 1 ml of culture was transferred to a new microcentrifuge tube, and 40 µl of chloroform was added and vortexed to mix it properly. After that, the culture was centrifuged for 5 minutes at 5000 rpm. The supernatant was transferred to a new centrifuge tube without disturbing the chloroform or any cell debris. This process was repeated thrice, and the lysate was stored at 4°C in fresh MCT with 20 µl chloroform.

For transduction, 2 ml overnight culture of recipient strain was inoculated in LB broth along with 5 mM CaCl₂. The culture was centrifuged for 5 minutes at 5000 rpm. The supernatant was discarded, and the pellet was resuspended in 500 µl LB medium with 2.5 mM CaCl₂ and 20 µl donor phage for 30 minutes at 37 °C without shaking. Cells were again centrifuged and resuspended in 500 µl LB media with 125 mM sodium citrate before

incubation at 30°C for 30 minutes with shaking. Cells were pelleted and dissolved in 100 mM solution of citrate buffer before they were spread on appropriate antibiotic Agar plate.

3.2.3. Plasmid and bacterial constructs

The reporter constructs plasmids, pUA66_*soxS*, pUA66_*ahpC*, and pUA66_*katG*, were gifts from Dr. Csaba Pal, Biological Research Centre of the Hungarian Academy of Sciences (Zaslaver et al., 2006). pBAD-*zwf* was a generous gift from Dr CC. Vasquez, Universidad de Santiago de Chile (Sandoval et al., 2011). *sodA*, *katG*, *ahpC*, and *speG* genes were PCR-amplified by DG12-DG13, RM7-RM8, DG9-DG10, and RK3- RK4 primer pairs (Supplementary file 3), respectively. The PCR products were double-digested at the primer-specific unique restriction sites and inserted into identically digested pET28a (+) plasmid vector so that the 6X His-tagged SodA, KatG, and AhpC proteins are being produced (Appendix Table 2). The protein expression vectors, pET-*sodA*, pET-*ahpC*, and pET-*katG*, were transformed to BL21 (DE3) cells, and expressions were induced by 0.4 mM IPTG. The overexpressed proteins were purified using Ni-NTA beads.

The bacterial strains containing recombinant plasmid were grown overnight at 37°C in 5 mL of LB/Kan broth in a shaker incubator for protein purification. The culture was then subcultured in flasks containing 1 L LB broth with antibiotic and allowed to grow at 37°C until the OD reaches 0.6, before being induced with 0.5 mM isopropyl -D-1-thiogalactopyranoside (IPTG) and continued to grow at 37°C in a shaker incubator for another 3 hrs. The culture was then centrifuged for 15 minutes at 8000 rpm to obtain a cell pellet, which was re-suspended in 30 mL of lysis solution (50 mM Tris-HCl, 200 mM NaCl, pH 8.0) containing 100 µg/ml lysozyme. Sonication was used to lyse the re-suspended cells. The sonicated mixture was treated with 1mM ice cold PMSF and centrifuged for 20 minutes to clear the cell lysate. Ni-NTA matrix was equilibrated by using an equilibration buffer having 50 mM Tris-HCl, 200 mM NaCl, 10% glycerol, pH 8.0. To facilitate binding, the supernatant was added to a Ni-NTA matrix and gently mixed for an hour at 4°C. After binding, the column was washed with 5 column volume of equilibration buffer + 25mM imidazole. The protein was eluted using equilibration buffer + 300 mM imidazole and then dialyzed using Amicon Ultra-15 centrifugal Filter Units (10 kDa for SodA and AhpC protein while 30 kDa for KatG protein).

sodA and *speG* were additionally subcloned in pDAK1, a derivative of pBAD/Myc-HisA vector to get pSodA, and pSpeG multicopy expressions for complementation assays

(Appendix Table 2). We also PCR-amplified *zwf* using RK55-RK56 primer pairs and cloned in the pDAK1 vector to get pZwf vector for complementation assays.

3.2.4. Antibody production

Following the standard protocol, rabbit polyclonal antibodies were raised using the purified proteins. A 1 ml glass syringe has been used to create an emulsion containing 200 g of protein and an equal volume of Freund's complete adjuvant (sigma). A drop of emulsion was floated to the water to assess the emulsion's quality. The NZW rabbit underwent primary immunisation by being injected with 200–300 l of the emulsion. Three weeks later, emulsion of Freund's incomplete adjuvant with purified protein was used as first booster. There was a total of 3-4 boosters administered at an interval of 14-21 days. To confirm the production of antibody, 1mL of blood was drawn after the second booster. A volume of 10 ml blood was collected in a 15 ml centrifuge tube from the marginal ear vein after 5 days of final immunisation and kept at room temperature to allow blood clotting. After 1 hour, the sample was centrifuged at 3000 rpm for 30 minutes to separate the serum from blood. The serum was tested in a blot to check the quality of antibody produced. For further purification of antibody, purified his-tagged proteins were mixed with the serum collected and this mixture was passed through Ni-NTA column (QIAGEN). Pure protein was eluted with 1M MgCl₂.

3.2.5. Determining relative ROS levels in the cells

pUA66_*soxS*, pUA66_*ahpC*, and pUA66_*katG* reporter plasmids were transformed into the *ΔspeG* strain. Cells transformed were grown overnight and diluted 100 times and cultured in the presence or absence of 3.2mM spermidine for 4 hrs. 25 μM Menadione treated cells were used as a positive control for O₂⁻ generation whenever it was specified. After two PBS washes, the cell pellets were dissolved in 500 μl phosphate buffer saline (PBS). Flow cytometry was performed on 0.05 million cells using the F11 laser and FACS Verse (BD Biosciences). We determined the mean fluorescence intensity (MFI) values from three biological replicates.

3.2.6. Quantitative real-time PCR (RT-qPCR)

The Qiagen bacterial RNA isolation kit and the TRIzol® reagent were used to isolate bacterial mRNA. The overnight culture was 100 times diluted and allowed to grow in the presence and absence of 3.2 mM spermidine for 4 hours. Cell lysis was carried out by dissolving 50 mg of cell pellet in 1ml TRIzol® reagent for 5 min at room temperature. The lysate was then mixed with 200 μl of chloroform and kept for another 2 minutes at room

temperature. Cell suspensions were then centrifuged at 13000 rpm for 15 minutes. The upper aqueous layer was transferred to a fresh MCT and 200 µl of ice-cold isopropanol was added to it. This mixture was then incubated in ice for approximately 20 minutes and centrifuged at 13000 rpm for 10 minutes at 4°C. The pellet so obtained was washed with 500 µl of 75% molecular grade ethanol, air dried and then dissolved in 45 µl nuclease-free water along with 1 unit DNase and 0.5 µl RNase inhibitor to eliminate any remaining DNA contaminants. RNA extracted was further purified by using QIAGEN RNeasy® mini kit. A Nano-drop spectrophotometer from Thermo Scientific was used to measure the RNA concentration.

For each reaction, 200 ng of RNA along with gene specific primers were used. GoTaq® 1-Step RT-qPCR System (Promega) was used for RT-qPCR. Non-template reaction mixtures were used as negative controls. At least three independent experiments were conducted for the determination of fold changes from Ct value differences ($\Delta\Delta C_T$) between -fed and unfed samples. A microarray measurement of constitutive expression of *betB* mRNA was used as an internal control to standardize the results.

3.2.7. β -galactosidase and GFP reporter assays

β -gal expression from a single copy *sodA-lacZ* transcriptional fusion was used to quantify promoter activity. Overnight culture of RKM1 strain was 100 times diluted and cultivated with or without 3.2 mM spermidine till mid-log phase. Cells were then incubated for 20' on ice to stop growth. Cell pellets were washed and diluted in 500 µl of Z-buffer (60 mM Na₂HPO₄, 40 mM NaH₂PO₄, 10 mM KCl, and 1 mM MgSO₄). Absorbance of mixture was recorded at 550 nm to get rid of cell debris. 100 µl of sample along with 900 µl Z-buffer was incubated with 100 µl of 4 mg/ml Ortho-nitrophenyl- β -D-galactopyranoside (ONPG) until yellow colour starts to appear. This reaction was terminated by adding 200 µl of 1M Na₂CO₃. The sample was centrifuged twice at 13000 rpm and the supernatant was quantified at 420nm. Enzyme activity was calculated using the following formula.

$$\text{Miller Units} = 1000 \times [(\text{OD}_{420} - 1.75 \times \text{OD}_{550})] / (\text{T} \times \text{V} \times \text{OD}_{600})$$

3.2.8. Western blotting experiments

Overnight cultures of *E. coli* strains were inoculated in fresh LB medium at 1:100 dilution and cultured at 37°C for 1.5 hours. The culture was then treated with 3.2 mM spermidine and incubated for another 2.5 hours. Cells were washed twice with 1X PBS. Bacterial protein extraction reagent (B-PER® Thermo Scientific) along with 100 µg/ml lysozyme and 2 units/ml DNase 1 was used to harvest and lyse cells. The Bradford assay kit

(Bio-Rad) was used to determine the total protein level. SDS-PAGE was used to separate 40 µg of total cellular proteins from each sample. To visualize protein resolution and equal loading in the PAGE, the proteins were transferred to a 0.22 µm nitrocellulose blotting membrane (Amersham, GE Healthcare Life Sciences) by using a semi-dry transfer method using ATTO semi-dry transfer apparatus at 10V for 45 minutes. To check the equal load of each protein lysate, the transferred Nitrocellulose membrane was stained with Ponceau S (sigma). The membrane was then washed with 1XTBST (20mM Tris-HCL, 150mM NaCl, 0.5% Tween20, pH 8.0). The nitrocellulose membrane was then immersed in 10 ml blocking buffer (5% Skimmed milk in 1X TBST buffer) for 1 hr at room temperature. The membrane was then washed thrice with 1X TBST buffer. The blotting membrane was incubated overnight with 1:5000 diluted primary antibody in shaking condition at 4°C. Next day, membrane was washed thrice with 1X TBST (10 minutes per wash). After washing, the membrane was incubated with 1:10000 diluted secondary antibody and kept at room temperature for an hour. After incubation, the membrane was further washed thrice with 1X TBST. Immobilon[®] Forte Western HRP substrate (Millipore) was used to develop the blot.

Polyclonal rabbit primary antibodies and HRP conjugated secondary antibodies were used for Western blotting and dilution of both primary and secondary antibody was done in 1X TBST.

3.3. Results

3.3.1. Spermidine blocks the induction of SoxR regulon

To understand the global impact of spermidine toxicity, we performed a microarray experiment on the *AspeG* strain in the presence and absence of spermidine. The genes that were >2-fold downregulated are involved in flagellar biogenesis, acid resistance, hydrogenase function, nitrogen metabolism, electron transport, aromatic and basic amino acid metabolism, etc. (Figure 3.2). Interestingly, transcription of the genes encoding chaperones, heat shock, and other stress factors (*groL*, *groS*, *dnaK*, *hdeAB*, *ibpAB*, *uspAB*, etc.) was also downregulated under spermidine stress (Supplementary file 1). On the other hand, among the highly upregulated category, the genes that encode for the ribosome, RNA polymerase, transcription factors, DNA polymerase, and enzymes for the fatty acid biosynthesis and Fe-S cluster biogenesis were prominent.

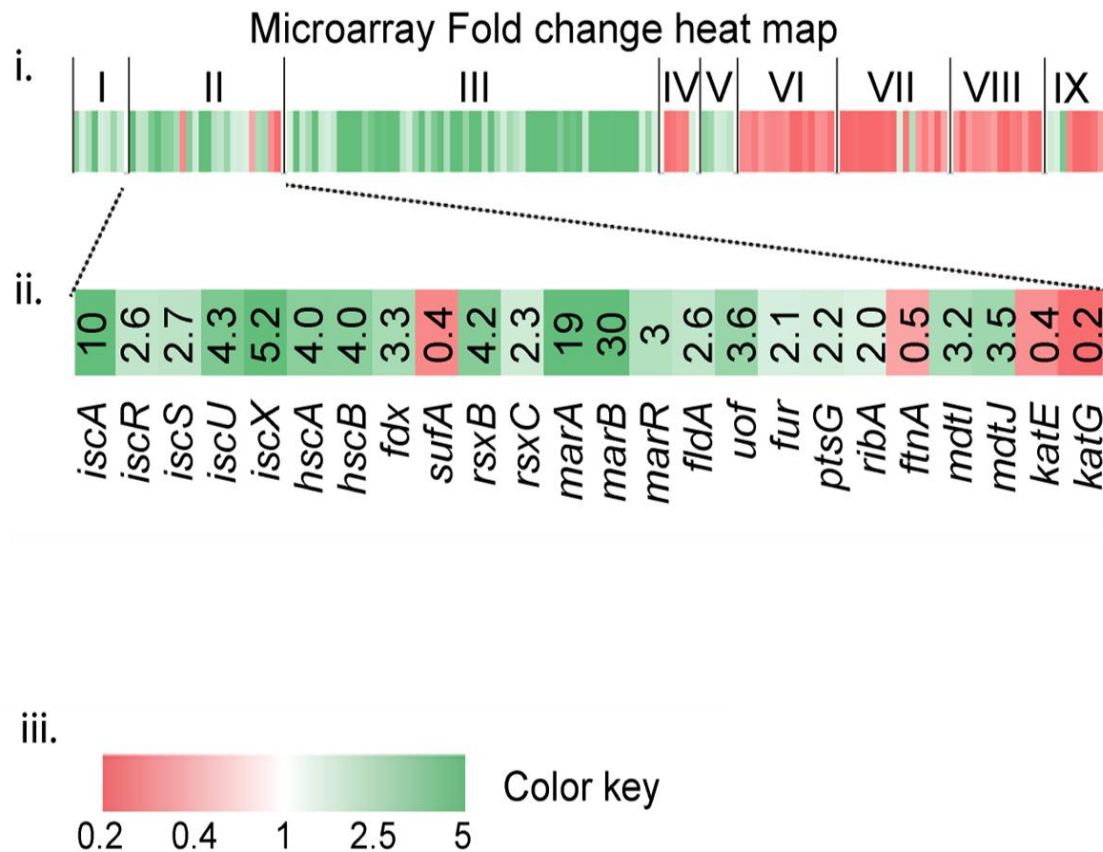


Figure 3.3. Microarray heat map showing various categories of genes I: Replication and transcription-associated genes, II: Fe homeostasis, ROS, multidrug resistance, and sugar metabolism genes, III: Ribosomal and ribosome biogenesis-associated genes, IV: Oxidoreductase and ATP synthesis genes, V: Fatty acid metabolism-related genes, VI: Flagellar biogenesis-related genes, VII: Acid resistance and chaperone genes, VIII: Hydrogenase and nitrogen metabolizing genes, IX: Amino acid metabolizing genes; see Supplementary file 1) that were differentially expressed under spermidine stress. (ii) Zoomed in the heat map of the category II genes responsible for Fe metabolism and reactive oxygen species (ROS) regulation. (iii) Color key represents the expression fold-change (FC) of the genes.

Fe-S center of SoxR senses the levels of cellular O_2^- or NO (Fujikawa et al., 2017; Hidalgo and Demple, 1994; Kobayashi, 2017; Liochev and Fridovich, 2011; Lo et al., 2012) and triggers transcription of a set of genes, including *soxS*, *sodA*, and *zwf* (Touati, 2000; Wu and Weiss, 1992). Surprisingly, none of the three critical genes was found to be activated in the microarray. RT-qPCR analyses verified the unaltered expression of *soxS*, *sodA*, and *zwf*

under spermidine stress (Figure 3.4B). Consistently, using $\Delta speG$ harboring pUA66_*soxS*, a reporter plasmid expressing *gfpmut2* from the *soxS* promoter (P_{soxS} -*gfpmut2*), and RKM1 strain containing a chromosomally fused *lacZ* reporter under *sodA* promoter (P_{sodA} -*lacZ*) (Appendix Table 1), we did not find any transcriptional activation of *soxS* and *sodA* promoters (Figure 3.4C and 3.4D). Therefore, we suspected whether spermidine in excess blocks the O_2^- -mediated activation of SoxR, thereby aggravating O_2^- toxicity. However, an alternative explanation for this observation would be that the redox cycling drugs, but not O_2^- , are the efficient activators of SoxR (Gu and Imlay, 2011b). Therefore, we used menadione, a redox cycling agent and O_2^- generator, to observe the P_{soxS} -*gfpmut2* reporter induction and chased it by spermidine in the $\Delta speG$ strain. Spermidine also suppressed the menadione-induced GFP reporter fluorescence (Figure 3.4C), suggesting that spermidine indeed blocks SoxR-mediated activation of *soxS* in *E. coli*. Among other ROS-responsive genes, the catalase coding genes (*katE* and *katG*) were downregulated, (Figure 3.1) while no change was observed in the expression of *ahpCF* genes under spermidine stress (GEO accession #154618). Using pUA66_*ahpC* and pUA66_*katG* reporter plasmids (P_{ahpC} -*gfpmut2* and P_{katG} -*gfpmut2*, respectively), we validated these microarray observations (Figure 3.3A).

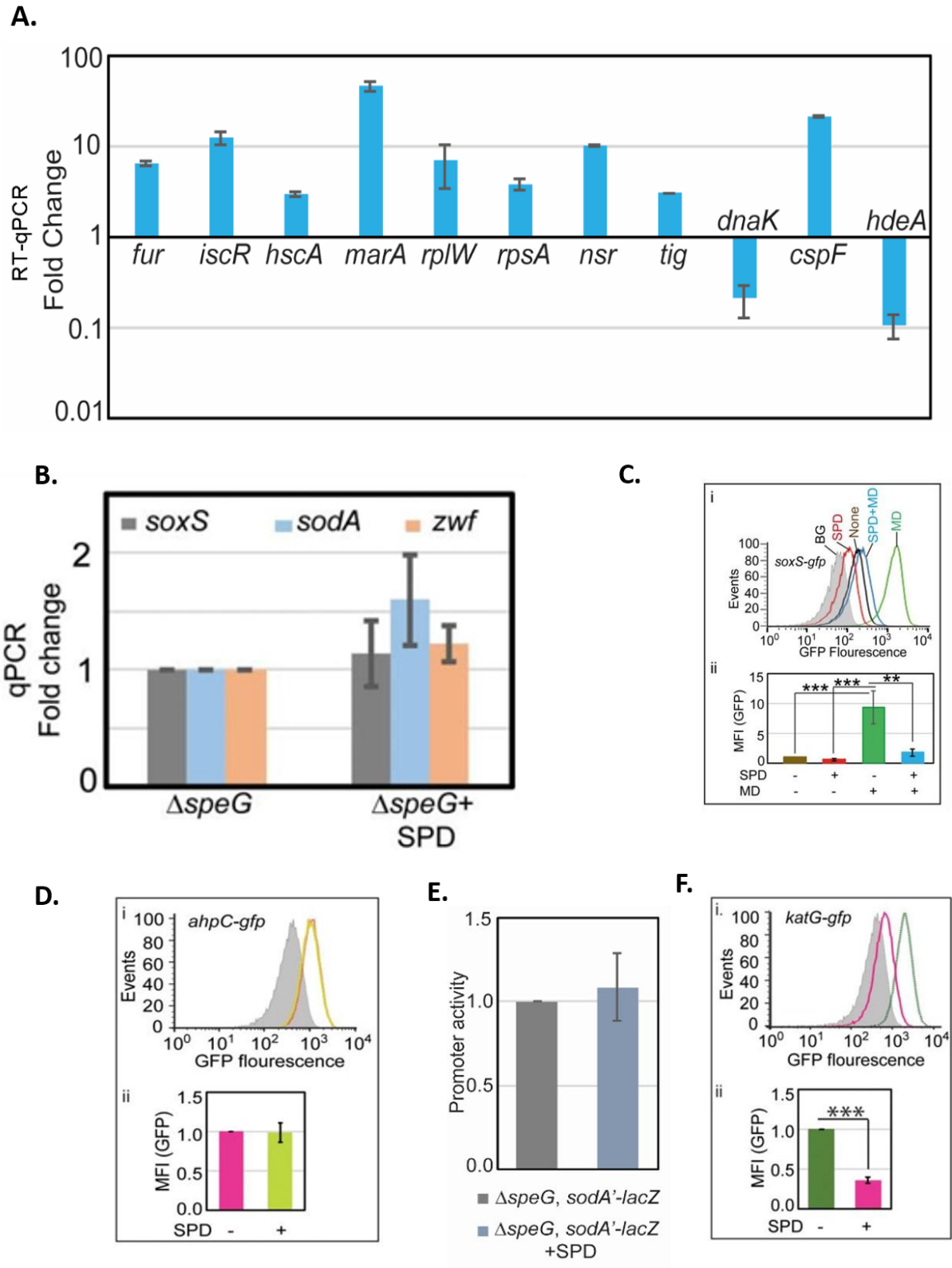


Figure 3.4. Validation of Microarray data.

A. Microarray data was validated by performing RT-qPCR against some of the genes that were up or down-regulated in the Microarray. **B.** RT-qPCR data to show that the spermidine

stress does not alter the expression of *soxS*, *sodA*, and *zwf* genes in the Δ *speG* strain. **C.** Flow cytometry experiments determined that spermidine stress does not upregulate P_{soxS} -*gfpmut2* reporter in the Δ *speG* strain. The upper portion of the panel (i) represents a flow cytometry histogram. Grey area is background fluorescence of the Δ *speG* cells. The areas within saffron-line and blue-line represent GFP fluorescence in the absence and presence of spermidine, respectively. The bar diagram in the lower part of the panel (ii) exhibits relative MFI values calculated from three independent flow cytometry experiments. **D.** β -galactosidase reporter assay shows that the promoter activity of *sodA* gene remains unchanged under spermidine stress. **E.** Flow cytometry experiments were performed to show that spermidine stress does not upregulate P_{ahpC} -*gfp* reporter in the Δ *speG* strain. The subpanel (i) represents a flow cytometry histogram of background fluorescence of the Δ *speG* cells (grey area). The pink-lined and green-lined areas of histogram represent fluorescence in the absence and presence of spermidine, respectively. The bar diagram in the subpanel (ii) exhibits relative MFI values calculated from three independent flow cytometry experiments. **F.** Flow cytometry experiments show that spermidine stress downregulates P_{katG} -*gfp* reporter expression in the Δ *speG* strain. The subpanel (i) represents the histogram of background fluorescence of the Δ *speG* cells (grey area). The green-lined and pink-lined areas of the histogram represent GFP fluorescence in the absence and presence of spermidine, respectively. The bar diagram in the lower part of panel (ii) exhibits relative MFI values in the presence or absence of spermidine calculated from three independent flow cytometry experiments. *** denotes P value <0.001; unpaired T-test.

Consistent with the microarray expressions, our western blotting experiments exhibited the unchanged expression of SodA and a decreased expression of KatG in the spermidine-treated Δ *speG* strain compared to untreated counterparts (Figure 3.5A and 3.4B). However, SodA level was slightly elevated in the Δ *speG* strain, and the spermidine-treated WT strain, in contrast to the untreated WT strain (Figure 3.5A). Contrary to the microarray data, a profound increase in AhpC level was observed (Figure 3.5C). while growing WT or Δ *speG* cells in the presence of spermidine, indicating a translational elevation of AhpC level under spermidine stress (Figure 3.5C).

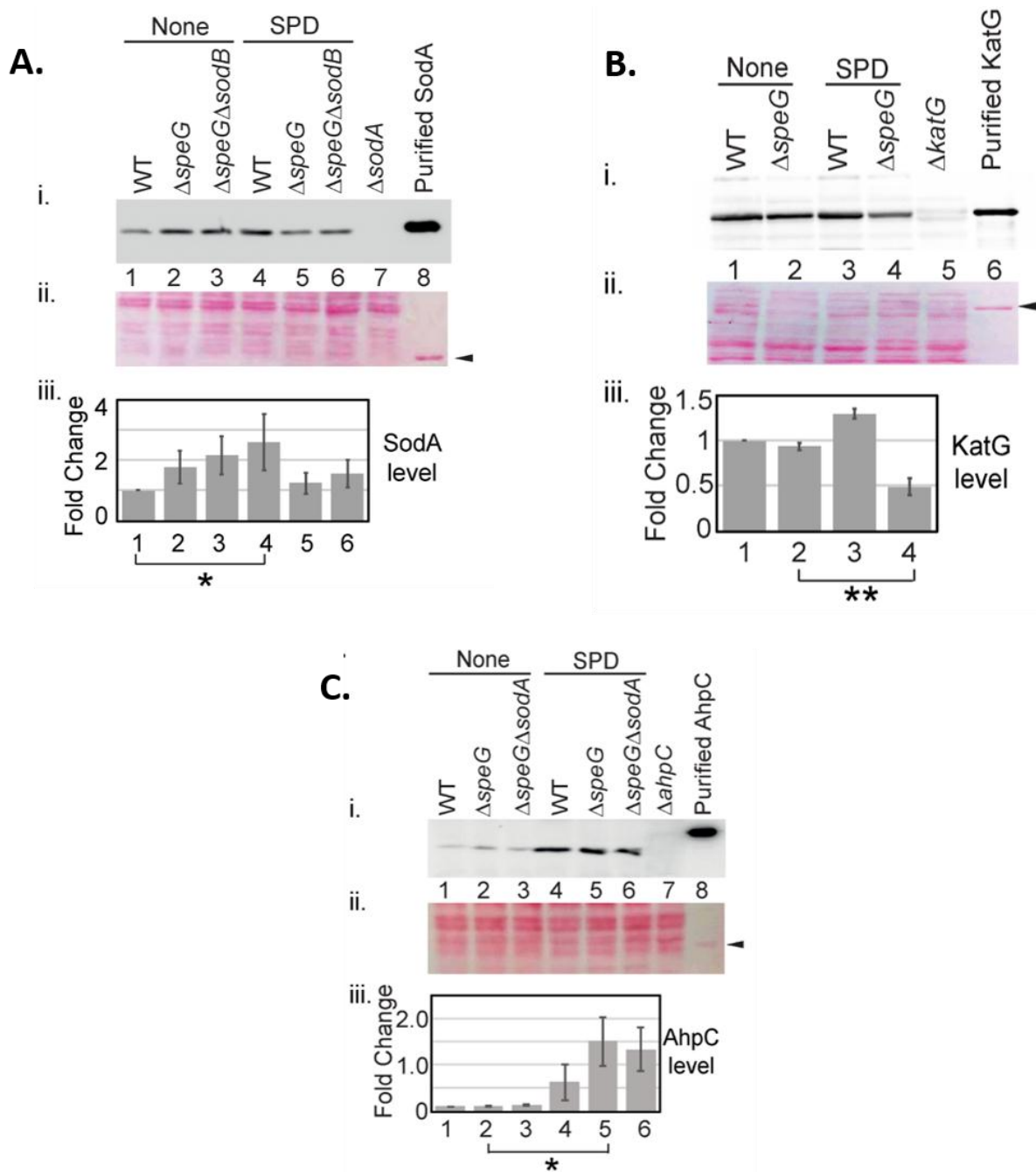


Figure 3.5. Western blotting experiments show SodA, KatG, and AhpC levels in the various strains in the presence or absence of spermidine; (i) developed blot, (ii) ponceau S-stained counterpart of the same blot, (iii) The bar diagrams represent relative fold change (FC) of the proteins under spermidine stress. The relative FC values were calculated from the band intensity values obtained from three independent blots in comparison to the untreated WT counterparts. Purified 6X his-tagged SodA, KatG and AhpC proteins were loaded as positive controls. The cellular protein extracts from Δ sodA, Δ katG and Δ ahpC strains were used for negative controls.

3.4. Discussion

In our previous study, we observed that spermidine, despite being an anti-ROS drug, spermidine causes O_2^- production inside the cell when it is over-accumulated (Fujikawa et al., 2017; Hidalgo and Demple, 1994; Kobayashi, 2017; Liochev and Fridovich, 2011; Lo et al., 2012). The Fe-S core of SoxR monitors the levels of cellular O_2^- or NO and causes transcription of a number of genes, including *soxS*, *sodA*, and *zwf* (Touati, 2000; Wu and Weiss, 1992). Surprisingly, the microarray analysis revealed that none of the three important genes were active (Figure 3.4C). This observation is consistent with the previous finding that redox cycling drugs, but not O_2^- are the efficient activators of SoxR function (Gu and Imlay, 2011). Menadione, a redox cycling drug, inhibited SoxR expression even when spermidine was present (Figure 3.4C). These two findings suggest that free spermidine may interfere with SoxR maturation by preventing the development of its Fe-S cluster. Because of this, apo-SoxR did not respond to the O_2^- or redox cycling medications, failing to activate the SoxR regulon genes. Another possibility is that an excess of spermidine might prevent SoxR from binding to the *soxS* and *sodA* promoter regions, thereby activating the genes (Igarashi and Kashiwagi, 2000; Jung and Kim, 2003; Miyamoto et al., 1993). Spermidine interacts with DNA ubiquitously and modulates gene expression in a variety of ways. Alternately, spermidine-mediated activation of *rsxA* and *rsxB* (Figure 3.1), which encode the essential elements of the ISC reduction enzyme, could cause inhibition of SoxR activation.

The protein expression of SodA, that neutralises O_2^- to less reactive H_2O_2 was found to be unchanged (Figure 3.5A) whereas the level of catalase (KatG) was decreased in presence of spermidine (Figure 3.4B). Increased AhpC levels indicates the activation of the alkyl hydroperoxidase (AhpCF) enzyme. The declined H_2O_2 level could be attributed to the slower rate of O_2^- anion dismutation due to the failure of SodA activation and the activation of alkyl hydroperoxidase (AhpCF) that neutralizes H_2O_2 , could be responsible for the decline in cellular H_2O_2 levels (discussed in Chapter 2). Thus, declined H_2O_2 concentration could be the limiting factor for the cellular $\bullet OH$ radical production under spermidine stress.

Spermidine has shown a diverse array of function. In our microarray data, apart from Fe metabolism, the genes that encode for the RNA polymerase, transcription factors, DNA polymerase, and enzymes for the fatty acid biosynthesis were prominent that suggests spermidine has many more roles in biological system that still to be investigated.

CHAPTER IV

BIOCHEMICAL IMPACT OF SPERMIDINE TOXICITY ON FE HOMEOSTASIS

4.1. Introduction

Polyamine frequently mimics the effects of cationic molecules such as Ca^{2+} and Mg^{2+} by competing for the same binding sites on receptors, enzymes, and membranes. As a result, polyamines may influence signal transmission and enzyme activity. Polyamines, for example, compete with Ca^{2+} for anionic sites on phospholipid membranes, altering receptor-mediated signal transduction and transmission (Koenig et al., 1987). Similarly, polyamines replace the ribosome's Mg^{2+} ion, which is necessary for translational operation (Ogasawara et al., 1989; Igarashi and Kashiwagi, 2015). Polyamines can also form complex with a variety of metal ions such as Ni^{2+} , Co^{2+} , Cu^{2+} , Fe^{2+} , and Zn^{2+} (Lovaas, 1997; Hares et al., 1956; Bertsch et al., 1958;). Polyamine's natural property as metal chelators has largely gone unnoticed by biologists. Furthermore, polyamines have an effect on Fe homeostasis in CHO cell lines (Gaboriau et al., 2004). Polyamines activate the translational expression of many genes, including *oppA*, *fecI*, *fis*, *rpoS*, and others (Yoshida et al., 2004). Subsequent research has confirmed that polyamines influence Fe transport in a variety of ways (Gaboriau et al., 2004). Polyamines regulate Fe uptake in *E. coli* through activating FecI, as evidenced by the enhanced transcription of *fecABCDE* mRNAs (Yoshida et al., 2004). It appears that polyamines play a significant role in metal ion homeostasis and function. Many major metalloenzymes require Mn^{2+} and Fe^{2+} to function properly. Fe and Mn dependent SODs catalyse O_2^- disproportionation using relatively comparable protein scaffolds and virtually identical active regions. Mn is essential metal under oxidative stress and Fe deficiency. Mn fights oxidative stress by activating Mn-SOD or SodA in *E. coli*. that keeps Fe-dependent enzymes functional (Anjem et al., 2009; Anjem and Imlay, 2012). Mn replaces Fe to restore the activities of various non-redox Fe-dependent enzymes in *E. coli*, including ribulose-5-phosphate-3-epimerase, peptide deformylase, threonine dehydrogenase, and cytosine deaminase. *E. coli* exposed to oxidative stress (Anjem and Imlay, 2012). When the Fe-dependent ribonucleotide reductase (NrdAB) in *E. coli* becomes nonfunctional due to Fe deficiency or oxidative stress, an alternative Mn dependent ribonucleotide reductase (NrdEF) largely restores DNA replication. Fe and manganese are substituted in similar or identical protein frameworks in enzymes such as epimerases, which are hypothesised to employ Fe^{2+}

as a Lewis acid under normal development conditions but switch to Mn^{2+} under oxidative stress (Martin et al., 2015).

4.2. Material and Methods

4.2.1. Bacterial strains and chemicals

BW25113 strain of *E. coli* was used as WT in this study. Oligonucleotides were purchased from IDT. Bacterial broths and agar media were purchased from BD Difco. The knockout strains of *E. coli* were procured from the KEIO library (Baba et al., 2006), verified by PCR, and freshly transduced into the WT background by P1 phage. The double and triple knockout mutants were generated following the standard procedure described by Datsenko and Wanner.

4.2.2. Aconitase activity

For aconitase activity, mid log phase cell was pelleted and resuspended in 1 ml of lysis buffer (1mM Tris-HCl, pH 8.0, 0.1 M KCl, 1mM PMSF, 0.6 μ g/ μ l lysozyme) . Cell lysis was done by freeze thaw in LN2 followed by, centrifugation at 13000 rpm for 10 min. The reaction mixture was made by adding 100 μ g of protein to 200 μ l 1X assay buffer (600 μ M $MnCl_2$, 25 mM sodium citrate, 250 μ M NADP and 50 mM Tris- HCl, pH 7.6). Absorbance was recorded at 340 nm.

4.2.3. ICP-MS analysis to estimate cellular Fe and Mn content

To determine the intracellular Fe and Mn concentration, overnight grown cells were diluted 100 times in LB media and cultured for 4 hours with and without spermidine treatment. Cell pellets were obtained by centrifuging the cells at 6,000 rpm for 6 minutes, after which they were pelleted and washed twice with 1X PBS supplemented with 1mM EDTA, and with 1X PBS. The Fe content was estimated at the ICP-MS facilities of the Punjab Biotechnology Incubator in Mohali, India. In brief, bacterial pellet was digested by using 5 mL of concentrated nitric acid and 0.5 mL of 30% H_2O_2 . Following digestion, the volume was increased to 50 ml with deionized water and the samples were tested for metals using ICP-MS. The microgram quantities of Fe and Mn per gram of cell pellets were plotted.

4.2.4. Spot assay

Overnight diluted culture was grown for 4 hours with and without treatment of spermidine. The concentration of spermidine used was 3.2 mM. $\Delta speG$ strain was grown under three different conditions; $\Delta speG$, $\Delta speG$ with 4.2 mM spermidine and $\Delta speG$ with 4.2

mM supplemented with 2mM Fe. Cells were serially diluted as 0, 10^{-2} , 10^{-4} , and 10^{-6} . 10 μ l of each dilution were used for spotting on LB Agar plate. The plate was kept overnight at 37°C.

In another set of experiment, overnight grown single and double mutant strains were spotted in similar way on LB Agar supplemented with spermidine to determine relative sensitivity.

4.2.5. RNA isolation

The Qiagen bacterial RNA isolation kit and the TRIzol® reagent were used to obtain bacterial mRNA. 50 mg of cell pellet were washed twice with nuclease free water and dissolved in 1ml TRIzol® reagent and allowed for 5 min to lyse the cell. 200 μ l of chloroform was added to the suspension and allowed another 2 minutes. Cell suspensions were then centrifuged at 13000 rpm for 15 minutes. The upper aqueous layer was then separated and transferred to fresh MCT. 200 μ l of ice-cold isopropanol was then added and the mixture was then kept on ice for 20 minutes. The samples were then centrifuged at 13000 rpm for 10 minutes at 4 °C. The RNA gets precipitated to form a pellet on the bottom of the MCT. Pellets were further washed with 500 μ l of 75% molecular grade ethanol. The pellets were then briefly air dried and dissolved in 45 μ l nuclease-free water along with 1 unit DNaseI, 5 μ l 10X DNaseI buffer and 0.5 μ l RNase inhibitor to eliminate any remaining DNA contaminants. RNA extracted was further purified by using QIAGEN RNeasy® mini kit. A Nano-drop spectrophotometer from Thermo Scientific and a UV-1800 Shimadzu UV-spectrophotometer were used to measure the RNA concentration.

4.2.6. Isothermal titration calorimetry

A MicroCal VP-ITC calorimeter, MicroCal Inc, was used for calorimetric measurements to probe the interaction of spermidine with Fe^{2+} and Fe^{3+} species. In order to achieve this, 100 μ M of spermidine solution was prepared in 20 mM sodium acetate buffer (pH 5.5) and add into the sample cell. The ligands (2.1 mM of FeCl_3 and ferrous ammonium sulfate) were also dissolved in the identical sodium acetate buffer. To avoid entrapment of any air bubble, the solutions were centrifuged at 13000 rpm for 10 minutes. The titrations involved 30 injections of individual ligands (5 μ l per shot) at 300 s intervals into the sample cell containing 1.8 ml of 100 μ M spermidine. The titration cell was kept at two different temperature (4°C and 25 °C) and stirred continuously at 286 rpm. The heat of dilution of ligand in the buffer alone was subtracted from the titration data. The data were analysed using Origin 5.0 software.

4.2.6. 2,2'-Bipyridyl and NBT assays

2,2'-Bipyridyl is a chemical compound that chelates Fe^{2+} and produces pink colour. The standard curve for 0 μM to 350 μM of Fe^{2+} ion was generated simply by recording A_{522} in the presence of 2,2'-Bipyridyl. Dissolved oxygen of medium and headspace oxygen was replaced by flushing N_2 gas in the medium for 5 minutes to create an anoxic condition as described (Stieglmeier et al., 2009). To check whether spermidine acts as a catalyst for Fe^{2+} to Fe^{3+} oxidation, we performed 2, 2'-bipyridyl assays probing leftover Fe^{2+} after the reaction. For this assay, 100 μM of spermidine was incubated with increasing concentrations (25 μM to 350 μM) of ferrous ammonium sulphate for 10 minutes at room temperature. 900 μl of the reaction products were mixed with 90 μl 4M sodium acetate buffer (pH 4.75) and 90 μl bipyridyl (0.5% in 0.1N HCl). The colour formation was recorded at 522 nm (A_{522}) using UV-1800 Shimadzu UV-spectrophotometer. In another experiment, the assay was performed in anoxic condition using rubber capped sealed glass vials containing anoxic reactants and needle-syringe-mediated mixing of the reagents. Here, three different concentrations (100 μM , 200 μM , and 300 μM) of ferrous ammonium sulphate were allowed to react with 100 μM of spermidine for 10 minutes. The standard curve for 0 μM to 350 μM of Fe^{2+} ion was generated simply by recording A_{522} of the mixture of 900 μl ferrous ammonium sulphate, 90 μl sodium acetate buffer, and 90 μl bipyridyl solutions.

We used Nitro blue tetrazolium (NBT) dye to probe whether spermidine-stimulated Fe^{2+} to Fe^{3+} oxidation liberates O_2^- anion *in vitro*. For this assay, different concentrations of Fe^{2+} were incubated with 100 μM of spermidine for 2 minutes. 100 μl of NBT (5 mg/ml) was added to the mixture and incubated at RT for another 5 minutes. The absorbance was recorded at 575 nm using UV-1800 Shimadzu UV-spectrophotometer.

Fe oxidation in the presence of RNA and spermidine was performed as described by Tadolini (1988a). 1 μg RNA and increasing concentrations of spermidine (10 μM -200 μM) were used in 5 mM MOPS buffer, pH 7.4. The oxidation was started adding 200 μM FeCl_2 . The reaction was incubated for 3 minutes at room temperature in triplicate in a 96 well plate. The reactions were terminated at desired time point by adding a stop solution (1:1 4M sodium acetate:4M glacial acetic acid) followed by 2,2'-Bipyridyl to detect Fe^{2+} levels. The absorbance was recorded at 522 nm using BIOTEK plate reader.

4.3. Results

4.3.1. Spermidine affects ISC biogenesis

O_2^- has the potential to oxidize the solvent-exposed Fe-S clusters of *E. coli* dehydratases, aconitase, and fumarase enzymes to liberate free Fe^{2+} (Benov, 2001; Fridovich,

1986; Imlay, 2008). Therefore, supplementation of Fe^{2+} ions helps to repair the damaged clusters (Gardner and Fridovich, 1992; Imlay, 2008). Consistently, we observed that the declined aconitase activity in the spermidine-stressed ΔspeG strain was rescued by supplementing Fe^{2+} ion (Figure 4.1A). Besides, the intracellular level of Fe in the ΔspeG strain was decreased more than 3-fold in the presence of spermidine (Figure 4.1B). Consequently, the addition of Fe^{2+} salt in the LB-agar plate rescued the growth of spermidine-fed ΔspeG strain supports this claim (Figure 4.1C). Interestingly, the Fe content in the *S. aureus* strains was found to be substantially lower than the *E. coli* WT cells (Figure 4.1B). Furthermore, while the Fe content of USA300 strain remained indifferent, the Fe content of RN4220 strain was significantly declined under spermidine stress (Figure 4.1B)

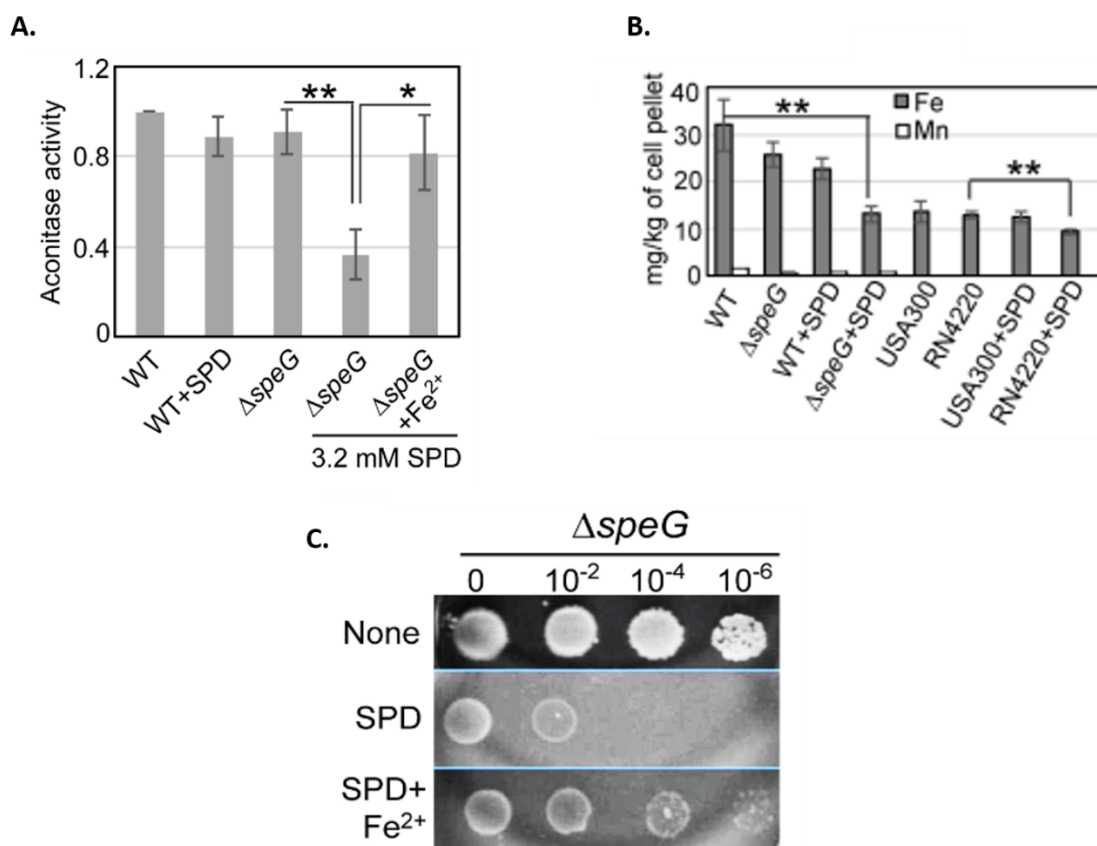


Figure 4.1. Spermidine-mediated O_2^- radical production affects Fe metabolism. **A.** The bar diagram represents relative aconitase activity in the *E. coli* WT and ΔspeG strains in the presence and absence of spermidine (spermidine). **B.** Intracellular levels of Fe and Mn levels for *E. coli* strains, and Fe levels for *S. aureus* strains determined in the presence or absence of spermidine stress were plotted. **C.** Spot assay using serially diluted ΔspeG cells demonstrated that Fe^{2+} can rescue spermidine stress (Reference - Dr. Vineet kumar's thesis, former PhD student, Dr Dipak Dutta lab, CSIR-IMTECH).

The Fe scarcity was also reflected in the gene expression pattern of IscR regulon in our microarray data (mentioned in Chapter 3). IscR forms a functional holoenzyme with the Fe-S cluster. The de-repression of ISC biogenesis operon (*iscRSUA-hscBA-fdx-iscX*) in the microarray signifies the presence of non-functional apo-IscR under the scarcity of cellular Fe²⁺ ion (Esquilin-Lebron et al., 2021; Schwartz et al., 2001). Besides, apo-IscR and apo-Fur activates and derepresses the alternative ISC assembly system (*sufABCDSE*), respectively (Esquilin-Lebron et al., 2021; Outten et al., 2004). Interestingly, no genes of the *suf* operon were found to be upregulated under spermidine stress. Instead, a 3-fold downregulation of *sufA* was observed in microarray data. Since *suf* operon is also positively regulated by OxyR (Esquilin-Lebron et al., 2021) but spermidine stress declined the cellular H₂O₂ levels (Chapter 2 figure 1C), we suggest that the combined action of apo-IscR, apo-Fur, and inactivated form of OxyR kept *suf* operon expression indifferent under spermidine stress. Spermidine also activated *rsxA* and *rsxB* which encodes the critical components of the ISC reducing system of SoxR (Koo et al., 2003).

The level of manganese, an antioxidant metal that determines *sodA* activity, is usually increased under Fe scarcity (Kaur et al., 2014, 2017; Martin et al., 2015; Waters et al., 2011).

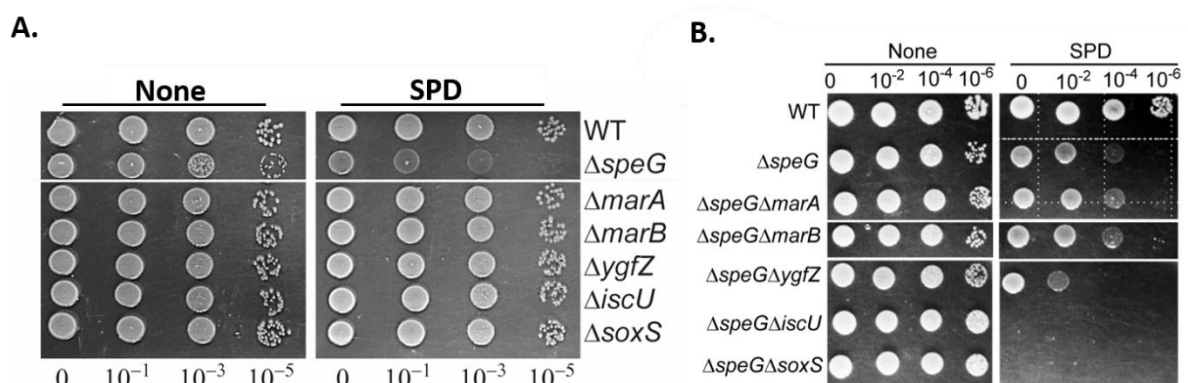


Figure 4.2. Spermidine accumulation affects Mn homeostasis *in vitro*. **A.** Spot assay shows the relative sensitivity of single mutants, $\Delta speG$, $\Delta marA$, $\Delta marB$, $\Delta ygfZ$, $\Delta iscU$ and $\Delta soxS$ strains to spermidine **B.** Spot assay shows the relative sensitivity of various double mutants, $\Delta speG\Delta ygfZ$, $\Delta speG\Delta iscU$, and $\Delta speG\Delta soxS$ strains to spermidine. Error bars in the panels are mean \pm SD from the three independent experiments. Whenever mentioned, the ***, **, and * denote p-values < 0.001 , < 0.01 , and < 0.1 respectively; unpaired t test.

However, a slight decrease in the level of cellular manganese under spermidine stress was observed (Figure 4.1 B). The low level of manganese could slow down the rate of

dismutation of O_2^- anion compromising SodA function, thereby elevating the O_2^- anion levels in the spermidine-treated cells.

Finally, we spotted serially diluted cultures of *E. coli* strains to show that the deletion of two individual genes (*iscU* and *ygfZ*), which are involved in the ISC biogenesis (Waller et al., 2010), affects the growth of the spermidine-treated $\Delta speG$ strain (Figure 4.2B). Interestingly, the $\Delta speG\Delta soxS$ strain was more sensitive to spermidine than the $\Delta speG$ strain (Figure 4.2B), indicating that the basal level of *soxS* expression has some potential to ameliorate O_2^- under spermidine stress. Although in our microarray data, *marA* and *marB* genes were expressed at the highest level in the spermidine-stressed $\Delta speG$ strain. $\Delta speG\Delta marA$ and $\Delta speG\Delta marB$ strains did not show any difference in growth compared to $\Delta speG$ strain under spermidine stress (Figure 4.2B). Note that, unlike $\Delta speG$ strain, the single mutants, viz., $\Delta marA$, $\Delta marB$, $\Delta ygfZ$, $\Delta iscU$, $\Delta soxS$, showed almost similar growth pattern as that of WT strain (Figure 4.2A).

4.3.2. Free spermidine directly interacts with Fe

To probe whether spermidine directly interacts with Fe, we performed isothermal titration calorimetry (ITC) using Fe^{3+} (ferric citrate) and Fe^{2+} (ferrous ammonium sulfate) ions. Titration of spermidine with Fe^{3+} generated exothermic peaks indicating a standard binding reaction with a stoichiometry (N) of 0.711 (Figure 4.3A). On the other hand, titration of spermidine with Fe^{2+} in two different isothermal conditions produced consistent and complex patterns (Figure 4.3B and 4.3C). To explain it, we divided the pattern into two halves. In the first half, Fe^{2+} injections to spermidine generated alternate exothermic and endothermic peaks till the ratio of spermidine to Fe^{2+} reaches about 1:1.3 (Figure 4.3B and 4.3C). In the second half of the profile, after the ratio of spermidine to Fe^{2+} crosses 1:1.3, no endothermic peaks were observed, and a gradual shortening of exothermic peaks was generated, leading to saturation (Figure 4.3B and 4.3C). From the first half of pattern, we suspected Fe^{2+} interaction with spermidine also involves some other reactions, such as oxidation of the Fe^{2+} to generate Fe^{3+} and O_2^- , Fe^{3+} release, and subsequent Fe^{3+} binding to spermidine.

4.3.3. Free spermidine interacts and oxidizes Fe^{2+} ion to generate O_2^- radicals in vitro

To test whether Fe^{2+} was oxidized in the presence of spermidine to liberate Fe^{3+} , we titrated spermidine by increasing amounts of Fe^{2+} followed by assessing the level of Fe^{2+} by using bipyridyl chelator. Chelation of Fe^{2+} ions by bipyridyl generates pink colour indicating

Fe²⁺ levels. No colour formation was observed till the ratio of spermidine to Fe²⁺ reaches 1:1.3 (Figure 4.4A), a number that exactly matches with the ratio of spermidine to Fe²⁺ in the first half of ITC experiments (Figure 4.3B and 4.3C). The development of colour starts when the ratio of spermidine to Fe²⁺ crosses 1:1.3 (Figure 4.4A), suggesting that 1 molecule of

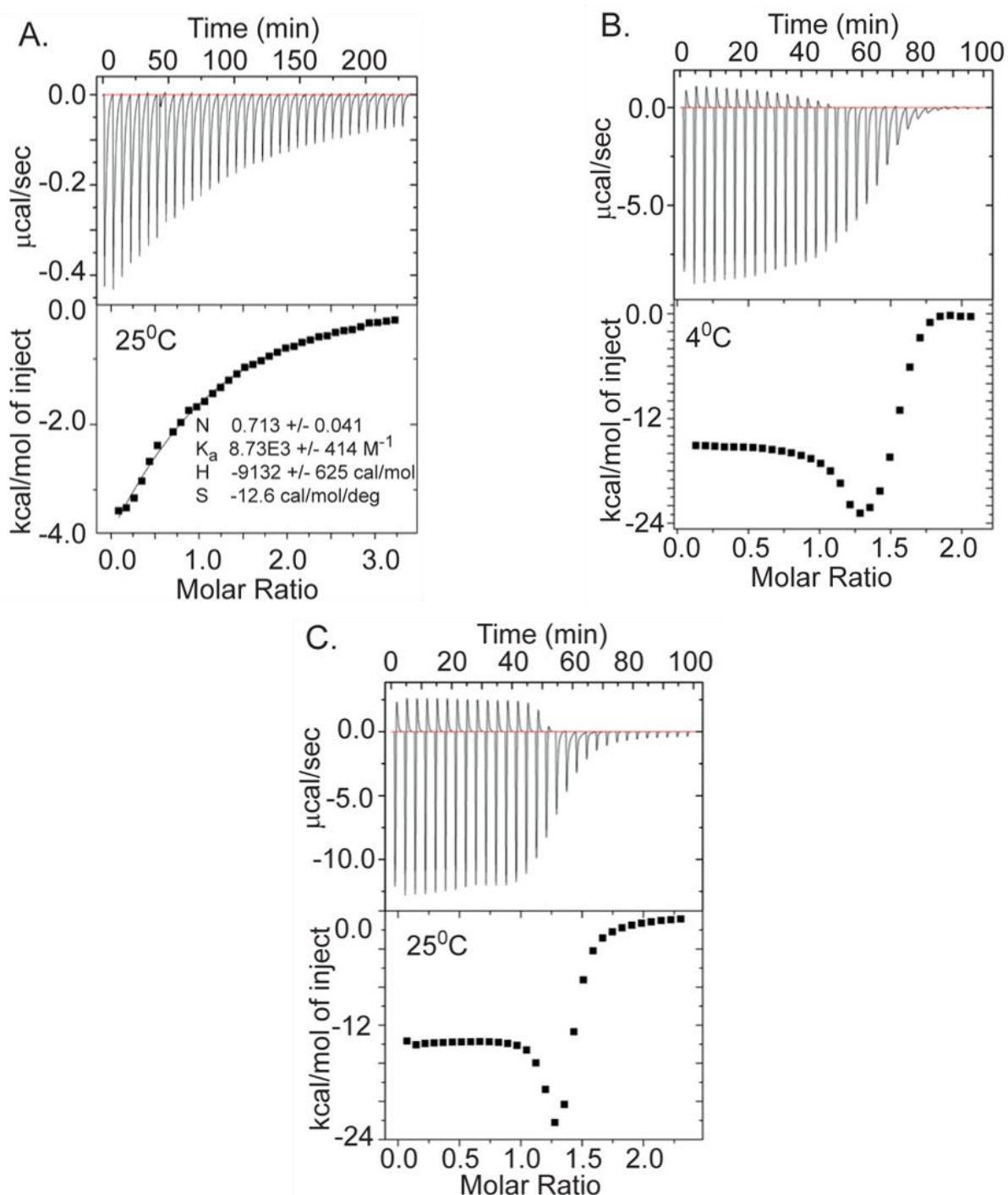


Figure 4.3. Spermidine directly interacts with Fe. **A.** Isothermal titration calorimetry (ITC) data demonstrates the interaction of spermidine with Fe³⁺. **B.** and **C.** ITC data shows the interaction of spermidine with Fe²⁺ ion at 4°C and 25°C, respectively.

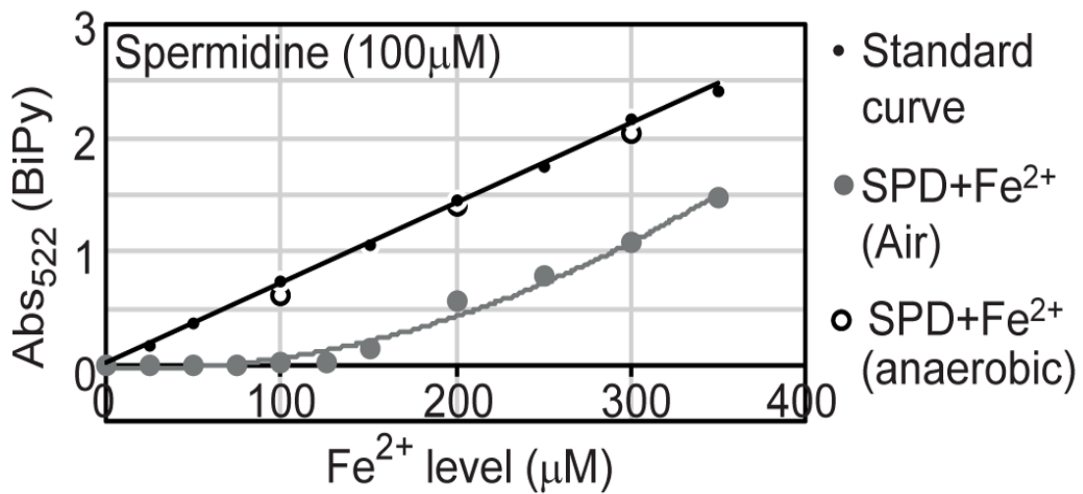
spermidine (or 10 molecules) exactly oxidizes 1.3 molecules (or 13 molecules) of Fe^{2+} . The colorimetric values overlap with the standard curve when reactions were under anoxic condition, indicating Fe^{2+} was not oxidized (Figure 4.4A). We used nitro bluetetrazolium (NBT) dye to check whether the loss of one electron from Fe^{2+} generates O_2^- anion under spermidine stress. An increased NBT absorption at 575nm till the ratio of spermidine to Fe^{2+} reaches 1:1.3 confirms that 1 molecule (or 10 molecule) of spermidine interacts with 1.3 molecules (or 13 molecules) of Fe^{2+} generating 1.3 molecules (or 13 molecules) O_2^- anion radical (Figure 4.4B).

4.3.3. Free spermidine interacts and oxidizes Fe^{2+} ion to generate O_2^- radicals in vitro

To test whether Fe^{2+} was oxidized in the presence of spermidine to liberate Fe^{3+} , we titrated spermidine by increasing amounts of Fe^{2+} followed by assessing the level of Fe^{2+} by using bipyridyl chelator. Chelation of Fe^{2+} ions by bipyridyl generates pink colour indicating Fe^{2+} levels. No colour formation was observed till the ratio of spermidine to Fe^{2+} reaches 1:1.3 (Figure 4.4A), a number that exactly matches with the ratio of spermidine to Fe^{2+} in the first half of ITC experiments (Figure 4.3B and 4.3C). The development of colour starts when the ratio of spermidine to Fe^{2+} crosses 1:1.3 (Figure 4.4A), suggesting that 1 molecule of spermidine (or 10 molecules) exactly oxidizes 1.3 molecules (or 13 molecules) of Fe^{2+} . The colorimetric values overlap with the standard curve when reactions were under anoxic condition, indicating Fe^{2+} was not oxidized (Figure 4.4A). We used nitro blue tetrazolium (NBT) dye to check whether the loss of one electron from Fe^{2+} generates O_2^- anion under spermidine stress. An increased NBT absorption at 575nm till the ratio of spermidine to Fe^{2+} reaches 1:1.3 confirms that 1 molecule (or 10 molecule) of spermidine interacts with 1.3 molecules (or 13 molecules) of Fe^{2+} generating 1.3 molecules (or 13 molecules) O_2^- anion radical (Figure 4.4B).

From the stoichiometry of 0.711 (which is close to 0.5) (Figure 4.3A), we postulate that two spermidine and one Fe^{3+} together could form a hexadentate co-ordination complex with an octahedral geometry (Figure 4.5A). It appears that when spermidine molecules engaged to form a hexadentate co-ordination complex with Fe^{2+} , the former helps oxidizing latter to form Fe^{3+} in sufficient concentrations. Fe^{3+} finally forms coordination complex with

A.



B.

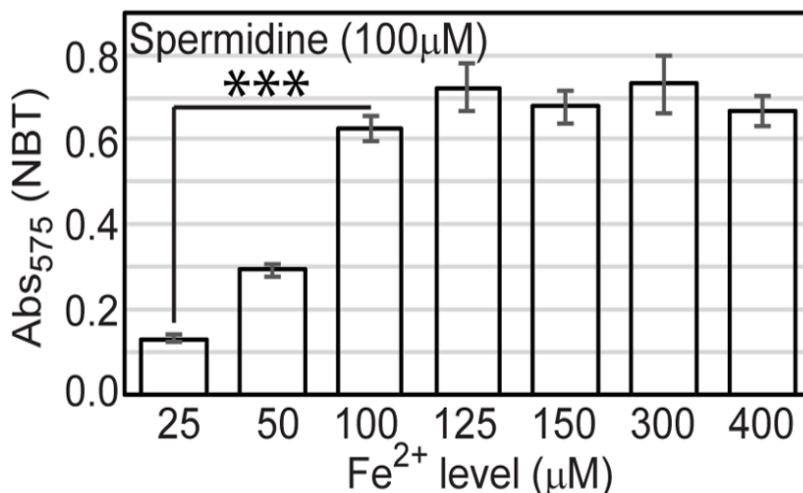


Figure 4.4. Spermidine oxidizes Fe²⁺ generating O₂⁻ radical in aerobic condition. **A.** 100 µM spermidine was incubated with different concentrations of Fe²⁺ followed by an estimation of Fe²⁺ levels by a bipyridyl chelator. The colour formation was recorded at 522 nm and plotted along with the standard curve. The panel depicts that the incubations of 100 µM spermidine with 100, 200, and 300 µM of Fe²⁺ in the anaerobic condition don't lead to the loss of Fe²⁺ ions detected by the bipyridyl chelator. However, when 100 µM spermidine was incubated with the different concentrations of Fe²⁺ (25–350 µM) in the aerobic condition, the bipyridyl-mediated color formation was observed when Fe²⁺ level was between above 125 µM and 150 µM (i.e., till spermidine to Fe²⁺ ratio reaches approximately 1.3). The mean values from the three independent experiments were plotted. SD is negligible and is not shown for clarity. **B.** Nitro blue tetrazolium (NBT) assay was performed to determine that

spermidine and Fe^{2+} interaction yields O_2^- radical. The colorimetry at 575 nm suggests that 100 μM of spermidine interacts with approximately 125 μM of Fe^{2+} (ratio 1:1.3) to generate a saturated colour. Error bars in the panel are mean \pm SD from the three independent experiments. *** denotes p-value < 0.001 ; unpaired t test.

spermidine (Figure 4.5A). It may be noted that the binding of spermidine and Fe^{3+} is entirely enthalpy driven, as indicated by a large negative ΔH . The negative entropy (ΔS) value presumably results from the ordering of spermidine from an extended conformation to a compact and rigid one after metal chelation (Figure 4.5A).

The cellular spermidine barely exists as a “free” species; rather, majority of them remain “bound” with RNA, DNA, nucleotides, and phospholipids (Igarashi and Kashiwagi, 2000; Miyamoto et al., 1993; Schuber, 1989; Tabor and Tabor, 1984b). It has been reported that these phosphate-containing biomolecules have the inherent property to inhibit Fe oxidation blocking O_2^- production (LØVaas, 1996; Tadolini, 1988a; Tadolini, 1988b). The bound spermidine further enhances the inhibitory effects of these biomolecules towards Fe oxidation. Consistent with the report (Tadolini, 1988b), we noticed that 1 μg of RNA inhibited the oxidation of 200 μM Fe^{2+} . The presence of 10 μM spermidine further decreased Fe oxidation (Figure 4.5B). However, increasing the concentrations of spermidine (50, 100, and 200 μM), accelerated Fe oxidation gradually (Figure 4.5B). This data clearly indicates that cell maintains a level of cellular spermidine that may remain optimally bound with the biomolecules inhibiting O_2^- generation. However, when homeostasis fails due to *speG* deletion, excess spermidine accumulates that can remain in a “free”-form inducing O_2^- radical toxicity.

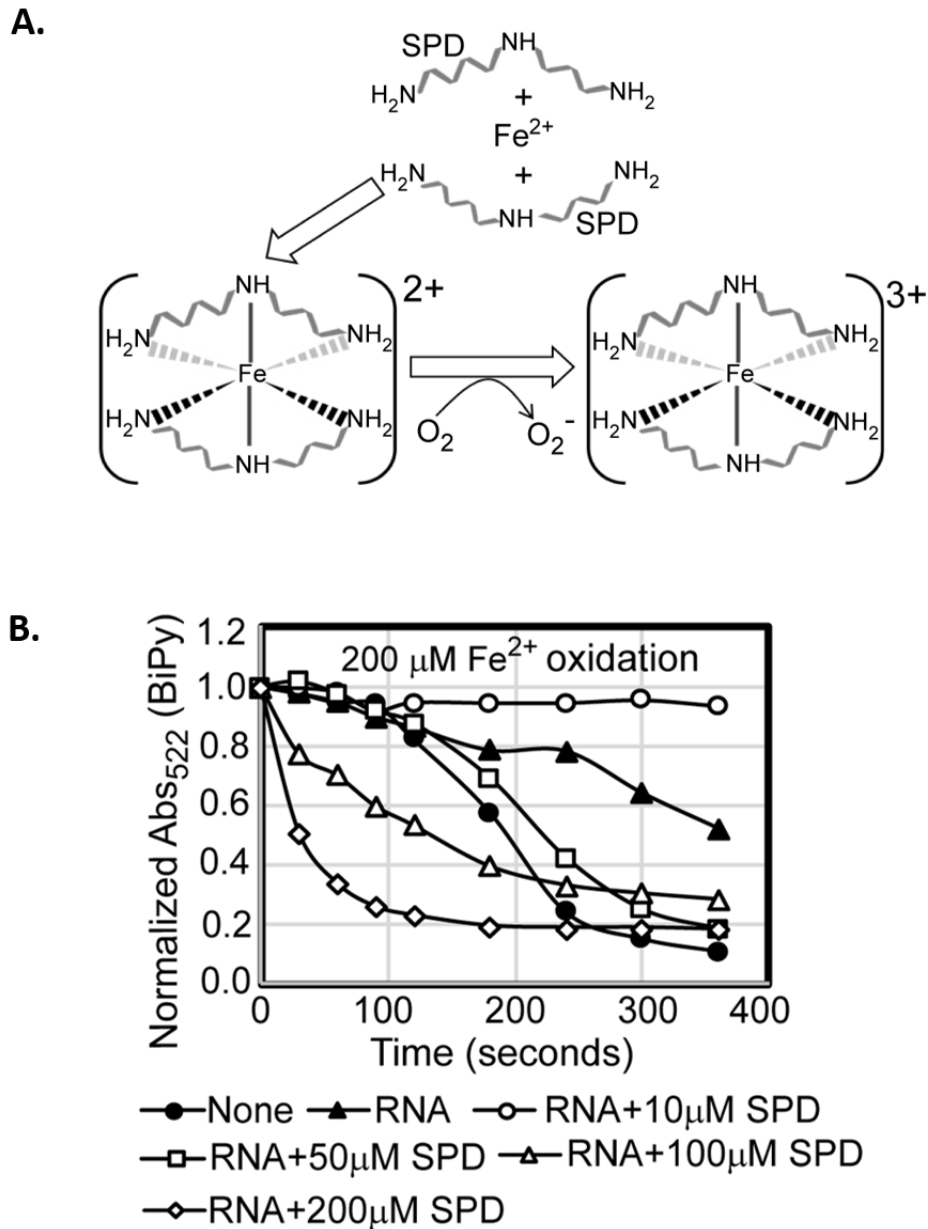


Figure 4.5. Model to show final coordination complex formation. A. An Fe^{2+} interacts with two spermidine molecules forming hexadentate co-ordination complex. This interaction oxidizes Fe^{2+} liberating one electron to reduce oxygen molecule. Finally, two spermidine coordinates one Fe^{3+} with an octahedral geometry. **B.** The curves represent that *E. coli* total RNA inhibits Fe oxidation. Spermidine further reduces the RNA-mediated Fe oxidation at concentration 10 μM but higher concentrations of spermidine increase the Fe oxidation despite the presence of RNA. The mean values are derived from the three independent experiments and plotted. SD is negligible and is not shown for clarity.

4.4. Discussion

We provide clear-cut evidence that excess spermidine, which remains as a free species stimulates the production of toxic levels of O_2^- radicals in *E. coli* (Reference- Chapter 2). O_2^- anion thus generated damages Fe-S clusters of the proteins. Since spermidine directly interacts with Fe (Figure 4.3), it may abstract Fe from some of the Fe-S clusters, thereby inactivating some of the proteins. On the other hand, when spermidine level is at optimum, most of it remain as bound form with the biomolecules, thereby slows down Fe oxidation and subsequent O_2^- production (LØVaas, 1996; Tadolini, 1988b, 1988a). Thus, spermidine deficiency would enhance the rate of Fe oxidation (Figure 4.5B), leading to ROS. This is why spermidine is a double-edged sword where in excess, it provokes O_2^- anion production, and in scarcity, it leads to higher ROS levels. Polyamines remain protonated at physiological pH, yet they are able to coordinate several positively charged metal ions, such as Ni^{2+} , Co^{2+} , Cu^{2+} , and Zn^{2+} , possibly via charge neutralization by counterions that reduces the coulombic repulsion between spermidine and the metals (LØVaas, 1996). Similar charge neutralization of the nitrogen atoms of spermidine likely allows coordinate covalent bonds with Fe^{3+} (Figure 4.5A). About 10 spermidine molecules oxidize Fe^{2+} to generate 13 Fe^{3+} cations and equivalent numbers of O_2^- radicals (Figure 4.4A and 4.4B). When sufficient concentration of Fe^{3+} is generated, two spermidine molecules coordinate one Fe^{3+} to form a hexadentate complex with an octahedral geometry (Figure 4.5A). We substantiated this in vitro spermidine-mediated Fe oxidation and subsequent O_2^- radical production phenomena (Figure 4.5B), showing that cells are highly toxic to the spermidine under aerobic condition but not under anaerobic condition. Besides, the activation of IscR, the low cellular Fe content (Figure 4.1B), and the rejuvenation of cell growth by Fe^{2+} supplementation (Figure 4.1C) indicate that the spermidine presumably lowers the Fe^{2+}/Fe^{3+} ratio in $\Delta speG$ strain.

Our study in *E. coli* observed quite a few biochemical aspects which might explain how the horizontal acquisition of *speG* gene could confer a pathogenic advantage to the *Staphylococcus aureus* USA 300 strain (Eisenberg et al., 2009). *S. aureus*, a Gram-positive commensal living on human skin, often causes severe disease upon access to deeper tissues. Since most of the Fe in mammals exists intracellularly, the extracellular pathogen, *S. aureus* faces hardship and competes with the host for the available Fe (Hammer and Skaar, 2011). As spermidine declines cellular Fe content (Figure 4.1B), it is thus possible that *S. aureus* does not synthesize spermidine (Joshi, 2012). Furthermore, the acquisition of *speG* gene by *S. aureus* USA300 could allow it to inactivate host-originated spermidine/spermine, thereby to

maintain cellular Fe content (Joshi, 2012). Corroborating to our findings, a recent observation has pointed out that spermine stress upregulates Fe homeostasis genes, indicating that spermine toxicity has a specific connection with Fe depletion in the *speG*-negative *S. aureus* strain, Mu50 (MRSA) (Yao and Lu, 2014). Besides, spermine-mediated Fe depletion may be responsible for the synergistic effect of spermine with the antibiotics against *S. aureus* (Kwon and Lu, 2007). Nevertheless, a thorough in vivo host-pathogen interaction study may unravel a specific link between spermine/spermidine and Fe depletion in *S. aureus*.

Summary of present study

Briefly, We proposed a model from previous chapters to summarise our study. Spermidine blocks O_2^- radical-mediated activation of SoxRS that upregulates *zwf* and *sodA*. Consequently, reduced NADPH production and dismutation of O_2^- radical to H_2O_2 were not accelerated, leading to redox imbalance and O_2^- mediated damage to the iron-sulfur clusters, respectively. Additionally, spermidine translationally upregulated alkyl hydroperoxidase (AhpCF) that lowers the level of H_2O_2 . Declined cellular Fe^{2+} and H_2O_2 levels weaken Fenton reaction to produce $\bullet OH$ radical.

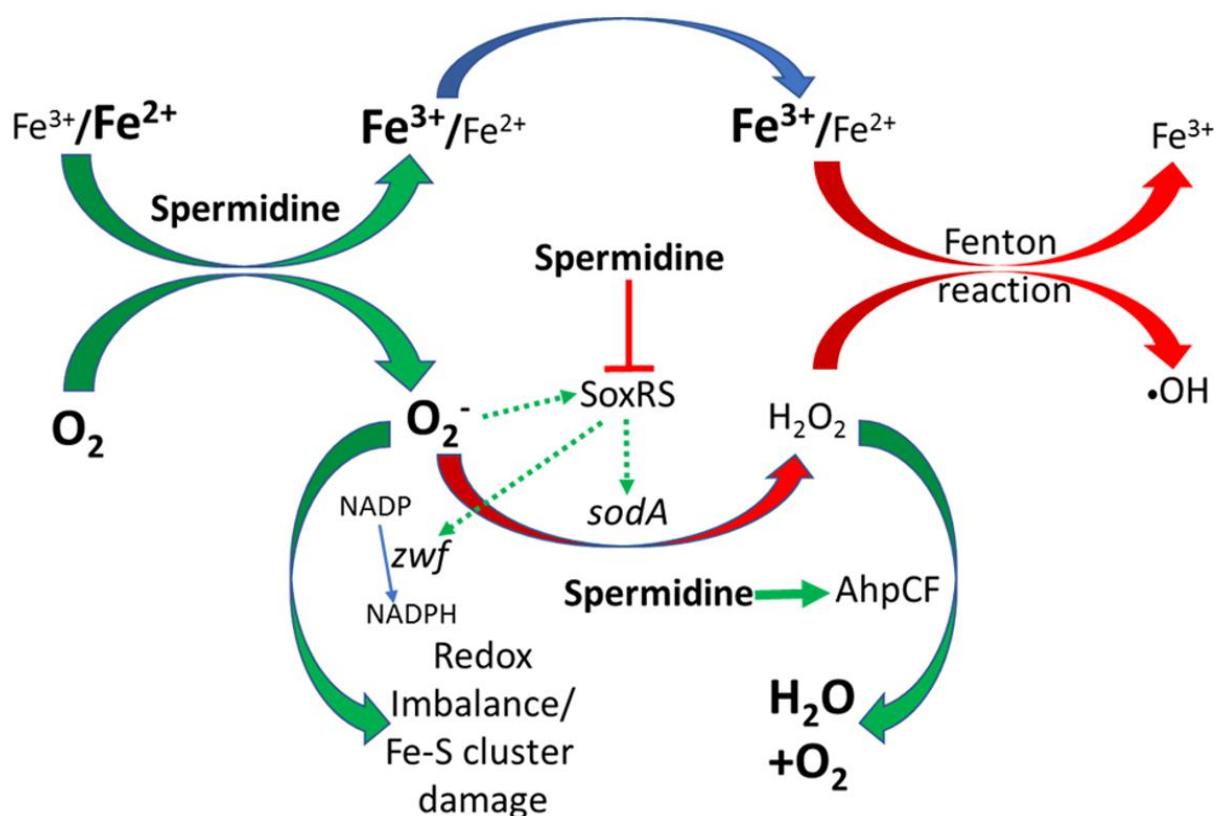


Figure. Flowchart explaining the reactive oxygen species (ROS) generation under spermidine stress. The model describes that the spermidine administration in the cell interacts with free iron and oxygen to generate O_2^- radical, increasing Fe^{3+}/Fe^{2+} ratio..

REFERENCES

- Algranati, I. D., and Goldemberg, S. H. (1977). Polyamines and their role in protein synthesis. *Trends in Biochemical Sciences*. 77, 272–274.
- Agostinelli, E. (2020). Biochemical and pathophysiological properties of polyamines. *Amino Acids* 52, 111–117.
- Andrews, S.C., Robinson, A.K., and Rodríguez-Quñones, F. (2003). Bacterial iron homeostasis. *FEMS Microbiol. Rev.* 27, 215–237.
- Anjem, A., and Imlay, J.A. (2012). Mononuclear Iron Enzymes Are Primary Targets of Hydrogen Peroxide Stress. *J. Biol. Chem.* 287, 15544–15556.
- Anjem, A., Varghese, S., and Imlay, J.A. (2009). Manganese import is a key element of the OxyR response to hydrogen peroxide in *Escherichia coli*. *Mol. Microbiol.* 72, 844–858.
- Antonelli, M.L., Balzamo, S., Carunchio, V., and Cernia, E. (1984). Complex formation of 4,9-diazadodecane-1,12-diamine with Copper(II) and Zinc(II) ions in aqueous solution. *Thermochim. Acta* 78, 1–8.
- Archibald, F.S., and Fridovich, I. (1981). Manganese, superoxide dismutase, and oxygen tolerance in some lactic acid bacteria. *J. Bacteriol.* 146, 928–936.
- Atiya Ali, M., Strandvik, B., Sabel, K.G., Palme Kilander, C., Strömberg, R., and Yngve, A. (2014). Polyamine levels in breast milk are associated with mothers' dietary intake and are higher in preterm than full-term human milk and formulas. *J. Hum. Nutr. Diet.* 27, 459–467.
- Atkins, J. F., Lewis, J. B., Anderson, C. W. and Gesteland, R. F. (1975) 'Enhanced differential synthesis of proteins in a mammalian cell-free system by addition of polyamines.', *The Journal of biological chemistry*, 250, 5688–9
- Baba, T., Ara, T., Hasegawa, M., Takai, Y., Okumura, Y., Baba, M., Datsenko, K.A., Tomita, M., Wanner, B.L., and Mori, H. (2006). Construction of *Escherichia coli* K-12 in-frame, single-gene knockout mutants: The Keio collection. *Mol. Syst. Biol.* 2, 2006.0008.
- BACHRACH, U., and COHEN, I. (1961). Spermidine in the bacterial cell. *J. Gen. Microbiol.* 26, 1–9.

- Balasundaram, D., Tabor, C.W., and Tabor, H. (1993). Oxygen toxicity in a polyamine-depleted *spe2Δ* mutant of *Saccharomyces cerevisiae*. *Proc. Natl. Acad. Sci. U. S. A.* *90*, 4693–4697.
- Barbagallo, M., Letizia, M., Martino, D., Marcocci, L., Pietrangeli, P., De Carolis, E., Casalino, M., Colonna, B., and Prosseda, G. (2011). A New Piece of the *Shigella* Pathogenicity Puzzle: Spermidine Accumulation by Silencing of the *speG* Gene.
- Benov, L. (2001). How superoxide radical damages the cell. In *Protoplasma*, (Springer), pp. 33–36.
- Benov, L., and Fridovich, I. (1999). Why superoxide imposes an aromatic amino acid auxotrophy on *Escherichia coli*. The transketolase connection. *J. Biol. Chem.* *274*, 4202–4206.
- Bertsch, C.R., Fernelius, W.C., and Block, B.P. (1958). A thermodynamic study of some complexes of metal ions with polyamines. *J. Phys. Chem.* *62*, 444–450.
- Beyer, W.F., and Fridovich, I. (1987). Effect of hydrogen peroxide on the iron-containing superoxide dismutase of *Escherichia coli*. *Biochemistry* *26*, 1251–1257.
- Bleeke, T., Zhang, H., Madamanchi, N., Patterson, C., and Faber, J.E. (2004). Catecholamine-Induced Vascular Wall Growth is Dependent on Generation of Reactive Oxygen Species. *Circ. Res.* *94*, 37–45.
- Bock, C.W., Katz, A.K., Markham, G.D., and Glusker, J.P. (1999). Manganese as a replacement for magnesium and zinc: Functional comparison of the divalent ions. *J. Am. Chem. Soc.* *121*, 7360–7372.
- Bors, W., Langebartels, C., Michel, C., and Sandermann, H. (1989). Polyamines as radical scavengers and protectants against ozone damage. *Phytochemistry* *28*, 1589–1595.
- Boukhalfa, H., and Crumbliss, A.L. (2002). Chemical aspects of siderophore mediated iron transport. *Biometals* *2002* *154* *15*, 325–339.
- Bradbeer, C., Woodrow, M.L., and Khalifah, L.I. (1976). Transport of vitamin B12 in *Escherichia coli*: common receptor system for vitamin B12 and bacteriophage BF23 on the outer membrane of the cell envelope. *J. Bacteriol.* *125*, 1032.
- Bsat, N., Herbig, A., Casillas-Martinez, L., Setlow, P., and Helmann, J.D. (1998). *Bacillus subtilis* contains multiple Fur homologues: identification of the iron uptake (Fur) and

- peroxide regulon (PerR) repressors. *Mol. Microbiol.* 29, 189–198.
- Burrell, M., Hanfrey, C.C., Murray, E.J., Stanley-Wall, N.R., and Michael, A.J. (2010). Evolution and multiplicity of arginine decarboxylases in polyamine biosynthesis and essential role in *Bacillus subtilis* biofilm formation. *J. Biol. Chem.* 285, 39224–39238.
- Buts, J.P., De Keyser, N., De Raedemaeker, L., Collette, E., and Sokal, E.M. (1995). Polyamine profiles in human milk, infant artificial formulas, and semi-elemental diets. *J. Pediatr. Gastroenterol. Nutr.* 21, 44–49.
- Buyukuslu, N. (2015). Dietary Polyamines and Diseases: Reducing Polyamine Intake Can Be Beneficial In Cancer Treatment. *J. Nutr.* 2, 27–38.
- Buyukuslu, N., Hizli, H., Esin, K., and Garipagaoglu, M. (2014). A Cross-Sectional Study: Nutritional Polyamines in Frequently Consumed Foods of the Turkish Population. 3, 541–557.
- Campilongo, R., Di Martino, M.L., Marcocci, L., Pietrangeli, P., Leuzzi, A., Grossi, M., Casalino, M., Nicoletti, M., Micheli, G., Colonna, B., et al. (2014). Molecular and Functional Profiling of the Polyamine Content in Enteroinvasive *E. coli*: Looking into the Gap between Commensal *E. coli* and Harmful Shigella. *PLoS One* 9, e106589.
- Canvin, J., Langford, P.R., Wilks, K.E., and Kroll, J.S. (1996). Identification of sodC encoding periplasmic [Cu,Zn]-superoxide dismutase in *Salmonella*. *FEMS Microbiol. Lett.* 136, 215–220.
- Casero, R.A., Murray Stewart, T., and Pegg, A.E. (2018). Polyamine metabolism and cancer: treatments, challenges and opportunities. *Nat. Rev. Cancer* 18, 681–695.
- Chattopadhyay, M.K., and Tabor, H. (2013). Polyamines are critical for the induction of the glutamate decarboxylase-dependent acid resistance system in *Escherichia coli*. *J. Biol. Chem.* 288, 33559–33570.
- Chattopadhyay, M.K., Tabor, C.W., and Tabor, H. (2003a). Polyamines protect *Escherichia coli* cells from the toxic effect of oxygen. *Proc. Natl. Acad. Sci. U. S. A.* 100, 2261–2265.
- Chattopadhyay, M.K., Tabor, C.W., and Tabor, H. (2003b). Polyamines protect *Escherichia coli* cells from the toxic effect of oxygen. *Proc. Natl. Acad. Sci. U. S. A.* 100, 2261–2265.

- Chattopadhyay, M.K., Tabor, C.W., and Tabor, H. (2006a). Polyamine deficiency leads to accumulation of reactive oxygen species in a *spe2Δ* mutant of *Saccharomyces cerevisiae*. *Yeast* 23, 751–761.
- Chattopadhyay, M.K., Tabor, C.W., and Tabor, H. (2006b). Polyamine deficiency leads to accumulation of reactive oxygen species in a *spe2Δ* mutant of *Saccharomyces cerevisiae*. *Yeast* 23, 751–761.
- Chattopadhyay, M.K., Chen, W., Poy, G., Cam, M., Stiles, D., and Tabor, H. (2009). Microarray studies on the genes responsive to the addition of spermidine or spermine to a *Saccharomyces cerevisiae* spermidine synthase mutant. *Yeast* 26, 531–544.
- Chattopadhyay, M.K., Keembiyehetty, C.N., Chen, W., and Tabor, H. (2015). Polyamines Stimulate the Level of the σ^{38} Subunit (RpoS) of *Escherichia coli* RNA Polymerase, Resulting in the Induction of the Glutamate Decarboxylase-dependent Acid Response System via the *gadE* Regulon. *J. Biol. Chem.* 290, 17809–17821.
- Chen, J., Rogers, S.C., and Kavdia, M. (2013). Analysis of kinetics of dihydroethidium fluorescence with superoxide using xanthine oxidase and hypoxanthine assay. *Ann. Biomed. Eng.* 41, 327–337.
- Chiang, S.M., and Schellhorn, H.E. (2012). Regulators of oxidative stress response genes in *Escherichia coli* and their functional conservation in bacteria. *Arch. Biochem. Biophys.* 525, 161–169.
- D’Orazio, M., Scotti, R., Nicolini, L., Cervoni, L., Rotilio, G., Battistoni, A., and Gabbianelli, R. (2008). Regulatory and structural properties differentiating the chromosomal and the bacteriophage-associated *Escherichia coli* O157:H7 Cu, Zn superoxide dismutases. *BMC Microbiol.* 8.
- Daly, M.J., Gaidamakova, E.K., Matrosova, V.Y., Vasilenko, A., Zhai, M., Venkateswaran, A., Hess, M., Omelchenko, M. V., Kostandarithes, H.M., Makarova, K.S., et al. (2004). Accumulation of Mn(II) in *Deinococcus radiodurans* facilitates gamma-radiation resistance. *Science* (80-.). 306, 1025–1028.
- Datsenko, K.A., and Wanner, B.L. (2000). One-step inactivation of chromosomal genes in *Escherichia coli* K-12 using PCR products. *Proc. Natl. Acad. Sci. U. S. A.* 97, 6640–6645.
- Dela Vega, A.L., and Delcour, A.H. (1996). Polyamines decrease *Escherichia coli* outer

- membrane permeability. *J. Bacteriol.* *178*, 3715–3721.
- Dikalov, S.I., Polienko, Y.F., and Kirilyuk, I. (2018). Electron Paramagnetic Resonance Measurements of Reactive Oxygen Species by Cyclic Hydroxylamine Spin Probes. *Antioxid. Redox Signal.* *28*, 1433.
- Ding, H., and Demple, B. (1997). In vivo kinetics of a redox-regulated transcriptional switch. *Proc. Natl. Acad. Sci. U. S. A.* *94*, 8445–8449.
- Dubbs, J.M., and Mongkolsuk, S. (2012). Peroxide-sensing transcriptional regulators in bacteria. *J. Bacteriol.* *194*, 5495–5503.
- Eisenberg, T., Knauer, H., Schauer, A., Büttner, S., Ruckenstuhl, C., Carmona-Gutierrez, D., Ring, J., Schroeder, S., Magnes, C., Antonacci, L., et al. (2009). Induction of autophagy by spermidine promotes longevity. *Nat. Cell Biol.* *11*, 1305–1314.
- Esquilin-Lebron, K., Dubrac, S., Barras, F., and Boyd, J.M. (2021). Bacterial Approaches for Assembling Iron-Sulfur Proteins. *MBio* *12*.
- Farr, S.B., D'Ari, R., and Touati, D. (1986). Oxygen-dependent mutagenesis in *Escherichia coli* lacking superoxide dismutase. *Proc. Natl. Acad. Sci. U. S. A.* *83*, 8268–8272.
- Fee, J.A. (1991). Regulation of *sod* genes in *Escherichia coli*: relevance to superoxide dismutase function. *Mol. Microbiol.* *5*, 2599–2610.
- Figuroa-Bossi, N., and Bossi, L. (1999). Inducible prophages contribute to *Salmonella* virulence in mice. *Mol. Microbiol.* *33*, 167–176.
- Finney, L.A., and O'halloran, T. V (2002). Transition Metal Speciation in the Cell: Insights from the Chemistry of Metal Ion Receptors.
- Franco, R., Panayiotidis, M.I., and Cidlowski, J.A. (2007). Glutathione depletion is necessary for apoptosis in lymphoid cells independent of reactive oxygen species formation. *J. Biol. Chem.* *282*, 30452–30465.
- Fridovich, I. (1986). Biological effects of the superoxide radical. *Arch. Biochem. Biophys.* *247*, 1–11.
- Fuangthong, M., and Helmann, J.D. (2003). Recognition of DNA by three ferric uptake regulator (Fur) homologs in *Bacillus subtilis*. *J. Bacteriol.* *185*, 6348–6357.
- Fujikawa, M., Kobayashi, K., Tsutsui, Y., Tanaka, T., and Kozawa, T. (2017). Rational Tuning of Superoxide Sensitivity in SoxR, the [2Fe-2S] Transcription Factor:

- Implications of Species-Specific Lysine Residues. *Biochemistry* 56, 403–410.
- Fukuchi, J.I., Kashiwagi, K., Takio, K., and Igarashi, K. (1994). Properties and structure of spermidine acetyltransferase in *Escherichia coli*. *J. Biol. Chem.* 269, 22581–22585.
- Fukuchi, J.I., Kashiwagi, K., Yamagishi, M., Ishihama, A., and Igarashi, K. (1995). Decrease in cell viability due to the accumulation of spermidine in spermidine acetyltransferase-deficient mutant of *Escherichia coli*. *J. Biol. Chem.* 270, 18831–18835.
- Gaboriau, F., Kreder, A., Clavreul, N., Moulinoux, J.P., Delcros, J.G., and Lescoat, G. (2004). Polyamine modulation of iron uptake in CHO cells. *Biochem. Pharmacol.* 67, 1629–1637.
- Gardner, P.R., and Fridovich, I. (1992). Inactivation-reactivation of aconitase in *Escherichia coli*. A sensitive measure of superoxide radical. *J. Biol. Chem.* 267, 8757–8763.
- Gawlitta, W., Stockem, W., and Weber, K. (1981). Visualization of actin polymerization and depolymerization cycles during polyamine-induced cytokinesis in living *Amoeba proteus*. *Cell Tissue Res.* 215, 249–261.
- Geiger, L.E., and Morris, D.R. (1980). Stimulation of deoxyribonucleic acid replication fork movement by spermidine analogs in polyamine-deficient *Escherichia coli*. *J. Bacteriol.* 141, 1192–1198.
- Giel, J.L., Rodionov, D., Liu, M., Blattner, F.R., and Kiley, P.J. (2006). IscR-dependent gene expression links iron-sulphur cluster assembly to the control of O₂⁻ regulated genes in *Escherichia coli*. *Mol. Microbiol.* 60, 1058–1075.
- Gilbertsen, A., and Williams, B. (2014). Development of a *Pseudomonas aeruginosa* Argmatine Biosensor. *Biosensors* 4, 387–402.
- Gómez-Gallego, C., Kumar, H., García-Mantrana, I., Du Toit, E., Suomela, J.P., Linderborg, K.M., Zhang, Y., Isolauri, E., Yang, B., Salminen, S., et al. (2017). Breast Milk Polyamines and Microbiota Interactions: Impact of Mode of Delivery and Geographical Location. *Ann. Nutr. Metab.* 70, 184–190.
- González-Flecha, B., and Demple, B. (1999). Role for the oxyS gene in regulation of intracellular hydrogen peroxide in *Escherichia coli*. *J. Bacteriol.* 181, 3833–3836.
- González-Flecha, B., and Demple, B. (2000). Genetic responses to free radicals. Homeostasis

- and gene control. *Ann. N. Y. Acad. Sci.* 899, 69–87.
- Gordon, M.A. (2008). *Salmonella* infections in immunocompromised adults. *J. Infect.* 56, 413–422.
- Goytia, M., Dhulipala, V.L., and Shafer, W.M. Spermine impairs biofilm formation by *Neisseria gonorrhoeae*.
- Gu, M., and Imlay, J.A. (2011a). The SoxRS response of *Escherichia coli* is directly activated by redox-cycling drugs rather than by superoxide. *Mol. Microbiol.* 79, 1136–1150.
- Gu, M., and Imlay, J.A. (2011b). The SoxRS response of *Escherichia coli* is directly activated by redox-cycling drugs rather than by superoxide. *Mol. Microbiol.* 79, 1136–1150.
- Ha, H.C., Yager, J.D., Woster, P.A., and Casero, R.A. (1998a). Structural specificity of polyamines and polyamine analogues in the protection of DNA from strand breaks induced by reactive oxygen species. *Biochem. Biophys. Res. Commun.* 244, 298–303.
- Ha, H.C., Sirisoma, N.S., Kuppusamy, P., Zweier, J.L., Woster, P.M., and Casero, R.A. (1998b). The natural polyamine spermine functions directly as a free radical scavenger. *Proc. Natl. Acad. Sci. U. S. A.* 95, 11140–11145.
- Hammer, N.D., and Skaar, E.P. (2011). Molecular mechanisms of *staphylococcus aureus* iron acquisition. *Annu. Rev. Microbiol.* 65, 129–147.
- Hares, G.B., Fernelius, W.C., and Douglas, B.E. (1956). Equilibrium Constants for the Formation of Complexes between Metal Ions Polyamines. *J. Am. Chem. Soc.* 78, 1816–1818.
- Hayashi, K., Ohsawa, T., Kobayashi, K., Ogasawara, N., and Ogura, M. (2005). The H₂O₂ stress-responsive regulator PerR positively regulates srfA expression in *Bacillus subtilis*. *J. Bacteriol.* 187, 6659–6667.
- Hidalgo, E., and Demple, B. (1994). An iron-sulfur center essential for transcriptional activation by the redox-sensing SoxR protein. *EMBO J.* 13, 138–146.
- Hidalgo, E., Ding, H., and Demple, B. (1997). Redox Signal Transduction: Mutations Shifting [2Fe-2S] Centers of the SoxR Sensor-Regulator to the Oxidized Form. *Cell* 88, 121–129.

- Higashi, K., Ishigure, H., Demizu, R., Uemura, T., Nishino, K., Yamaguchi, A., Kashiwagi, K., and Igarashi, K. (2008). Identification of a spermidine excretion protein complex (MdtJI) in *Escherichia coli*. *J. Bacteriol.* *190*, 872–878.
- Hoet, P.H.M., and Nemery, B. (2000). invited review Polyamines in the lung: polyamine uptake and polyamine-linked pathological or toxicological conditions.
- Horsburgh, M.J., Wharton, S.J., Cox, A.G., Ingham, E., Peacock, S., and Foster, S.J. (2002). MntR modulates expression of the PerR regulon and superoxide resistance in *Staphylococcus aureus* through control of manganese uptake. *Mol. Microbiol.* *44*, 1269–1286.
- Igarashi, K., and Kashiwagi, K. (1999). Polyamine transport in bacteria and yeast. *Biochem. J.* *344*, 633–642.
- Igarashi, K., and Kashiwagi, K. (2000). Polyamines: Mysterious modulators of cellular functions. *Biochem. Biophys. Res. Commun.* *271*, 559–564.
- Igarashi, K., and Kashiwagi, K. (2019). The functional role of polyamines in eukaryotic cells. *Int. J. Biochem. Cell Biol.* *107*, 104–115.
- Igarashi, K., Kishida, K., Kashiwagi, K., Tatokoro, I., Kakegawa, T., and Hirose, S. (1981). Relationship between methylation of adenine near the 3' end of 16-S ribosomal RNA and the activity of 30-S ribosomal subunits. *Eur. J. Biochem.* *113*, 587–593.
- Igarashi, K., Sugawara, K., Izumi, I., Nagayama, C. and Hirose, S. (1974) 'Effect of Polyamines on Polyphenylalanine Synthesis by *Escherichia coli* and Rat-Liver Ribosomes', *European Journal of Biochemistry*, *48*, 495–502.
- Igarashi, K., Kashiwagi, K., Aoki, R., Kijima, M. and Hirose, S. (1979). Comparative studies on the increase by polyamines of fidelity of protein synthesis in *Escherichia coli* and wheat germ cell free systems. *BBRC*, *91*, 440–448.
- Imlay, J.A. (1995). A Metabolic Enzyme That Rapidly Produces Superoxide, Fumarate Reductase of *Escherichia coli*. *J. Biol. Chem.* *270*, 19767–19777.
- Imlay, J.A. (2008). Cellular defenses against superoxide and hydrogen peroxide. *Annu. Rev. Biochem.* *77*, 755–776.
- Imlay, J.A. (2009). Oxidative Stress. *EcoSal Plus* *3*, 5.4.
- Imlay, J.A. (2013). The molecular mechanisms and physiological consequences of oxidative

- stress: lessons from a model bacterium. *Nat. Publ. Gr.*
- Imlay, J.A. (2015). Diagnosing oxidative stress in bacteria: not as easy as you might think.
- Imlay, J.A., and Fridovich, I. (1991). Superoxide production by respiring membranes of *Escherichia coli*. *Free Radic. Res. Commun. 12-13 Pt 1*, 59–66.
- Iyer, R., and Delcour, A.H. (1997). Complex inhibition of OmpF and OmpC bacterial porins by polyamines. *J. Biol. Chem.* 272, 18595–18601.
- Jacquamet, L., Traoré, D.A.K., Ferrer, J.L., Proux, O., Testemale, D., Hazemann, J.L., Nazarenko, E., El Ghazouani, A., Caux-Thang, C., Duarte, V., et al. (2009). Structural characterization of the active form of PerR: insights into the metal-induced activation of PerR and Fur proteins for DNA binding. *Mol. Microbiol.* 73, 20–31.
- Jakubovics, N.S., and Jenkinson, H.F. (2001). Out of the iron age: new insights into the critical role of manganese homeostasis in bacteria. *Microbiology* 147, 1709–1718.
- Jang, S., and Imlay, J.A. (2007a). Micromolar intracellular hydrogen peroxide disrupts metabolism by damaging iron-sulfur enzymes. *J. Biol. Chem.* 282, 929–937.
- Jang, S., and Imlay, J.A. (2007b). Micromolar intracellular hydrogen peroxide disrupts metabolism by damaging iron-sulfur enzymes. *J. Biol. Chem.* 282, 929–937.
- Jastrzab, R., Kaczmarek, M.T., Nowak, M., Trojanowska, A., and Zabiszak, M. (2017). Complexes of polyamines and their derivatives as living system active compounds. *Coord. Chem. Rev.* 351, 32–44.
- Jelenc, P.C., and Kurland, C.G. (1979). Nucleoside triphosphate regeneration decreases the frequency of translation errors. *Proc. Natl. Acad. Sci. U. S. A.* 76, 3174.
- Joshi, G. (2012). ACME encoded speG abrogates the unique hypersensitivity of *Staphylococcus aureus* to exogenous polyami. *Mol Microbiol* 82, 9–20.
- Jung, I.L., and Kim, I.G. (2003). Transcription of *ahpC*, *katG*, and *katE* genes in *Escherichia coli* is regulated by polyamines: Polyamine-deficient mutant sensitive to H₂O₂-induced oxidative damage. *Biochem. Biophys. Res. Commun.* 301, 915–922.
- Kalač, P. (2014). Health effects and occurrence of dietary polyamines: a review for the period 2005-mid 2013. *Food Chem.* 161, 27–39.
- Kalyanaraman, B., Darley-USmar, V., Davies, K.J.A., Dennery, P.A., Forman, H.J., Grisham, M.B., Mann, G.E., Moore, K., Roberts, L.J., and Ischiropoulos, H. (2012). Measuring

- reactive oxygen and nitrogen species with fluorescent probes: Challenges and limitations. *Free Radic. Biol. Med.* *52*, 1–6.
- Kammler, M., Schon, C., and Hantke, K. (1993). Characterization of the Ferrous Iron Uptake System of *Escherichia coli*. *J. Bacteriol.* *175*, 6212–6219.
- Karatan, E., and Michael, A.J. (2013). A wider role for polyamines in biofilm formation. *Biotechnol. Lett.* *35*, 1715–1717.
- Kashiwagi, K., and Igarashi, K. (1988). Adjustment of polyamine contents in *Escherichia coli*. *J. Bacteriol.* *170*, 3131–3135.
- Kashiwagi, K., Kobayashi, H., and Igarashi, K. (1986). Apparently unidirectional polyamine transport by proton motive force in polyamine-deficient *Escherichia coli*. *J. Bacteriol.* *165*, 972–977.
- Kaur, G., Sengupta, S., Kumar, V., Kumari, A., Ghosh, A., Parrack, P., and Dutta, D. (2014). Novel MntR-Independent mechanism of manganese homeostasis in *Escherichia coli* by the ribosome-associated protein HflX. *J. Bacteriol.* *196*, 2587–2597.
- Kaur, G., Kumar, V., Arora, A., Tomar, A., Ashish, Sur, R., and Dutta, D. (2017). Affected energy metabolism under manganese stress governs cellular toxicity. *Sci. Rep.* *7*, 11645.
- Keseler, I.M., Mackie, A., Peralta-Gil, M., Santos-Zavaleta, A., Gama-Castro, S., Bonavides-Martínez, C., Fulcher, C., Huerta, A.M., Kothari, A., Krummenacker, M., et al. (2013a). EcoCyc: Fusing model organism databases with systems biology. *Nucleic Acids Res.* *41*.
- Keseler, I.M., Mackie, A., Peralta-Gil, M., Santos-Zavaleta, A., Gama-Castro, S., Sar Bonavides-Martínez, C., Fulcher, C., Huerta, A.M., Kothari, A., Krummenacker, M., et al. (2013b). EcoCyc: fusing model organism databases with systems biology. *Nucleic Acids Res.* *41*, 605–612.
- Khademian, M., and Imlay, J.A. (2017). *Escherichia coli* cytochrome c peroxidase is a respiratory oxidase that enables the use of hydrogen peroxide as a terminal electron acceptor. *Proc. Natl. Acad. Sci. U. S. A.* *114*, E6922–E6931.
- Khan, A.U., Mei, Y.H., and Wilson, T. (1992a). A proposed function for spermine and spermidine: protection of replicating DNA against damage by singlet oxygen. *Proc. Natl. Acad. Sci.* *89*, 11426–11427.

- Khan, A.U., Di Mascio, P., Medeiros, M.H.G., and Wilson, T. (1992b). Spermine and spermidine protection of plasmid DNA against single-strand breaks induced by singlet oxygen. *Proc. Natl. Acad. Sci. U. S. A.* *89*, 11428–11430.
- Khan, A.U., Mei, Y.H., and Wilson, T. (1992c). A proposed function for spermine and spermidine: Protection of replicating DNA against damage by singlet oxygen. *Proc. Natl. Acad. Sci. U. S. A.* *89*, 11426–11427.
- Kobayashi, K. (2017). Sensing Mechanisms in the Redox-Regulated, [2Fe-2S] Cluster-Containing, Bacterial Transcriptional Factor SoxR. *Acc. Chem. Res.* *50*, 1672–1678.
- Koenig, H., Goldstone, A. D., Trout, J. j. and Lu, C. Y. (1987). Polyamine mediate uncontrolled calcium entry and cell damage in rat heart in the calcium paradox. *Journal of Clinical Investigation.* *80*, 1322-1331.
- Kóña, J., and Brinck, T. (2006). A combined molecular dynamics simulation and quantum chemical study on the mechanism for activation of the OxyR transcription factor by hydrogen peroxide. *Org. Biomol. Chem.* *4*, 3468–3478.
- Koo, M.S., Lee, J.H., Rah, S.Y., Yeo, W.S., Lee, J.W., Lee, K.L., Koh, Y.S., Kang, S.O., and Roe, J.H. (2003). A reducing system of the superoxide sensor SoxR in *Escherichia coli*. *EMBO J.* *22*, 2614–2622.
- Korshunov, S., and Imlay, J.A. (2006). Detection and quantification of superoxide formed within the periplasm of *Escherichia coli*. *J. Bacteriol.* *188*, 6326–6334.
- Korshunov, S., and Imlay, J.A. (2010). Two sources of endogenous hydrogen peroxide in *Escherichia coli*. *Mol Microbiol.* *7059*, 1389..1401.
- Kreiswirth, B.N., Löfdahl, S., Betley, M.J., O'reilly, M., Schlievert, P.M., Bergdoll, M.S., and Novick, R.P. (1983). The toxic shock syndrome exotoxin structural gene is not detectably transmitted by a prophage. *Nature* *305*, 709–712.
- Krishnakumar, R., Craig, M., Imlay, J.A., and Slauch, J.M. (2004). Differences in Enzymatic Properties Allow SodCI but Not SodCII To Contribute to Virulence in *Salmonella enterica* Serovar *Typhimurium* Strain 14028. *J. Bacteriol.* *186*, 5230.
- Krüger, A., Vowinckel, J., Mülleler, M., Grote, P., Capuano, F., Bluemlein, K., and Ralser, M. (2013). Tpo1-mediated spermine and spermidine export controls cell cycle delay and times antioxidant protein expression during the oxidative stress response. *EMBO Rep.* *14*, 1113–1119.

- Kussmaul, L., and Hirst, J. (2006). The mechanism of superoxide production by NADH:ubiquinone oxidoreductase (complex I) from bovine heart mitochondria. *Proc. Natl. Acad. Sci. U. S. A.* *103*, 7607–7612.
- Kwon, D.H., and Lu, C.D. (2007). Polyamine effects on antibiotic susceptibility in bacteria. *Antimicrob. Agents Chemother.* *51*, 2070–2077.
- Lee, J.W., and Helmann, J.D. (2006). The PerR transcription factor senses H₂O₂ by metal-catalysed histidine oxidation. *Nature* *440*, 363–367.
- Li, H., Singh, A.K., McIntyre, L.M., and Sherman, L.A. (2004). Differential Gene Expression in Response to Hydrogen Peroxide and the Putative PerR Regulon of *Synechocystis* sp. Strain PCC 6803. *J. Bacteriol.* *186*, 3331.
- Limsuwun, K., and Jones, P.G. (2000). Spermidine acetyltransferase is required to prevent spermidine toxicity at low temperatures in *Escherichia coli*. *J. Bacteriol.* *182*, 5373–5380.
- Liochev, S.I., and Fridovich, I. (1992). Fumarase C, the stable fumarase of *Escherichia coli*, is controlled by the soxRS regulon. *Proc. Natl. Acad. Sci. U. S. A.* *89*, 5892.
- Liochev, S.I., and Fridovich, I. (2011). Is superoxide able to induce SoxRS? *Free Radic. Biol. Med.* *50*, 1813.
- Lo, F.-C., Lee, J.-F., Liaw, W.-F., Hsu, I.-J., Tsai, Y.-F., Chan, S.I., and Yu, S.S.-F. (2012). The Metal Core Structures in the Recombinant *Escherichia coli* Transcriptional Factor SoxR. *Chem. - A Eur. J.* *18*, 2565–2577.
- Löser, C. (2000). Polyamines in human and animal milk. *Br. J. Nutr.* *84 Suppl 1*.
- LØVaas, E. (1996). Antioxidative and Metal-Chelating Effects of Polyamines. *Adv. Pharmacol.* *38*, 119–149.
- Lu, Y. (2018). Assembly and transfer of iron–sulfur clusters in the plastid. *Front. Plant Sci.* *9*, 336.
- Lushchak, V.I., and Storey, K.B. (2021). Oxidative stress concept updated: Definitions, classifications, and regulatory pathways implicated. *EXCLI J.* *20*, 956–967.
- Madeo, F., Eisenberg, T., Pietrocola, F., and Kroemer, G. (2018). Spermidine in health and disease. *Science (80-.)*. *359*.
- Makui, H., Roig, E., Cole, S.T., Helmann, J.D., Gros, P., and Cellier, M.F.M. (2000).

- Identification of the *Escherichia coli* K-12 Nramp orthologue (MntH) as a selective divalent metal ion transporter. *Mol. Microbiol.* *35*, 1065–1078.
- Martin, J.E., and Imlay, J.A. (2011). The alternative aerobic ribonucleotide reductase of *Escherichia coli*, NrDEF, is a manganese-dependent enzyme that enables cell replication during periods of iron starvation. *Mol. Microbiol.* *80*, 319–334.
- Martin, J.E., Waters, L.S., Storz, G., and Imlay, J.A. (2015). The *Escherichia coli* Small Protein MntS and Exporter MntP Optimize the Intracellular Concentration of Manganese. *PLOS Genet.* *11*, e1004977.
- Massé, E., and Gottesman, S. A small RNA regulates the expression of genes involved in iron metabolism in *Escherichia coli*.
- Massey, V., Strickland, S., Mayhew, S.G., Howell, L.G., Engel, P.C., Matthews, R.G., Schuman, M., and Sullivan, P.A. (1969). The production of superoxide anion radicals in the reaction of reduced flavins and flavoproteins with molecular oxygen. *Biochem. Biophys. Res. Commun.* *36*, 891–897.
- Maurelli, A.T., Fernández, R.E., Bloch, C.A., Rode, C.K., and Fasano, A. (1998). “Black holes” and bacterial pathogenicity: A large genomic deletion that enhances the virulence of *Shigella* spp. and enteroinvasive *Escherichia coli*. *Proc. Natl. Acad. Sci. U. S. A.* *95*, 3943–3948.
- McHugh, J.P., Rodríguez-Quñones, F., Abdul-Tehrani, H., Svistunenko, D.A., Poole, R.K., Cooper, C.E., and Andrews, S.C. (2003). Global iron-dependent gene regulation in *Escherichia coli*: A new mechanism for iron homeostasis. *J. Biol. Chem.* *278*, 29478–29486.
- Messner, K.R., and Imlay, J.A. (1999). The identification of primary sites of superoxide and hydrogen peroxide formation in the aerobic respiratory chain and sulfite reductase complex of *Escherichia coli*. *J. Biol. Chem.* *274*, 10119–10128.
- Mettert, E.L., and Kiley, P.J. (2015). Fe-S proteins that regulate gene expression. *Biochim. Biophys. Acta* *1853*, 1284–1293.
- Michael, A.J. (2018). Polyamine function in archaea and bacteria. *J. Biol. Chem.* *293*, 18693–18701.
- Miller-Fleming, L., Olin-Sandoval, V., Campbell, K., and Ralser, M. (2015). Remaining Mysteries of Molecular Biology: The Role of Polyamines in the Cell. *J. Mol. Biol.*

427, 3389–3406.

Minois, N., Carmona-Gutierrez, D., and Madeo, F. (2011). Polyamines in aging and disease. *Aging (Albany, NY)*. *3*, 716–732.

Minton, K.W., TABORt, H., and WHITE TABORt, C. (1990). Paraquat toxicity is increased in *Escherichia coli* defective in the synthesis of polyamines (spermidine/putresdne/superoxide/oxygen-dependent toxidy/methyl viologen).

Mishra, S., and Imlay, J. (2012). Why do bacteria use so many enzymes to scavenge hydrogen peroxide? *Arch. Biochem. Biophys.* *525*, 145.

Miyamoto, S., Kashiwagi, K., Ito, K., Watanabe, S.I., and Igarashi, K. (1993). Estimation of Polyamine Distribution and Polyamine Stimulation of Protein Synthesis in *Escherichia coli*. *Arch. Biochem. Biophys.* *300*, 63–68.

Mongkolsuk, S., and Helmann, J.D. (2002). Regulation of inducible peroxide stress responses. *Mol. Microbiol.* *45*, 9–15.

Morikawa, K., Ohniwa, R.L., Kim, J., Maruyama, A., Ohta, T., and Takeyasu, K. (2006). Bacterial nucleod dynamics: Oxidative stress response in *Staphylococcus aureus*. *Genes to cells* *11*, 409-423.

Morris, D.R., and Fillingame, R.H. (1974). Regulation of amino acid decarboxylation. *Annu. Rev. Biochem.* *43*, 303–325.

Morris, D. R. and Igarashi, K.(1984). Physiological Effects in Bovine Lymphocytes of Inhibiting Polyamine Synthesis with Ethylglyoxal Bis(guanylhydrazone)', *Cancer Research*, *44*, 5332–5337.

Motomura, N., and Tomota, Y. (2006). Olfactory dysfunction in dementia of Alzheimer's type and vascular dementia. *Psychogeriatrics* *6*, 19–20.

Napolitano, R., Janel-Bintz, R., Wagner, J., and Fuchs, R.P.P. (2000). All three SOS-inducible DNA polymerases (Pol II, Pol IV and Pol V) are involved in induced mutagenesis. *EMBO J.* *19*, 6259.

Nimse, S.B., and Pal, D. (2015). Free radicals, natural antioxidants, and their reaction mechanisms. *RSC Adv.* *5*, 27986–28006.

Nishibori, N., Fujihara, S., and Akatuki, T. (2007). Amounts of polyamines in foods in Japan and intake by Japanese. *Food Chem.* *100*, 491–497.

- Nnyepi, M.R., Peng, Y., and Broderick, J.B. (2007). Inactivation of *E. coli* pyruvate formate-lyase: role of AdhE and small molecules. *Arch. Biochem. Biophys.* *459*, 1–9.
- Nunoshiba, T., Hidalgo, E., Cuevas, C.F.A., and Demple, B. (1992). Two-stage control of an oxidative stress regulon: the *Escherichia coli* SoxR protein triggers redox-inducible expression of the soxS regulatory gene. *J. Bacteriol.* *174*, 6054–6060.
- Ogasawara, T., Ito, K., and Igarashi, K. (1989). Effect of polyamines on globin synthesis in a rabbit reticulocyte polyamine-free protein synthetic system. *J. Biochem.* *105*, 164–167.
- Olavarría, K., Valdés, D., and Cabrera, R. (2012). The cofactor preference of glucose-6-phosphate dehydrogenase from *Escherichia coli*- modeling the physiological production of reduced cofactors. *FEBS J.* *279*, 2296–2309.
- Oriol-Audit, C. (1978). Polyamine-Induced Actin Polymerization. *Eur. J. Biochem.* *87*, 371–376.
- Outten, F.W., Djaman, O., and Storz, G. (2004). A suf operon requirement for Fe-S cluster assembly during iron starvation in *Escherichia coli*. *Mol. Microbiol.* *52*, 861–872.
- Oves-Costales, D., Kadi, N., Fogg, M.J., Song, L., Wilson, K.S., and Challis, G.L. (2007). Enzymatic logic of anthrax stealth siderophore biosynthesis: AsbA catalyzes ATP-dependent condensation of citric acid and spermidine. *J. Am. Chem. Soc.* *129*, 8416–8417.
- Patel, C.N., Wortham, B.W., Lines, J.L., Fetherston, J.D., Perry, R.D., and Oliveira, M.A. (2006). Polyamines Are Essential for the Formation of Plague Biofilm. *J. Bacteriol.* *188*, 2355–2363.
- Pegg, A.E. (2013). Toxicity of polyamines and their metabolic products. *Chem. Res. Toxicol.* *26*, 1782–1800.
- Pegg, A.E. (2016). Functions of polyamines in mammals. *J. Biol. Chem.* *291*, 14904–14912.
- Pegg, A.E. (2018). Introduction to the thematic minireview series: Sixty plus years of polyamine research. *J. Biol. Chem.* *293*, 18681–18692.
- Pérez-Cano, F.J., González-Castro, A., Castellote, C., Franch, À., and Castell, M. (2010). Influence of breast milk polyamines on suckling rat immune system maturation. *Dev. Comp. Immunol.* *34*, 210–218.

- Pick, U., Rental, M., Chitlaru, E., and Weiss, M. (1990). Polyphosphate-hydrolysis--a protective mechanism against alkaline stress? *FEBS Lett.* 274, 15–18.
- Pistocchi, R., Kashiwagi, K., Miyamoto, S., Nukui, E., Sadakata, Y., Kobayashi, H., and Igarashi, K. (1993). Characteristics of the operon for a putrescine transport system that maps at 19 minutes on the *Escherichia coli* chromosome. *J. Biol. Chem.* 268, 146–152.
- Plaza-Zamora, J., Sabater-Molina, M., Rodríguez-Palmero, M., Rivero, M., Bosch, V., Nadal, J.M., Zamora, S., and Larqué, E. (2005). Polyamines in human breast milk for preterm and term infants.
- Pohjanpelto, P., Virtanen, I., and Hölttä, E. (1981). Polyamine starvation causes disappearance of actin filaments and microtubules in polyamine-auxotrophic CHO cells. *Nature* 293, 475–477.
- Pomposiello, P.J., Koutsolioutsou, A., Carrasco, D., and Demple, B. (2003). SoxRS-Regulated Expression and Genetic Analysis of the *yggX* Gene of *Escherichia coli*. *J. Bacteriol.* 185, 6624.
- Poole, L.B. (2005). Bacterial defenses against oxidants: mechanistic features of cysteine-based peroxidases and their flavoprotein reductases. *Arch. Biochem. Biophys.* 433, 240–254.
- Putignani, L., Gesù, B., Pediatrico, O., Bogomolnaya, L., Fang, S.-B., Huang, C.-J., Huang, C.-H., Wang, K.-C., Chang, N.-W., Pan, H.-Y., et al. (2017).) *speG* Is Required for Intracellular Replication of Salmonella in Various Human Cells and Affects Its Polyamine Metabolism and Global Transcriptomes. *Front. Microbiol.* 8, 2245.
- Py, B., and Barras, F. (2010). Building Fe-S proteins: bacterial strategies. *Nat. Rev. Microbiol.* 8, 436–446.
- Rabellotti, E., Sessa, A., Tunici, P., Bardocz, S., Grant, G., Pusztai, A., and Perin, A. (1998). Oxidative degradation of polyamines in rat pancreatic hypertrophy. *Biochim. Biophys. Acta - Mol. Basis Dis.* 1406, 321–326.
- Rahman, I., Kode, A., and Biswas, S.K. (2007). Assay for quantitative determination of glutathione and glutathione disulfide levels using enzymatic recycling method. *Nat. Protoc.* 2007 16 1, 3159–3165.
- Rai, A.N., Thornton, J.A., Stokes, J., Sunesara, I., Swiatlo, E., and Nanduri, B. (2016).

- Polyamine transporter in *Streptococcus pneumoniae* is essential for evading early innate immune responses in *pneumococcal pneumonia*. *Sci. Reports* 2016 6, 1–15.
- Rider, J.E., Hacker, A., Mackintosh, C.A., Pegg, A.E., Woster, P.M., and Casero, R.A. (2007). Spermine and spermidine mediate protection against oxidative damage caused by hydrogen peroxide. *Amino Acids* 33, 231–240.
- Roche, B., Aussel, L., Ezraty, B., Mandin, P., Py, B., and Barras, F. (2013). Reprint of: Iron/sulfur proteins biogenesis in prokaryotes: Formation, regulation and diversity. *Biochim. Biophys. Acta - Bioenerg.* 1827, 923–937.
- Romain, N., Dandrifosse, G., Jeusette, F., and Forget, P. (1992). Polyamine concentration in rat milk and food, human milk, and infant formulas. *Pediatr. Res.* 32, 58–63.
- Sabater-Molina, M., Larqué, E., Torrella, F., Plaza, J., Lozano, T., Muñoz, A., and Zamora, S. (2009). Effects of dietary polyamines at physiologic doses in early-weaned piglets. *Nutrition* 25, 940–946.
- Sagar, N.A., Tarafdar, S., Agarwal, S., Tarafdar, A., and Sharma, S. (2021). medical sciences Polyamines: Functions, Metabolism, and Role in Human Disease Management.
- Sakai, A., Nakanishi, M., Yoshiyama, K., and Maki, H. (2006). Impact of reactive oxygen species on spontaneous mutagenesis in *Escherichia coli*. *Genes Cells* 11, 767–778.
- Sakamoto, A., Terui, Y., Yoshida, T., Yamamoto, T., Suzuki, H., Yamamoto, K., Ishihama, A., Igarashi, K., and Kashiwagi, K. (2015). Three Members of Polyamine Modulon under Oxidative Stress Conditions: Two Transcription Factors (SoxR and EmrR) and a Glutathione Synthetic Enzyme (GshA).
- Sandoval, J.M., Arenas, F.A., and Vásquez, C.C. (2011). Glucose-6-Phosphate Dehydrogenase Protects *Escherichia coli* from Tellurite-Mediated Oxidative Stress. *PLoS One* 6, e25573.
- Schellhorn, H.E., and Hassan, H.M. (1988). Transcriptional regulation of *katE* in *Escherichia coli* K-12. *J. Bacteriol.* 170, 4286–4292.
- Schiller, D., Kruse, D., Kneifel, H., Kramer, R., and Burkovski, A. (2000). Polyamine transport and role of *potE* in response to osmotic stress in *Escherichia coli*. *J. Bacteriol.* 182, 6247–6249.
- Schuber, F. (1989). Influence of polyamines on membrane functions. *Biochem. J.* 260, 1–10.

- Schwartz, C.J., Giel, J.L., Patschkowski, T., Luther, C., Ruzicka, F.J., Beinert, H., and Kiley, P.J. (2001). IscR, an Fe-S cluster-containing transcription factor, represses expression of *Escherichia coli* genes encoding Fe-S cluster assembly proteins. *Proc. Natl. Acad. Sci. U. S. A.* 98, 14895–14900.
- Seaver, L.C., and Imlay, J.A. (2004). Are respiratory enzymes the primary sources of intracellular hydrogen peroxide? *J. Biol. Chem.* 279, 48742–48750.
- Sen, A., and Imlay, J.A. (2021). How Microbes Defend Themselves From Incoming Hydrogen Peroxide. *Front. Immunol.* 12, 1104.
- Shah, P., and Swiatlo, E. (2008). A multifaceted role for polyamines in bacterial pathogens. *Mol. Microbiol.* 68, 4–16.
- Sissi, C., and Palumbo, M. (2009). Effects of magnesium and related divalent metal ions in topoisomerase structure and function. *Nucleic Acids Res.* 37, 702.
- Slade, D., and Radman, M. (2011). Oxidative Stress Resistance in *Deinococcus radiodurans*. *Microbiol. Mol. Biol. Rev.* 75, 133.
- Soda, K. (2010). Polyamine intake, dietary pattern, and cardiovascular disease. *Med. Hypotheses* 75, 299–301.
- Song, M.K., and Hunt, J.A. (1988). Specific role of manganese and magnesium on RNA synthesis in rabbit bone marrow erythroid cell nuclei. *Biol. Trace Elem. Res.* 16, 203–219.
- Stadtman, E.R., Berlett, B.S., and Chock, P.B. (1990). Manganese-dependent disproportionation of hydrogen peroxide in bicarbonate buffer. *Proc. Natl. Acad. Sci. U. S. A.* 87, 384–388.
- Stewart, T.M., Dunston, T.T., Woster, P.M., and Casero, R.A. (2018). Polyamine catabolism and oxidative damage. *J. Biol. Chem.* 293, 18736–18745.
- Stieglmeier, M., Wirth, R., Kminek, G., and Moissl-Eichinger, C. (2009). Cultivation of anaerobic and facultatively anaerobic bacteria from spacecraft-associated clean rooms. *Appl. Environ. Microbiol.* 75, 3484–3491.
- Sun, S.Y. (2010). N-acetylcysteine, reactive oxygen species and beyond. *Cancer Biol. Ther.* 9.
- Tabor, C.W., and Tabor, H. (1984a). Polyamines. *Annu. Rev. Biochem.* 53, 749–790.

- Tabor, C.W., and Tabor, H. (1984b). Polyamines. *Annu. Rev. Biochem.* 53, 749–790.
- Tabor, C.W., and Tabor, H. (1985). Polyamines in microorganisms. *Microbiol. Rev.* 49, 81.
- Tadolini, B. (1988a). The influence of polyamine-nucleic acid complexes on Fe²⁺ autoxidation. *Mol. Cell. Biochem.* 83, 179–185.
- Tadolini, B. (1988b). Polyamine inhibition of lipoperoxidation. The influence of polyamines on iron oxidation in the presence of compounds mimicking phospholipid polar heads. *Biochem. J.* 249, 33–36.
- Tang, Y., Quail, M.A., Artymiuk, P.J., Guest, J.R., and Green, J. (2002). *Escherichia coli* aconitases and oxidative stress: Post-transcriptional regulation of *sodA* expression. *Microbiology* 148, 1027–1037.
- Tardat, B., and Touati, D. (1991). Two global regulators repress the anaerobic expression of MnSOD in *Escherichia coli*::Fur (ferric uptake regulation) and Arc (aerobic respiration control). *Mol. Microbiol.* 5, 455–465.
- Thomas, V., Chaudhari, S., Jones, J., Zimmerman, M., and Bayles, K. (2015). Electron Paramagnetic Resonance (EPR) Spectroscopy to Detect Reactive Oxygen Species in *Staphylococcus aureus*. *Bio-Protocol* 5.
- Touati, D. (2000). Sensing and protecting against superoxide stress in *Escherichia coli* - How many ways are there to trigger soxRS response? *Redox Rep.* 5, 287–293.
- Vashishtha, A.K., Wang, J., and Konigsberg, W.H. (2016). Different Divalent Cations Alter the Kinetics and Fidelity of DNA Polymerases. *J. Biol. Chem.* 291, 20869.
- Van Vliet, A.H.M., Baillon, M.L.A., Penn, C.W., and Ketley, J.M. (1999). *Campylobacter jejuni* Contains Two Fur Homologs: Characterization of Iron-Responsive Regulation of Peroxide Stress Defense Genes by the PerR Repressor. *J. Bacteriol.* 181, 6371.
- Wallace, H.M., Fraser, A. V., and Hughes, A. (2003). A perspective of polyamine metabolism. *Biochem. J.* 376, 1–14.
- Waller, J.C., Alvarez, S., Naponelli, V., Lara-Nuñez, A., Blaby, I.K., Da Silva, V., Ziemak, M.J., Vickers, T.J., Beverley, S.M., Edison, A.S., et al. (2010). A role for tetrahydrofolates in the metabolism of iron-sulfur clusters in all domains of life. *Proc. Natl. Acad. Sci. U. S. A.* 107, 10412–10417.
- Waters, L.S., Sandoval, M., and Storz, G. (2011). The *Escherichia coli* MntR miniregulon

- includes genes encoding a small protein and an efflux pump required for manganese homeostasis. *J. Bacteriol.* *193*, 5887–5897.
- Watanabe, S. I., Kusama-Eguchi, K., Kobayashi, H. and Igarashi, K. (1991) ‘Estimation of polyamine binding to macromolecules and ATP in bovine lymphocytes and rat liver’, *Journal of Biological Chemistry*, *266*, 20803–20809
- Weatherburn, D.C., Billo, E.J., Jones, J.P., and Margerum, D.W. (2002). Effect of ring size on the stability of polyamine complexes containing linked consecutive rings. *Inorg. Chem.* *9*, 1557–1559.
- Wilmes-Riesenberg, M.R., Bearson, B., Foster, J.W., and Curtiss, R. (1996). Role of the acid tolerance response in virulence of *Salmonella typhimurium*. *Infect. Immun.* *64*, 1085.
- Worst, D.J., Gerrits, M.M., Vandenbroucke-Grauls, C.M.J.E., and Kusters, J.G. (1998). *Helicobacter pylori* ribBA-mediated riboflavin production is involved in iron acquisition. *J. Bacteriol.* *180*, 1473–1479.
- Wright, J.M., Satishchandran, C., and Boyle, S.M. (1986). Transcription of the *speC* (ornithine decarboxylase) gene of *Escherichia coli* is repressed by cyclic AMP and its receptor protein. *Gene* *44*, 37–45.
- Wu, J., and Weiss, B. (1992). Two-stage induction of the *soxRS* (superoxide response) regulon of *Escherichia coli*. *J. Bacteriol.* *174*, 3915–3920.
- Wu, H.J., Seib, K.L., Srikhanta, Y.N., Kidd, S.P., Edwards, J.L., Maguire, T.L., Grimmond, S.M., Apicella, M.A., McEwan, A.G., and Jennings, M.P. (2006). PerR controls Mn-dependent resistance to oxidative stress in *Neisseria gonorrhoeae*. *Mol. Microbiol.* *60*, 401–416.
- Yao, X., and Lu, C.-D. (2014). Characterization of *Staphylococcus aureus* Responses to Spermine Stress. *Curr. Microbiol.* *69*, 394–403.
- Yoshida, M., Kashiwagi, K., Shigemasa, A., Taniguchi, S., Yamamoto, K., Makinoshima, H., Ishihama, A., and Igarashi, K. (2004). A unifying model for the role of polyamines in bacterial cell growth, the polyamine modulon. *J. Biol. Chem.* *279*, 46008–46013.
- Zaslaver, A., Bren, A., Ronen, M., Itzkovitz, S., Kikoin, I., Shavit, S., Liebermeister, W., Surette, M.G., and Alon, U. (2006). A comprehensive library of fluorescent transcriptional reporters for *Escherichia coli*. *Nat. Methods* *3*, 623–628.

Appendix

Appendix Table 1. The list of strains and plasmids used in this work.

Strains	Genotype/Features	References
BW25113	<i>Escherichia coli</i> ; <i>rrnB3</i> Δ <i>lacZ4787</i> <i>hsdR514</i> Δ (<i>araBAD</i>) 567 Δ (<i>rhaBAD</i>)568 <i>rph-1</i>	(Baba et al., 2006)
<i>S. aureus</i> RN4220	NCTC8325-4; mutation in <i>sauI</i> <i>hsdR</i>	(Kreiwirth et al., 1983)
<i>S. aureus</i> USA300	<i>Staphylococcus aureus</i> subsp. <i>aureus</i> Rosenbach ATCC BAA- 1717	(Kreiwirth et al., 1983)
Δ <i>speG</i>	BW25113, Δ <i>speG</i> :: <i>kan</i> ^R	(Baba et al., 2006)
Δ <i>sodA</i>	BW25113, Δ <i>sodA</i> :: <i>kan</i> ^R	(Baba et al., 2006)
Δ <i>sodB</i>	BW25113, Δ <i>sodB</i> :: <i>kan</i> ^R	(Baba et al., 2006)
Δ <i>zwf</i>	BW25113, Δ <i>sodC</i> :: <i>kan</i> ^R	(Baba et al., 2006)
Δ <i>fis</i>	BW25113, Δ <i>fis</i> :: <i>kan</i> ^R	(Baba et al., 2006)
Δ <i>ihfA</i>	BW25113, Δ <i>ihfA</i> :: <i>kan</i> ^R	(Baba et al., 2006)
Δ <i>iscU</i>	BW25113, Δ <i>iscU</i> :: <i>kan</i> ^R	(Baba et al., 2006)
Δ <i>ygfZ</i>	BW25113, Δ <i>ygfZ</i> :: <i>kan</i> ^R	(Baba et al., 2006)
Δ <i>soxS</i>	BW25113, Δ <i>soxS</i> :: <i>kan</i> ^R	(Baba et al., 2006)
Δ <i>marA</i>	BW25113, Δ <i>marA</i> :: <i>kan</i> ^R	(Baba et al., 2006)
Δ <i>marB</i>	BW25113, Δ <i>marB</i> :: <i>kan</i> ^R	(Baba et al., 2006)
Δ <i>ahpC</i>	BW25113, Δ <i>ahpC</i> :: <i>kan</i> ^R	(Baba et al., 2006)
Δ <i>katG</i>	BW25113, Δ <i>katG</i> :: <i>kan</i> ^R	(Baba et al., 2006)
Δ <i>speGΔ<i>sodA</i></i>	BW25113, Δ <i>speG</i> , Δ <i>sodA</i> :: <i>kan</i> ^R	This study
Δ <i>speGΔ<i>sodB</i></i>	BW25113, Δ <i>speG</i> , Δ <i>sodB</i> :: <i>kan</i> ^R	This study
Δ <i>speGΔ<i>sodAΔ<i>sodB</i></i></i>	BW25113, Δ <i>speG</i> , Δ <i>sodA</i> , Δ <i>sodB</i> :: <i>kan</i> ^R	This study
Δ <i>speGΔ<i>zwf</i></i>	BW25113, Δ <i>speG</i> , Δ <i>zwf</i> :: <i>kan</i> ^R	This study

<i>ΔspeGΔsoxS</i>	BW25113, <i>ΔspeG</i> , <i>ΔsoxS::kan^R</i>	This study
<i>ΔspeGΔfis</i>	BW25113, <i>ΔspeG</i> , <i>Δfis::kan^R</i>	This study
<i>ΔspeGΔihfA</i>	BW25113, <i>ΔspeG</i> , <i>ΔihfA::kan^R</i>	This study
<i>ΔspeGΔiscU</i>	BW25113, <i>ΔspeG</i> , <i>ΔiscU::kan^R</i>	This study
<i>ΔspeGΔygfZ</i>	BW25113, <i>ΔspeG</i> , <i>ΔygfZ::kan^R</i>	This study
<i>ΔspeGΔmarA</i>	BW25113, <i>ΔspeG</i> , <i>ΔmarA::kan^R</i>	This study
<i>ΔspeGΔmarB</i>	BW25113, <i>ΔspeG</i> , <i>ΔmarB::kan^R</i>	This study
JRG3533	MC4100 ϕ (<i>sodA-lacZ</i>)49, <i>cm^R</i>	(Tang et al., 2002)
RKM1	BW25113, <i>ΔspeG</i> , <i>sodA-lacZ:cm^R</i>	This study
Plasmids		
pET28a (+)	<i>kan^R</i> ; T7-promoter; IPTG inducible	Novagen
pBAD/Myc-His A	<i>amp^R</i> ; pBAD-promoter; Ara inducible	ThermoFisher
pBAD- <i>zwf</i>	<i>zwf</i> cloned in pBAD TOPO (Invitrogen)	(Sandoval et al., 2011)
pBAD- <i>sodA</i>	<i>sodA</i> cloned in pBAD/Myc-His A vector	This study
pET- <i>sodA</i>	<i>sodA</i> cloned in pET28a (+) vector	This study
pET- <i>ahpC</i>	<i>ahpC</i> cloned in pET28a (+) vector	This study
pET- <i>katG</i>	<i>katG</i> cloned in pET28a (+) vector	This study
pBAD- <i>speG</i>	<i>speG</i> cloned in pBAD/Myc-His A vector	This study
pUA66- <i>soxS</i>	<i>kan^R</i> ; <i>soxS</i> promoter cloned upstream of <i>gfpmut2</i> reporter in pUA66	(Zaslaver et al., 2006)
pUA66- <i>ahpC</i>	<i>kan^R</i> ; <i>ahpC</i> promoter cloned upstream of <i>gfpmut2</i> reporter in pUA66	(Zaslaver et al., 2006)
pUA66- <i>katG</i>	<i>kan^R</i> ; <i>katG</i> promoter cloned upstream of <i>gfpmut2</i> reporter in	(Zaslaver et al., 2006)

Appendix Table 2. The list of oligonucleotides used in this work

Cloning Primers	Nucleotide sequence	Description
DG12	GCTACACATATGAGCTATACCCTGCC	Forward primer with NdeI site
DG13	GCACCGAAGCTTATTTTTTCGCCGC	Reverse primer with HindIII site
DG14	CAATCAGCTAGCATGTCATTCGAATTACC	Forward primer with NheI
DG16	CGATCAAGCTTATGCAGCGAGATTTTTC	Reverse primer with HindIII
RM7	GCAGTACATATGAGCACGTCAGACG	Forward primer with NdeI
RM8	GCTTACAAGCTTTTACAGCAGGTCGAAACG	Reverse primer with HindIII
DG9	GTCACGATCATATGTCCTTGATTAACACC	Forward primer with NdeI
DG10	CTGATGAGGATCCTTAGATTTTACCAACCAG	Reverse primer with BamHI
RK3	CGAGTGCCATATGCCAAGCGCCACAGTGT	Forward primer with NdeI
RK4	CGAGTGGAATTCCTATTGTGCGGTCGGCTTC	Reverse primer with EcoRI
RK55	GAGTGCCATATGGCGGTAACGCAAACAGCC	Forward primer with NdeI site
RK56	CGAGTGGAATTCTTACTCAAACCTCATTCCAG	Reverse primer with EcoRI site
RT Primers	Nucleotide sequence	Description
sodAF	GCTAACCACAGCCTGTTCTG	Forward and reverse

sodAR	CGCCAGTTTATCGCCTTTCA	primer pairs for <i>sodA</i> gene
<i>soxS</i> F	CGATTACATTCGCCAACGC	Forward and reverse
<i>soxS</i> R	GATCAAACCTGCCGACGGAAA	primer pairs for <i>soxS</i> gene
<i>zwf</i> F	TGTGCCATTCTACCTGCGTA	Forward and reverse
<i>zwf</i> R	CCTTCATCAGGTTGCAGACG	primer pairs for <i>zwf</i> gene
<i>fur</i> F	GGTATCGTCACCCGCCACAA	Forward and reverse
<i>fur</i> R	TGCGGCAATTCACGCTGAC	primer pairs for <i>fur</i> gene
<i>tig</i> F	TTCGGCGTTGAAGATGGTTC	Forward and reverse
<i>tig</i> R	GATCGCCTGAGACTTAACGC	primer pairs for <i>tig</i> gene
<i>hscA</i> F	GCTGCCATCTGTTGTTCCT	Forward and reverse
<i>hscA</i> R	TGATAAGGCAGATGCGGATA	primer pairs for <i>hscA</i> gene
<i>cspA</i> FF	AAAGCGGCAAGGGTCTTAT	Forward and reverse
<i>cspA</i> FR	TAAACATTGGCAGCTGAAGG	primer pairs for <i>cspA</i> gene
<i>nsrR</i> F	GGCGGATGACCAGTATTTCT	Forward and reverse
<i>nsrR</i> R	ACCAATACGTATCGCACTCG	primer pairs for <i>nsrR</i> gene
<i>recA</i> F	GGGCCAGATTGAGAAACAAT	Forward and reverse
<i>recA</i> R	GGTCCGTAGATTTGACGAT	primer pairs for <i>recA</i> gene
<i>rplW</i> F	TGAAGAACGTCTGCTGAAGG	Forward and reverse
<i>rplW</i> R	CAGGGTGTTAACGACTTCGAC	primer pairs for <i>rplW</i> gene
<i>rpsA</i> F	GAAGTTGACGTTGCTCTGGA	Forward and reverse
<i>rpsA</i> R	CCCTTAACTTTGCCGTTGAT	primer pairs for <i>rpsA</i> gene
<i>iscR</i> F	GCTGATATTTCCGAACGTCA	Forward and reverse
<i>iscR</i> R	GCTAATACTTCGCCAACGG	primer pairs for <i>iscR</i> gene
<i>nhaA</i> F	GGGTTGGTTCACCTCGAAATC	Forward and reverse

nhaAR	GCACAATCATCCCACCAATA	primer pairs for <i>nhaA</i> gene
cmrF	CTGAAAGAACTCGGTCGTGA	Forward and reverse
cmrR	TTGCAGCAAGCCATATTCAT	primer pairs for <i>cmr</i> gene
hdeAF	CCTGTGAAGATTTCTGGCT	Forward and reverse
hdeAR	TCCCATTCGCCTTTAACTTT	primer pairs for <i>hdeA</i> gene
dnaKF	ACTCGTATGCCAATGGTTCA	Forward and reverse
dnaKR	GGTAACGTCCAGCAGCAGTA	primer pairs for <i>dnaK</i> gene
betBF	AACTTCTTCAGCTCCGGTCA	Forward and reverse
betBR	GCCGAAGTTAGTTTGC GGAT	primer pairs for <i>betB</i> gene

Appendix Table 3. Microarray data representing upregulated (green) and downregulated (red) genes

Category	Gene name	Accession	Function	Fold Change
	dinG	b0799	ATP-dependent DNA helicase	3.95112827
	dnaG	b3066	DNA primase	2.05896767
I	dnaX	b0470	DNA polymerase III/DNA elongation factor III,	3.04534103
	rpoA	b3295	RNA polymerase, alpha subunit	5.68043539
Replication and Transcription associated genes	rpoZ	b3649	RNA polymerase, omega subunit	2.1063241
	nusB	b0416	transcription antitermination protein	2.33160864
	nusG	b3982	transcription termination factor	3.53514598
	rho	b3783	transcription termination factor	2.31318956
	iscA	b2528	FeS cluster assembly protein	10.4221496
II	iscR	b2531	isc operon transcriptional repressor; suf operon	2.60700843
	iscS	b2530	cysteine desulfurase (tRNA sulfurtransferase),	2.74162783
Iron Homeostasis, ROS, Multidrug resistance and sugar metabolism-associated genes	iscU	b2529	iron-sulfur cluster assembly scaffold protein	4.34152603
	iscX	b2524	Iron binding protein associated with IscS; puta	5.17706274
	hscA	b2526	DnaK-like molecular chaperone specific for Isc	4.01669472
	hscB	b2527	HscA co-chaperone, J domain-containing prote	4.00285371
	fdx	b2525	[2Fe-2S] ferredoxin	3.27489118
	rsxB	b1628	SoxR iron-sulfur cluster reduction factor comp	4.14944455
	rsxC	b1629	SoxR iron-sulfur cluster reduction factor comp	2.25586478
	marA	b1531	multiple antibiotic resistance transcriptional r	19.5347826
	marB	b1532	mar operon regulator, periplasmic	29.8378577
	marR	b1530	transcriptional repressor of multiple antibiotic	2.96438538
	fldA	b0684	flavodoxin 1	2.61823514
	uof	b4637	ryhB-regulated fur leader peptide	3.5942784
	fur	b0683	ferric iron uptake regulon transcriptional repre	2.05192138
	ptsG	b1101	fused glucose-specific PTS enzymes: IIB compo	2.14685021
	ribA	b1277	GTP cyclohydrolase II	1.95546985
	ftnA	b1905	ferritin iron storage protein (cytoplasmic)	0.51528032
	mdtI	b1599	multidrug efflux system transporter	3.20377632
	mdtJ	b1600	multidrug efflux system transporter	3.47120617
	katE	b1732	catalase HPII, heme d-containing	0.40909253
	katG	b3942	catalase-peroxidase HPI, heme b-containing	0.22398699

Category	Gene name	Accession	Function	Fold Change
	rimI	b4373	ribosomal-protein-S18-alanine N-acetyltransferase	2.04821544
	rimM	b2608	16S rRNA processing protein	8.01132574
III	rimO	b0835	ribosomal protein S12 methylthiotransferase;	2.46225187
	rimP	b3170	ribosome maturation factor for 30S subunits	3.34924484
Ribosomal and ribosome biogenesis-associated genes	rlmA	b1822	23S rRNA m(1)G745 methyltransferase, SAM-d	4.97190678
	rlmH	b0636	23S rRNA m(3)Psi1915 pseudouridine methyltr	2.3403622
	rlmL	b0948	fused 23S rRNA m(2)G2445 and m(7)G2069 met	2.09460831
	rluB	b1269	23S rRNA pseudouridine(2605) synthase	2.56272859
	rplA	b3984	50S ribosomal subunit protein L1	7.98603219
	rplB	b3317	50S ribosomal subunit protein L2	7.28516588
	rplC	b3320	50S ribosomal subunit protein L3	7.50404155
	rplD	b3319	50S ribosomal subunit protein L4	7.41094836
	rplE	b3308	50S ribosomal subunit protein L5	3.8774636
	rplF	b3305	50S ribosomal subunit protein L6	4.55513068
	rplI	b4203	50S ribosomal subunit protein L9	5.4238731
	rplJ	b3985	50S ribosomal subunit protein L10	4.86396766
	rplK	b3983	50S ribosomal subunit protein L11	5.40776063
	rplL	b3986	50S ribosomal subunit protein L7/L12	6.05065951
	rplM	b3231	50S ribosomal subunit protein L13	2.77822142
	rplN	b3310	50S ribosomal subunit protein L14	2.19186396
	rplO	b3301	50S ribosomal subunit protein L15	3.71810794
	rplP	b3313	50S ribosomal subunit protein L16	5.92042941
	rplQ	b3294	50S ribosomal subunit protein L17	2.9721687
	rplR	b3304	50S ribosomal subunit protein L18	4.35410934
	rplS	b2606	50S ribosomal subunit protein L19	6.14857535
	rplU	b3186	50S ribosomal subunit protein L21	3.11625296
	rplV	b3315	50S ribosomal subunit protein L22	5.40932369
	rplW	b3318	50S ribosomal subunit protein L23	10.9802773
	rplX	b3309	50S ribosomal subunit protein L24	3.72152915
	rplY	b2185	50S ribosomal subunit protein L25	5.65241773
	rpmA	b3185	50S ribosomal subunit protein L27	5.34942238
	rpmB	b3637	50S ribosomal subunit protein L28	2.81037901
	rpmC	b3312	50S ribosomal subunit protein L29	7.54130725
	rpmD	b3302	50S ribosomal subunit protein L30	3.2492543
	rpmF	b1089	50S ribosomal subunit protein L32	2.19649389
	rpmG	b3636	50S ribosomal subunit protein L33	3.34337768

Category	Gene name	Accession	Function	Fold Change
	rpmH	b3703	50S ribosomal subunit protein L34	2.82972896
	rpmI	b1717	50S ribosomal subunit protein L35	2.41728177
	rpmJ	b3299	50S ribosomal subunit protein L36	6.75481043
	rpsA	b0911	30S ribosomal subunit protein S1	7.50900472
	rpsB	b0169	30S ribosomal subunit protein S2	5.08408331
	rpsC	b3314	30S ribosomal subunit protein S3	5.90830813
	rpsD	b3296	30S ribosomal subunit protein S4	6.29468752
	rpsE	b3303	30S ribosomal subunit protein S5	4.14945828
	rpsF	b4200	30S ribosomal subunit protein S6	5.44536845
	rpsG	b3341	30S ribosomal subunit protein S7	4.70514293
	rpsH	b3306	30S ribosomal subunit protein S8	5.03927988
	rpsI	b3230	30S ribosomal subunit protein S9	2.44726822
	rpsJ	b3321	30S ribosomal subunit protein S10	7.31960456
	rpsK	b3297	30S ribosomal subunit protein S11	6.60295935
	rpsM	b3298	30S ribosomal subunit protein S13	5.01492776
	rpsN	b3307	30S ribosomal subunit protein S14	4.99620468
	rpsQ	b3311	30S ribosomal subunit protein S17	7.24086559
	rpsR	b4202	30S ribosomal subunit protein S18	8.45069592
	rpsS	b3316	30S ribosomal subunit protein S19	10.4145676
	rpsU	b3065	30S ribosomal subunit protein S21	6.67203774
	rsmH	b0082	16S rRNA m(4)C1402 methyltransferase, SAM-co	2.14324556
	tsf	b0170	translation elongation factor EF-Ts	3.70087628
	tufB	b3980	translation elongation factor EF-Tu 2	2.04539434
IV	ynfG	b1589	oxidoreductase, Fe-S subunit	0.2312421
Oxidoreductase	ynfF	b1588	S- and N-oxide reductase, A subunit, periplasmic	0.27367166
and ATP	cydA	b0733	cytochrome d terminal oxidase, subunit I	0.34893479
synthesis	cydB	b0734	cytochrome d terminal oxidase, subunit II	0.31578747
related genes	atpI	b3739	ATP synthase, membrane-bound accessory factor	2.06546314
V	fabD	b1092	malonyl-CoA-[acyl-carrier-protein] transacylase	3.8809974
Fatty acid	fabF	b1095	3-oxoacyl-[acyl-carrier-protein] synthase II	3.49672226
metabolism-	fabG	b1093	3-oxoacyl-[acyl-carrier-protein] reductase	2.16851668
related	fabH	b1091	3-oxoacyl-[acyl-carrier-protein] synthase III	2.30511292
genes	fabZ	b0180	(3R)-hydroxymyristol acyl carrier protein dehydrogenase	2.73663282

Category	Gene name	Accession	Function	Fold Change
	flgC	b1074	flagellar component of cell-proximal portion of flagellum	0.38113378
	flgD	b1075	flagellar hook assembly protein	0.38372757
VI	flgE	b1076	flagellar hook protein	0.29745148
	flgF	b1077	flagellar component of cell-proximal portion of flagellum	0.46619933
Flagellar biogenesis-related genes	flgK	b1082	flagellar hook-filament junction protein 1	0.35795609
	flgM	b1071	anti-sigma factor for FliA (sigma 28)	0.3390667
	flgN	b1070	export chaperone for FlgK and FlgL	0.36265926
	fliA	b1922	RNA polymerase, sigma 28 (sigma F) factor	0.41683165
	fliC	b1923	flagellar filament structural protein (flagellin)	0.05160497
	fliD	b1924	flagellar filament capping protein	0.18677943
	fliS	b1925	flagellar protein potentiates polymerization	0.32239647
	fliT	b1926	putative flagellar synthesis and assembly chaperone	0.14683468
	fliZ	b1921	RpoS antagonist; putative regulator of FliA activity	0.40852723
	fimA	b4314	major type 1 subunit fimbrin (pilin)	0.39195484
	motB	b1889	protein that enables flagellar motor rotation	0.26737931
	gadA	b3517	glutamate decarboxylase A, PLP-dependent	0.13053199
	gadB	b1493	glutamate decarboxylase B, PLP-dependent	0.06907889
	gadC	b1492	glutamate:gamma-aminobutyric acid antiporter	0.23534929
	gadE	b3512	gad regulon transcriptional activator	0.19047099
VII	hdeA	b3510	stress response protein acid-resistance protein	0.02250208
	hdeB	b3509	acid-resistance protein	0.00950182
Acid-resistance and chaperone genes	groL	b4143	Cpn60 chaperonin GroEL, large subunit of GroE	0.18031685
	groS	b4142	Cpn10 chaperonin GroES, small subunit of GroE	0.25781914
	dnaK	b0014	chaperone Hsp70, with co-chaperone DnaJ	0.21533484
	tig	b0436	peptidyl-prolyl cis/trans isomerase (trigger factor)	2.00420055
	clpB	b2592	protein disaggregation chaperone	0.28567572
	ftsH	b3178	protease, ATP-dependent zinc-metallo	3.00608194
	elaD	b2269	protease, capable of cleaving an AMC-ubiquitin	0.46527625
	ibpA	b3687	heat shock chaperone	0.31514539
	ibpB	b3686	heat shock chaperone	0.48395966
	uspA	b3495	universal stress global response regulator	0.16494791
	uspB	b3494	universal stress (ethanol tolerance) protein B	0.52139802

Category	Gene name	Accession	Function	Fold Change
	hyaA	b0972	hydrogenase 1, small subunit	0.47988936
	hybA	b2996	hydrogenase 2 4Fe-4S ferredoxin-type component	0.20474257
VIII	hybB	b2995	putative hydrogenase 2 cytochrome b type component	0.46592208
	hybC	b2994	hydrogenase 2, large subunit	0.36131142
Hydrogenase and nitrogen metabolizing genes	hybD	b2993	maturation protease for hydrogenase 2	0.37801963
	hybE	b2992	hydrogenase 2-specific chaperone	0.41100931
	hybF	b2991	protein involved with the maturation of hydrogenase 2	0.48389836
	hybO	b2997	hydrogenase 2, small subunit	0.24022274
	nrfA	b4070	nitrite reductase, formate-dependent, cytoplasmic	0.08855544
	nrfB	b4071	nitrite reductase, formate-dependent, pentameric	0.31659208
	nrfC	b4072	formate-dependent nitrite reductase, 4Fe4S sulfur	0.28490247
	nrfD	b4073	formate-dependent nitrite reductase, membrane-associated	0.46217211
	dmsA	b0894	dimethyl sulfoxide reductase, anaerobic, subunit	0.22652659
	dmsB	b0895	dimethyl sulfoxide reductase, anaerobic, subunit	0.15413292
	aroB	b3389	3-dehydroquinate synthase	2.26121472
IX	aroK	b3390	shikimate kinase I	2.04243602
	aroM	b0390	AroM family protein	4.42282202
Amino acid metabolizing genes	pheA	b2599	chorismate mutase and prephenate dehydratase	0.36073883
	tnaA	b3708	tryptophanase/L-cysteine desulfhydrase, PLP-dependent	0.10262431
	tnaB	b3709	tryptophan transporter of low affinity	0.14420319
	tnaC	b3707	tryptophanase leader peptide	0.2131414
	cadA	b4131	lysine decarboxylase, acid-inducible	0.26703994
	cadB	b4132	putative lysine/cadaverine transporter	0.4444759

Appendix Table 4. List of Fis and IHF regulated genes that were upregulated (green) and downregulation (red).

Gene name	Accession	Function	Fold Change	Regulators
gadB	b1493	glutamate decarboxylase B, PLP-	0.069078892	Fis regulated
nrfA	b4070	nitrite reductase, formate-deper	0.088555437	Fis regulated
gadA	b3517	glutamate decarboxylase A, PLP-	0.130531988	Fis regulated
ansB	b2957	periplasmic L-asparaginase 2	0.146419696	Fis regulated
dmsB	b0895	dimethyl sulfoxide reductase, an	0.154132923	Fis/IHF regulated
osmY	b4376	periplasmic protein	0.191358332	Fis regulated
ompC	b2215	outer membrane porin protein C	0.201420092	IHF regulated
katG	b3942	catalase-peroxidase HPI, heme b	0.223986992	Fis regulated
dmsA	b0894	dimethyl sulfoxide reductase, an	0.226526587	Fis/IHF regulated
fumB	b4122	anaerobic class I fumarate hydrat	0.22664556	Fis regulated
gadC	b1492	glutamate:gamma-aminobutyric	0.23534929	Fis regulated
nrfC	b4072	formate-dependent nitrite reduct	0.284902474	Fis regulated
nrfB	b4071	nitrite reductase, formate-deper	0.316592077	Fis regulated
acs	b4069	acetyl-CoA synthetase	0.402722895	Fis regulated
fliZ	b1921	RpoS antagonist; putative regulat	0.40852723	IHF regulated
katE	b1732	catalase HP11, heme d-containing	0.409092533	Fis regulated
mgIA	b2149	fused methyl-galactoside transpo	0.413486179	Fis regulated
fliA	b1922	RNA polymerase, sigma 28 (sigma	0.416831651	IHF regulated
nrfD	b4073	formate-dependent nitrite reduct	0.46217211	Fis regulated
hybB	b2995	putative hydrogenase 2 cytochro	0.465922083	Fis regulated
hyaA	b0972	hydrogenase 1, small subunit	0.479889356	Fis regulated
uspB	b3494	universal stress (ethanol toleran	0.521398024	IHF regulated
dps	b0812	Fe-binding and storage protein; s	0.542404641	Fis regulated
msrA	b4219	methionine sulfoxide reductase	0.548398438	Fis regulated
pflB	b0903	formate C-acetyltransferase 1, ar	0.552198154	Fis regulated
aldB	b3588	aldehyde dehydrogenase B	0.55443503	Fis regulated
hyaD	b0975	hydrogenase 1 maturation protea	0.583348099	Fis regulated
actP	b4067	acetate transporter	0.585936145	Fis regulated
rnpB	b3123	-	0.591970183	Fis regulated
acnB	b0118	bifunctional aconitate hydratase	0.622308282	Fis regulated
nanK	b3222	N-acetylmannosamine kinase	0.624725	Fis regulated
deoA	b4382	thymidine phosphorylase	0.626971766	Fis regulated
deoD	b4384	purine-nucleoside phosphorylas	0.631287757	Fis regulated
osmE	b1739	osmotically-inducible lipoprotein	0.645105105	Fis/IHF regulated
hyaC	b0974	hydrogenase 1, b-type cytochrom	0.647886429	Fis regulated
norW	b2711	NADH:flavorubredoxin oxidored	0.648068466	IHF regulated
dmsC	b0896	dimethyl sulfoxide reductase, an	0.648628991	Fis/IHF regulated
yjch	b4068	DUF485 family inner membrane p	0.652255398	Fis regulated
gadX	b3516	acid resistance regulon transcript	0.658769469	Fis regulated

Gene name	Accession	Function	Fold Change	Regulators
marB	b1532	mar operon regulator, periplasm	29.83785772	Fis regulated
marA	b1531	multiple antibiotic resistance tra	19.53478257	Fis regulated
marR	b1530	transcriptional repressor of mult	2.964385379	Fis regulated
proV	b2677	glycine betaine transporter subu	3.71054895	IHF regulated
rimP	b3170	ribosome maturation factor for 3	3.349244841	Fis regulated
ompF	b0929	outer membrane porin 1a (Ia;b;F	2.782105818	IHF regulated
mazF	b2782	mRNA interferase toxin, antitoxi	2.528091569	Fis regulated
fnr	b1334	oxygen-sensing anaerobic growth	2.409449044	IHF regulated
proP	b4111	proline/glycine betaine transpor	2.340555777	Fis regulated
proW	b2678	glycine betaine transporter subu	2.210573557	IHF regulated
tufB	b3980	translation elongation factor EF-T	2.045394337	Fis regulated
glpQ	b2239	periplasmic glycerophosphodies	1.992814577	Fis regulated
rpsO	b3165	30S ribosomal subunit protein S1	1.920604414	Fis regulated
prfA	b1211	peptide chain release factor RF-1	1.902731669	IHF regulated
nusA	b3169	transcription termination/antiter	1.780656817	Fis regulated
mazE	b2783	antitoxin of the ChpA-ChpR toxin	1.67434581	Fis regulated
gltX	b2400	glutamyl-tRNA synthetase	1.670333108	Fis regulated
htrE	b0139	putative outer membrane usher	1.663641295	IHF regulated
pnp	b3164	polynucleotide phosphorylase/p	1.626036246	Fis regulated
pspE	b1308	thiosulfate:cyanide sulfurtransfe	1.603971958	IHF regulated
cspA	b3556	RNA chaperone and antiterminat	1.562064216	Fis regulated
guaB	b2508	IMP dehydrogenase	1.554487182	Fis regulated
focA	b0904	formate channel	1.545236752	IHF regulated

Appendix Table 5. List of the major chemicals used in this study.

Sl.NO	Chemical Name	Vendor	Catalog number
1	LB Broth	Difco	244620
2	Spermidine	Sigma	85558
3	Thiourea	Sigma	T7875
4	Tyron	Sigma	172553
5	Sodium pyruvate	HIMEDIA	PCT0503
6	L-Ascorbic acid	HIMEDIA	TC094
7	NAC	Sigma	A7250
8	LB Agar	Difco	244520
9	NaCl	Sigma	S7653
10	Hexane-diamine	GLR	GLRIN19020026
11	Perchloric acid	Sigma	244252
12	Sodium carbonate	Sigma	S7795
13	Dansyl chloride	Sigma	D-2625
14	Proline	Sigma	P0380
15	Toluene	Sigma	34866
16	Acetonitrile	Merck	DJ4DF41174
17	H2DCFDA	Sigma	D6883
18	DHE	Sigma	D7008
19	Hydrogen peroxide	merck	HE8H580416
20	Arabinose	Sigma	A3256
21	KCl	Sigma	P9333
22	CaCl ₂	Sigma	C5080
23	MgSO ₄	Sigma	63138
24	Na ₂ CO ₃	Hi-media	GRM851
25	KH ₂ PO ₄	Sigma	P5655
26	HEPES	Sigma	H3375
27	D-glucose	Sigma	G7528
28	DETC	Sigma	D-3506
29	Deferoxamine mesylate salt	Sigma	D9533
30	DMTU	Sigma	D188700
31	Uric acid	Sigma	2625
32	CMH Hydrochloride	Sigma	ALX-430-117
33	HCl	RANKEM	H0080

34	DTNB	Sigma	D218200
35	Triethanolamine	Sigma	90279
36	2-vinyl pyridine	Sigma	132292
37	NaOH	MERCK	ME9D590006
38	Trizma base	Sigma	T1503
39	EDTA	Sigma	E5134
40	Chloroform	FiSher Scientific	12307
41	Sodium citrate	Sigma	311421
42	Kanamycin sulfate	Sigma	60615
43	IPTG	Biosynth	I-8000
44	Lysozyme	Sigma	62970
45	PMSF	Sigma	97626
46	Glycerol	Fisher Scientific	15457
47	Imidazole	Sigma	I2399
48	Friend's complete adjuvant	Sigma	F5881
49	Friend's incomplete adjuvant	Sigma	F5506
50	Menadione	Sigma	M5625
51	TRIzol®	Ambion	15596018
52	Isopropanol	MP biomedicals	194006
53	Ethanol	MP biomedicals	180077
54	DNaseI	Roche (Merck)	10104159001
55	RNase inhibitor	NEB	M0314S
56	ONPG	Sigma	N1127
57	B-PER®	Thermo scientific	90084
58	Nitrocellulose blotting membrane	GE healthcare life sciences	10600017
59	Ponceau S	Sigma	P3504
60	Skimmed milk	Difco	232100
61	Immobilon® Forte Western HRP substrate	Millipore	WBLUF0500
62	FeCl ₂	Sigma	372870
63	Ammonium iron sulfate	Sigma	215406
64	2,2'-Bipyridyl	Sigma	D216305
65	NBT dye	Thermo	N6495
66	TEMED	Sima	T9281
67	Glacial acetic acid	SRL	85801

68	Sodium acetate	Sigma	71188
69	SDS	Sigma	L3771
70	Ampicillin sodium salt	Sigma	A9518
71	Kanamycin	Sigma	60615
72	APS	Sigma	A9164
73	Tween 20	Sigma	P1379
74	TEMED	Sigma	T9281
75	Ethidium bromide	Merck	K39420515
76	Glycine	Sigma	G8790
77	Acrylamide	Sigma	A9099
78	Bis acrylamide	Sigma	M7279
79	Peroxidase conjugate Goat anti-Rabbit Antibody	Sigma	A6667
80	Glutathione reductase	Sigma	G3664
81	Agarose	Sigma	A9539
82	Methanol	SRL	65524
83	Nuclease free water	Sigma	W3513

Free spermidine evokes superoxide radicals that manifest toxicity

Vineet Kumar^{1†‡}, Rajesh Kumar Mishra^{1†}, Debarghya Ghose¹, Arunima Kalita¹, Pulkit Dhiman^{1,2}, Anand Prakash¹, Nirja Thakur¹, Gopa Mitra³, Vinod D Chaudhari^{1,2}, Amit Arora^{1*§}, Dipak Dutta^{1*}

¹Division of Molecular Biochemistry and Microbiology, CSIR Institute of Microbial Technology, Chandigarh, India; ²Division of Medicinal Chemistry, CSIR Institute of Microbial Technology, Chandigarh, India; ³Clinical Proteomics Unit, Division of Molecular Medicine, St. John's Research Institute, St John's Medical College, Bangalore, India

Abstract Spermidine and other polyamines alleviate oxidative stress, yet excess spermidine seems toxic to *Escherichia coli* unless it is neutralized by SpeG, an enzyme for the spermidine *N*-acetyl transferase function. Thus, wild-type *E. coli* can tolerate applied exogenous spermidine stress, but Δ speG strain of *E. coli* fails to do that. Here, using different reactive oxygen species (ROS) probes and performing electron paramagnetic resonance spectroscopy, we provide evidence that although spermidine mitigates oxidative stress by lowering overall ROS levels, excess of it simultaneously triggers the production of superoxide radicals, thereby causing toxicity in the Δ speG strain. Furthermore, performing microarray experiment and other biochemical assays, we show that the spermidine-induced superoxide anions affected redox balance and iron homeostasis. Finally, we demonstrate that while RNA-bound spermidine inhibits iron oxidation, free spermidine interacts and oxidizes the iron to evoke superoxide radicals directly. Therefore, we propose that the spermidine-induced superoxide generation is one of the major causes of spermidine toxicity in *E. coli*.

Editor's evaluation

The authors argue that a polyamine, spermidine, causes the production of reactive oxygen species (ROS) in *Escherichia coli* by oxidizing Fe²⁺, but spermidine can also be protective against ROS at lower concentrations when bound to other cellular molecules such as RNA. Thus, spermidine has both protective and antagonistic effects on ROS stress, depending on the cellular concentration.

Introduction

Polyamines are ubiquitously present in all life forms. They tweak a diverse array of biological processes, for example, nucleic acid and protein metabolism, ion channel functions, cell growth and differentiation, mitochondrial function, autophagy and aging, protection from oxidative damage, actin polymerization, and perhaps many more (Casero et al., 2018; Gawlitta et al., 1981; Madeo et al., 2018; Michael, 2018; Miller-Fleming et al., 2015; Oriol-Audit, 1978; Pegg, 2016; Pohjanpelto et al., 1981; Tabor and Tabor, 1984; Wallace et al., 2003). The cationic amine groups of polyamines can avidly bind to the negatively charged molecules, such as RNA, DNA, phospholipids, etc. (Igarashi and Kashiwagi, 2000; Miyamoto et al., 1993; Schuber, 1989; Tabor and Tabor, 1984). Polyamines have been demonstrated to protect DNA from reactive oxygen species (ROS) such as singlet oxygen, hydroxyl radical (\bullet OH), or hydrogen peroxide (H₂O₂) (Balasundaram et al., 1993; Ha et al., 1998a; Ha et al., 1998b; Jung and Kim, 2003; Khan et al., 1992a; Khan et al., 1992b; LØVaas, 1996;

*For correspondence:

aarora.pgi@gmail.com (AA);
dutta@imtech.res.in (DD)

†These authors contributed equally to this work

Present address: †Regional Centre for Biotechnology, Faridabad, India; §Department of Medical Microbiology, Post Graduate Institute of Medical Education and Research, Chandigarh, India

Competing interest: The authors declare that no competing interests exist.

Funding: See page 20

Preprinted: 05 September 2021

Received: 08 February 2022

Accepted: 11 April 2022

Published: 13 April 2022

Reviewing Editor: Joseph T Wade, New York State Department of Health, United States

© Copyright Kumar et al. This article is distributed under the terms of the [Creative Commons Attribution License](https://creativecommons.org/licenses/by/4.0/), which permits unrestricted use and redistribution provided that the original author and source are credited.




Cite this: *Metallomics*, 2017, 9, 1596

Received 9th August 2017,
Accepted 12th October 2017

DOI: 10.1039/c7mt00231a

rsc.li/metallomics

Cobalt and nickel impair DNA metabolism by the oxidative stress independent pathway†

Vineet Kumar, Rajesh Kumar Mishra, Gursharan Kaur and Dipak Dutta *

The oxidative stress that evolves under cobalt and nickel exposure is thought to exert toxicity, though the exact routes of such metal poisoning remain ambiguous. We revisited the metal toxicity in *Escherichia coli* to show that cobalt and nickel exposure at levels as low as 0.5 and 1 mM, respectively, visibly inhibits growth. We also observed that acidic conditions aggravated, while alkaline conditions alleviated the metal toxicity. Besides, 1 mM manganese, which is non-cytotoxic, as judged by the growth of *E. coli*, synergistically elevated cobalt and nickel stress. However, the metal toxicity did not lead to oxidative stress in *E. coli*. On the other hand, we show that cobalt and nickel, but not manganese, reduced the rate of DNA replication to 50% within 2 hours. Interestingly, the metal ions promoted DNA double-strand breaks but did not induce SOS repair pathways, indicating that the metal ions could block SOS induction. To test this, we show that cobalt and nickel, but not manganese, suppressed the nalidixic acid-induced SOS response. Finally, using an *in vitro* assay system, we demonstrated that cobalt and nickel inhibit RecBCD function, which is essential for SOS induction. Therefore, our data indicate that cobalt and nickel affect DNA replication, damage DNA, and inhibit the SOS repair pathway to exert toxicity.

Significance to metallomics

The ionic forms of cobalt and nickel are globally toxic. However, their mechanism of action is poorly understood. In this study, using the bacteria *Escherichia coli* as a model organism, we show that the metal ions do not evoke oxidative stress but directly affect DNA replication and repair processes to exert their toxicity. We also show how a nontoxic level of manganese ions synergistically aggravates the toxicities of cobalt and nickel. These observations may help novel drug formulation by combining metal ions with genotoxic antibacterial drugs.

Introduction

Small amounts of biologically occurring transition metal ions are required for metabolic functioning. Among them, cobalt (Co) and nickel (Ni) regulate the functions of a few specific enzymes. Essentially Co is a part of vitamin B12 and other cobalamins, which are mainly associated with the biological activity of methionine synthase.¹ On the other hand, a Ni ion is an integral part of the [Ni-Fe] hydrogenase, urease, glyoxylase and several other enzymes.^{2–4} However, the presence of these metals in excess can be hazardous at systemic and cellular levels in humans. The sources of such metal poisoning are manifold. Mining, smelting and refining of the metals, Ni plating, cupronickel coins, military decorative pins, orthopaedic metal-on-metal joint implants, and haemodialysis are reported to

increase the Co and Ni levels in the blood and other organs.^{5–18} Co and Ni exposure by direct contact, inhalation or ingestion can lead to disease conditions like allergy, contact dermatitis, nasal septum perforation *etc.*^{5–14,19–22} Co and Ni compounds are also cytotoxic, genotoxic, and carcinogenic to humans.^{23–25} The combination of Co and Ni exposure can act synergistically to exert cytotoxicity.^{26–28} In *E. coli* and other microorganisms, Co and Ni affect growth and propagation.^{29,30} Co and Ni pollution in farmland soils and seawater inhibits rice production, and fertilization of coral gametes, respectively.^{15–17} Co and Ni are also highly toxic to freshwater mussels.³¹ A series of studies have proposed that exposure to Co and Ni alters the redox chemistry in the cells by producing reactive oxygen species (ROS).^{28,32–37} Thus, Co- and Ni-mediated posttranslational modification and carbonylation of the proteins and the genotoxic effects were attributed to the oxidative stress.^{28,38–42} Co reacts with H₂O₂ in a phosphate-buffer system, especially in the presence of glutathione or histidine, to produce both superoxide (O₂^{•-}) and hydroxyl radical (•OH) species that damage nucleotides and DNA.^{43–46} In contrast,

CSIR-Institute of Microbial Technology, Sector 39-A, Chandigarh 160036, India.

E-mail: dutta@imtech.res.in

† Electronic supplementary information (ESI) available. See DOI: 10.1039/c7mt00231a